Materials Research

DOI: 10.1002/anie.200603675

Combinatorial and High-Throughput Materials Science

Wilhelm F. Maier, Klaus Stöwe, and Simone Sieg*

Keywords:
catalysts · combinatorial chemistry · high-throughput analysis · materials libraries · materials science

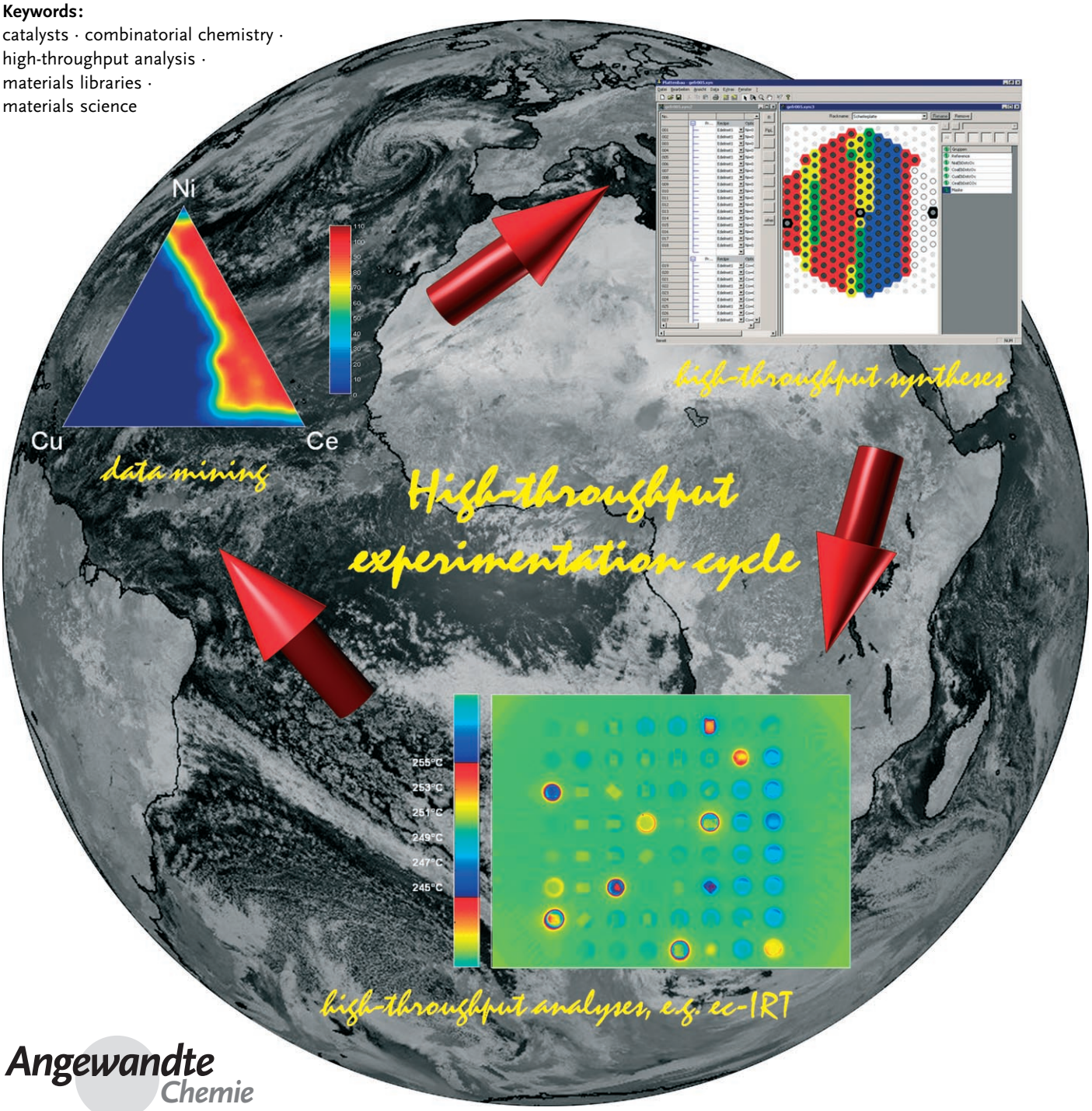

There is increasing acceptance of high-throughput technologies for the discovery, development, and optimization of materials and catalysts in industry. Over the years, the relative synchronous development of technologies for parallel synthesis and characterization has been accompanied by developments in associated software and information technologies. This Review aims to provide a comprehensive overview on the state of the art of the field by selected examples. Technologies developed to aid research on complex materials are covered as well as databases, design of experiment, data-mining technologies, modeling approaches, and evolutionary strategies for development. Different methods for parallel synthesis provide single sample libraries, gradient libraries for electronic or optical materials, similar to polymers and catalysts, and products produced through formulation strategies. Many examples illustrate the variety of isolated solutions and document the barely recognized variety of new methods for the synthesis and analysis of almost any material. The Review ends with a summary of success stories and statements on still-present problems and future tasks.

From the Contents

1. Introduction

Our standard of living is closely associated with industrial products based on functional materials (hard and soft matter with a function). The worldwide demand for new or improved materials is unlimited. The development and improvement of materials have always been demanding, time-consuming, and costly processes. High-throughput (HT) technologies, which promise to speed up the discovery and development processes, have evolved rapidly during the last decade. The aim of this Review is to present an overview of the current state of this field. Combinatorial and HT materials science is an approach to the rapid discovery, study, and optimization of new and known materials that combines rapid synthesis, high-throughput testing, and high-capacity information processing to prepare, analyze, and interpret large numbers of diverse material compositions.

The use of the terms "combinatorial" and "high-throughput" in the literature is still confusing. In an early approach, IUPAC defined the terms used in combinatorial chemistry;[1] these definitions were guided by drug research and do not always consider the problems associated with combinatorial materials research. Schüth has paid particular attention to these two terms in a review article,[2] but we feel a need for further clarification. The term "combinatorial" should refer to experiments in which groups or elements of different materials or components of a recipe, such as solvents, additives, or other components, are combined. Combinatorial thus refers to a change in the nature of the parameters, not to the change in the value of the parameters. The systematic variation of given compositions, temperatures, pressures, or other single parameters to explore a wide parameter space is not a combinatorial, but a high-throughput experiment.

Although "high-throughput" as a term only refers to the number of experiments and not to any intelligence associated with the experimental design and combinatorial strategies for discoveries, it also does not exclude those, and in the following the term high-throughput will be used to describe both combinatorial approaches and numeric variations. In this Review we will frequently use the abbreviations: HT (high-throughput), HTT (high-throughput technology), HTE (high-throughput experimentation), and HTS (high-throughput screening).

High-throughput experiments have a long history; early activities were exclusively manual operations, while the latest developments have been technology driven. Some early examples of high-throughput experimentation can be traced back to Edison (1878) and Ciamician (1912; as outlined in a review by Schubert and co-workers)[3] as well as to the development of the catalyst for ammonia synthesis by Mitasch at BASF in 1909. Despite these early activities, HTE did not become a research subject for a long time. In 1970, Hanak successfully prepared and applied what we now call composition spread or gradient libraries for research and development purposes at the laboratories of the firm RCA. His work led to several new products, which successfully entered the market. It also resulted in 28 publications and 12

[*] Prof. Dr. W. F. Maier, Prof. Dr. K. Stöwe, Dipl.-Math. S. Sieg
Technische Chemie, Universität des Saarlandes
Gebäude C4.2, 66123 Saarbrücken (Germany)
Fax: (+49) 681–302–2343
E-mail: w.f.maier@mx.uni-saarland.de
Homepage: http://www.uni-saarland.de/fak8/maier

Supporting information for this article is available on the WWW under http://www.angewandte.org or from the authors.

patents, which were reviewed in detail recently.[4,5] In one of his publications Hanak stated: "… *the present approach to the search for new materials suffers from a chronic ailment, that of handling one sample at a time in the processes of synthesis, analysis and testing of properties. It is an expensive and time consuming approach, which prevents highly-trained personnel from taking full advantage of its talents and keeps the tempo of discovery of new materials at a low level*."[6] Despite the potential importance and validity of this statement, the work of Hanak went unnoticed; his message was not appreciated at the time. In the following years there was very little HT activity of note. In 1980 the first article on parallel reactors for applications in heterogeneous catalysis was published by the Moulijn research group,[7] which was followed in 1986 by a detailed report on six parallel reactors for the testing of heterogeneous catalysts.[8]

In the early 1990s the bioorganic chemist Schultz assembled a team of physicists and materials scientists at the Lawrence Berkely National Laboratory of UC Berkeley to apply combinatorial principles from drug development to materials research. The famous publication from 1995 concerning a search for superconductors from a materials library marked the actual start of combinatorial materials science as a discipline.[9] At that time scepticism was high and critical voices were common. There were those who were impressed and believed that this technology would rapidly solve many of the materials problems versus a critical majority afraid of the replacement of intelligent science by sheer number crunching and automation. However, the idea continued to spread and high-throughput experiments were started in many laboratories. In 1997 the newly formed company Symyx Technologies published a library of over 25000 distinct compounds, thereby documenting the state of the art of this technique.[10] The first extensive review appeared in 1999.[11] It covered 207 publications on a large variety of technological developments and provided a critical, but positive view on a rapidly developing field.

Today the initial euphoria has abated and combinatorial materials science has matured. HTTs have been developed for and applied to an ever increasing number of materials, such as catalysts, electronic and magnetic materials, polymer-based materials, optical materials, biomaterials, paints, drug formulations, detergents, cosmetics, glues, and others. Often, the use of HTTs in the development or discovery of new materials is not even mentioned in the title of publications, abstract, or key words and is only found in the detailed description or is completely omitted. It has become impossible to accurately identify all HTT activities. About 10000 publications in which such methods have been applied can already be found, which clearly exceeds the coverage of a comprehensive review. We have therefore restricted this Review to selected publications and attempt to provide an overview on the state of the art, the areas in which HTTs have already made an impact, and the problems HTTs are still facing. Thus, HTTs related to drug discovery and homogeneous catalysis are largely excluded, because the two fields have little in common with materials research. Combinatorial drug discovery and development is based on molecular structures and their variation, while in materials research access to composition, processing parameters, and a large variation of HT characterization methods have dominated the developments in the field. Nevertheless, there are some overlapping areas, such as the development of polymers for drug transport and release, the acceleration of the formulations of drugs (galenics), and development of compatible biomaterials, such as bone substitutes, which are associated with HTTs and combinatorial chemistry but these are also not covered in this Review. Another rapidly developing field, the use of HTTs in formulation developments, such as detergents, paints, adhesives, and others, is confined to industrial laboratories and rarely the subject of scientific reports.

High-throughput experiments in materials research are defined by the types of materials of interest, and typically requires the preparation of an array of materials (libraries), a fast method to screen for properties (characterization and testing), and suitable software for experimental control, data storage, data analysis, and experimental design (computational tools).

A high-throughput experiment often starts with a first set of experiments that cover the parameter space selected. The hits detected during the early stage of the study will usually dominate the later experiments, that is, the search focuses with time. There are two principally different scenarios for high-throughput experiments: discovery and optimization. The discovery strategy (often termed primary screening) is applied when totally new (alternative) materials are the target

Wilhelm F. Maier, born in 1949 in Kaufbeuren, is professor of Technical Chemistry at Saarland University. After studying chemical engineering at the Ohm-Polytechnic in Nürnberg, he studied chemistry at the Philipps University in Marburg and received his PhD with M. T. Reetz. After postdoctoral research with P. von R. Schleyer at the University of Erlangen, he joined the University of California as Assistant Professor, and in 1988 he became Professor for Technical Chemistry at the University of Essen. In 1992 he joined the Max Planck Institut für Kohlenforschung as head of a research group for heterogeneous catalysis before taking up his current position in 2000.

Klaus Stöwe, born in 1962 in Nürnberg, completed his PhD in chemistry in 1990 under the direction of H. P. Beck at the Friedrich-Alexander University in Erlangen. After sabbaticals at the Max-Planck-Institut für Festkörperforschung in Stuttgart and the group of D. C. Johnson in Eugene, Oregon, in 1997 he completed his habilitation in Saarbrücken at the Institute for Inorganic and Analytical Chemistry, where he focused on homonuclear interactions in selected lanthanide and actinide chalcogenides. In 2004 he joined the Technical Chemistry at Saarland University, where he is involved in high-throughput synthesis and characterization techniques. At the beginning of 2007 he was appointed extraordinary professor.

of the search (motivations may be: scientific curiosity, existing materials have little potential for further improvements, and no suitable materials are known). Discovery strategies aim at sampling broad and highly diverse parameter spaces. Experimental conditions are compromised for throughput. The disadvantage of this approach is that the number of mistakes often increases (false positives and false negatives). Additional problems in the search for new or alternative materials are search conditions, which are oriented at the conditions for the best performance of existing materials, which give the latter an advantage and contribute to false negatives and a significant reduction in the number of hits. Inherent deviations between primary screening conditions and those of real applications means that it is imperative to reproduce effective materials (hits) resulting from primary screening data by conventional synthesis and confirm the expected function by conventional measurements. Hits, which are usually amplified during a study, should always be validated under conventional or realistic conditions. Optimization aims to accelerate the development of materials (often termed secondary screening). Here, relatively narrow, well-defined parameter spaces around known materials are sampled at high speed under conditions as close to conventional experimentation as possible. The known material to be optimized may be a hit discovered by primary screening or it may be any known material. Secondary screening describes experimental set-ups, where the conditions used to measure the functional behavior of materials is as close as possible to traditional measurement procedures. Here, the compromise calls for high accuracy of the data, which is often paid for by a slowing down of the experiment and a reduction in the number of samples studied in the HT experiment. The goals are reliable trends and optimized materials rather than hits and local optima.

There have been an impressive number of reviews on this subject, which is typical for a rapidly developing new field. Since many of these reviews are relevant for the HT topic as well as related areas, a summary of selected review articles, books, and special issues has been assembled. Their large number and space limitations has necessitated the reviews being summarized in the Supporting Information, which can be accessed by the interested reader.

Simone Sieg, born in 1978 in Zweibrücken, completed her studies of mathematics with a minor in chemistry in 2003 at the University of Technology in Kaiserslautern, working in the field of optimization and traffic planning (thesis title: "Algorithms for Multicovering Models with Application to Line Planning"). She then joined the team of W. F. Maier to start her PhD thesis in the field of heterogeneous catalysis and combinatorial chemistry. Her current work focuses on the modeling of quantitative structure–activity relationships for heterogeneous catalysts by Kriging and multilevel B-Spline approaches.

2. Computational Tools

A major bottleneck in high-throughput techniques is no longer the development of experimental procedures for the preparation and testing of materials, it is often data management and data analysis. Although the development of the computational methods has progressed rapidly in recent years, many laboratories are hesitant to use these methods because of a lack of manpower, complexity, and lack of access to established software.

2.1. Design of Experiments (DoE)

The number of factors to consider increases dramatically with the desire to discover or develop new or better materials. Elements of the periodic table, suitable precursors and their concentrations, functional group variations, sequence order of the addition of reagents during the preparation, solvents, additives, modifiers, treatment and reaction times, pretreatment, activation procedures, and microstructures are all parameters which affect the function of solids. Clearly, systematic variation of all the potential parameters rapidly approaches infinity. Although present high-throughput experiments allow the acceleration of investigations by a factor of 10–100, this is by no means sufficient to support mindless systematic screening. While DoE is still often ignored in conventional research, it is essential for the planning of high-thoughput experiments. Since high-throughput experiments are significantly more cost intensive than conventional research, it is only successful if they deliver the promised progress in a shorter time, which requires careful planning of the experimental parameter space. DoE can be described as techniques that minimize experimental effort at maximal information output. DoE has developed rapidly with the onset of high-throughput experiments and a large variety of methods have become available to serve the needs of HTE.

Since experiments are costly and time-consuming, intelligent selection of experiments has a long tradition. Statistical DoE allows the effective determination of those parameters as well as parameter interactions which have a main effect on the property of interest. Systematic variations of up to four parameters (so-called complete factorials or fractional factorials) can be carried out manually and have long become part of the education of experimental scientists (factorial design). Ramos et al.[12] compared the performance of an inert membrane reactor (IMR) for the oxidative dehydrogenation of propane to that of a conventional fixed-bed reactor with identical catalysts and operating conditions. A factorial DoE led to the maximum yield of propene. The statistical design of experiments has been used by Salim and co-workers[13] for analyzing the precipitation and aging steps used during the preparation of silica-supported nickel catalysts. A model could be developed which describes the specific surface area of the catalyst as a function of the rate of formation of the nickel silicate. With the help of this model, the preparative conditions could be optimized to maximize the catalytic activity. The effective application of such a systematic DoE to large sample numbers or parameter spaces has been the

objective of recent studies. A legitimate approach is the so-called full-grid search to sample the whole parameter space defining individual step sizes for each of the parameters considered. In this approach, all the samples have to be screened for their functional performance to obtain insight into the impact each factor has on the property of interest. A clear drawback is the large number of experiments to be carried out, which rapidly increases with the number of selected factors. Castillo et al.[14] presented the use of a split-plot experimental design, developed for high-throughput studies of catalysts (see Figure 2 in Ref. [14]), but demonstrated this with only two catalysts. Here two levels of the parameters temperature (T) and pressure (p) were combined with the variation of two catalysts at two concentrations. With each experiment carried out twice for statistical reasons, this resulted in 32 parallel experiments. Four modules out of eight allow variation of temperature and pressure. This design can be increased to cover any number of catalysts. Furthermore, the study focused on the unique error structure of these designs. The approach has been elaborated upon during a case study at Dow Chemical Company.[15] A good overview on experimental design approaches for HTE can also be found in Ref. [16], while examples of split-plot designs realized in industry can be found in Refs. [17–19]. A factorial design was selected by Corma et al. to study experimental variations in zeolite synthesis (Figure 1). A Pareto analysis was applied to interpret and quantify the factor effects. The new zeolite ITQ-30 was discovered by this technique.[20]

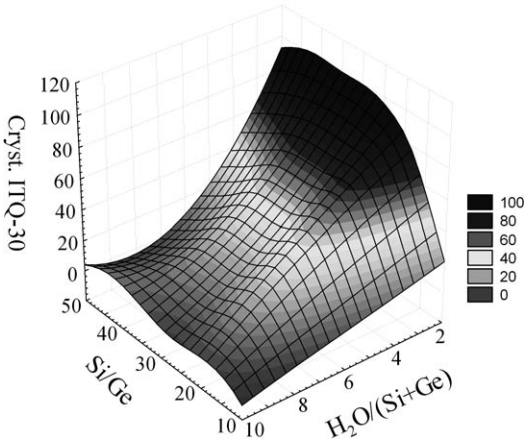

Figure 1. Evolution of zeolite ITQ-30; crystallinity is shown as a function of synthesis conditions on varying the molar ratios of Si/Ge and $H_2O/(Si+Ge)$ (see Figure 5 in Ref. [20]).

With the development of computation, complex DoEs became common, and now standard software can be used to plan and evaluate effective and statistically meaningful optimizations. Unfortunately, in most cases the use of factorial design for simultaneous optimization is limited to a maximum of five parameters at two levels. One approach to reduce the parameter space is by intuition or knowledge available from prior experimentation and research. Another is the use of a "primary screening" strategy, in which hundreds or thousands of potential samples are prescreened for the property of interest. Primary screening is therefore a means to reduce the parameter space for a final optimization.

Another way to limit the parameter space is by the use of structure–activity relationships, which turn random searches into well-structured searches. Quantitative structure–activity relationships (QSARs) are important aspects of modern drug development, which provide descriptors that link molecular structure with pharmacological effects. Structural diversity is an essential question of concern in the search for new drugs. Much effort has been devoted to the question of how to design a structurally very diverse library for general purpose screening,[21–25] and many methods have been proposed to optimize experimental designs.[26,27] For example, scientists rely on the "similar property principle", which means that molecules with similar structures or with similar functional groups will show similar physicochemical and biological properties.[28,29] This approach is reasonable for drug development, and very effective codes or algorithms have been developed to represent molecular structures for rapid computation. "Descriptors" (for example, dipole moment, distance between selected functional groups, etc.) are identified which correlate molecular structure with specific drug function. Algorithms can then be applied to sort molecules into different classes depending on the chosen similarity measure (for example, Euclidian distance, Tanimoto coefficient, etc.). The design of a screening library for primary screening usually selects only a few representatives from each class to achieve the largest diversity with the least possible effort.

Unfortunately, most materials cannot be represented by exact structures, and functional solids do not lend themselves easily to simple representation by a computer. The much higher complexity of materials and the diverse preparation methods of such functional solids do not allow such developments to be directly transferred from drug research to materials research. Nevertheless, the mathematical techniques used can still be applied. In materials research, quantitative structure–property relationships (QSPRs)[30] and quantitative composition–activity relationships (QCARs)[31] have been developed, which attempt to link the materials function with structure or chemical composition.

Reynolds reported that the concepts of molecular diversity and similarity that have shown to be useful in the field of biologically active molecules can also be applied successfully to the design of synthetic polymers.[32] A first serious effort to extend the descriptor approach to heterogeneous catalysts was recently published by the research groups of Schüth and Mirodatos.[33–35] They described a search for descriptors based on data obtained by testing a library of 467 catalysts for the oxidation of propene. Experimental data were supplemented by physical data of the elements and phases. Principal component analysis (PCA) and clustering methods were applied to identify characteristic features correlating with catalysis (Figure 2). The clusters allowed the catalysts to be grouped into classes, but descriptor identification turned out to be difficult.

The lack of correlation between catalytic performance and composition is understandable since catalyst preparation varied greatly. The best descriptors identified were atomic

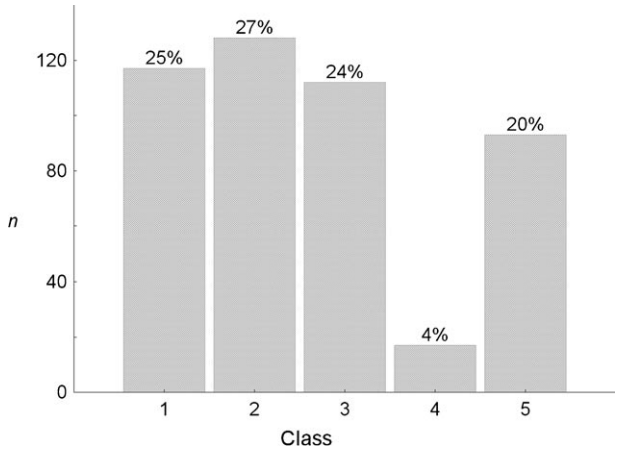

Figure 2. Number of catalysts *n* in each class for *k*-means analysis based on eight principal components that characterize the catalytic performance of 467 very different materials for propene oxidation (from Ref. [35]). Class 1: low conversion, high selectivity for CO_2; class 2: medium conversion, high selectivity for CO_2; class 3: low conversion, high selectivity for CO, partial oxidation products; class 4: low selectivity for CO_2, CO, and hydrocarbons; class 5: high conversion, high selectivity for CO_2.

radius, electron affinity, and free enthalpy of the most stable oxides. The authors concluded that a broader database and more comparable data were required for this type of analysis. Corma et al. reported the successful unsupervised construction of QSPR models from spectra characterization descriptors and synthesis descriptors for epoxidation catalysts based on Ti silicates.[36]

Searching for an optimal composition or a synthesis route to a material is a multidimensional optimization problem. Since many factors influence the properties of materials (for example, chemical composition, synthesis route, pore structure, surface properties, etc.), 20–30 descriptors are not exceptional. At the start, the functions to be optimized (objective functions) that describe the relationship between a performance measure (for example, activity, durability, hardness, flexibility, conductivity, etc.) of a material and its composition or certain other descriptors are unknown. To date, no theory exists that helps this relationship to be described in an analytical way. Only discrete values of these underlying functions are available from experimental measurements, and therefore standard mathematical optimization approaches cannot be used directly. In most cases, analytic expressibility is an important prerequisite for the application of efficient optimization methods such as gradient methods, conjugate gradient methods, or methods that also need second-order derivatives (for example, Gauss–Newton, Levenberg–Marquardt).

To solve this problem for applications in materials research, Holena[37] proposed two possible solutions: 1) Employing optimization methods that do not require gradient or second-order derivatives of the optimized function. These can be deterministic, such as the simplex method,[38] stochastic, such as simulated annealing,[39–41] or genetic algorithms (GAs). Holena remarked that GAs have become very attractive for catalysis research, since they seem to establish a straight-forward correspondence between the optimization paths followed by the algorithm and the channels of a high-throughput reactor in which the proposed new materials are to be tested and validated. 2) Construction of an analytically expressible function using the available data such that the gradient and second-order derivatives can be estimated with sufficient precision. Standard optimization methods can then be applied. Thus, methods to approximate very general functions are needed. Various classes of neural networks seem to yield the most promising results for this approach. Applications in materials research are nearly all based on a particular kind of neural network, the so-called multiplayer perception (see for example, Ref. [37] and references therein).

2.2. Genetic Algorithms and Evolutionary Strategies

GAs are ideally suited for high-throughput experiments since they require a population of individual samples and thus rely on high-throughput. GAs have been applied to materials research for nearly ten years. The history of GAs goes back to the 1960s when Holland started his work in this field and the fundamental concepts and ideas were published in 1975.[42] De Jong published the first application (parameter optimization) in the same year.[43] It was not until 10 years later that this new approach to solve complex practical problems became more and more accepted within the community. In 1989, Goldbergs book *Genetic Algorithms in Search, Optimization and Machine Learning*[44] introduced the theory and application of genetic algorithms to a wide audience. In general, GAs are a class of nonlinear, adaptive, and often heuristic methods for solving optimization and search problems. As in nature, genetic algorithms are often used as so-called "black-box" functions. In nature, populations evolve over many generations following the principles of natural selection and the "survival of the fittest". By copying and imitating these principles from nature, genetic algorithms can generate artificial populations to undergo an evolution that approaches an optimal solution of a predefined problem. In contrast to other methods, a GA need not to be trained and does not need nor collect information about gradients or other specific information on the problem to be solved, and theoretically there is no limit to the number of parameters or algorithms that can be applied. This may be the reason why GAs are often applied to fields that are not well understood or where a complete modeling is not possible because of mathematical or computational restrictions or efforts.

A good overview on genetic algorithms and neural networks and their use in heterogeneous catalysis has been given by Holena.[37] The author lists the most relevant practical applications of both techniques and the reader is also referred to references in that review. Figure 3 illustrates the idea and procedure of a genetic algorithm.

The aim of applying a GA is to improve a starting solution (library of individuals) for a given problem within each iteration. The individuals are evaluated by the fitness function (desired property). The best individuals are used to produce an offspring generation with the help of selected algorithms,

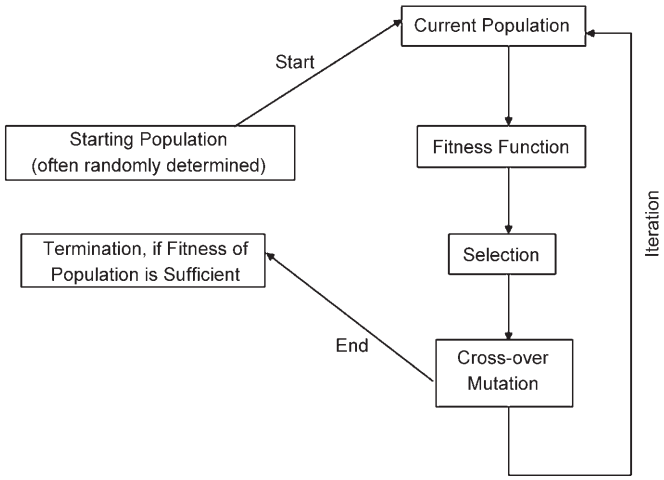

Figure 3. Flow scheme of a genetic algorithm.

such as mutation, cross-over, or recombination operations. The offspring generation is then evaluated and the process starts again. Genetic algorithms for materials research can be simply described as follows: the best members of the starting library with respect to the fitness function are selected as hits. From these hits (parents), the next library (offspring generation) is formed. It is up to the researcher to develop suitable algorithms that form an offspring generation which improves upon the parents. Such algorithms may exchange the elements of the parents, exchange their molar contents, or introduce random dopant elements. As long as there is an improvement in the offspring generations, the evolution towards the desired function is working. If there is no improvement in early offspring generations, the algorithms chosen may be poor. If this happens in later generations, an optimum may have been reached. Contrary to most other optimization procedures, GAs are not limited by the boundaries of the starting library or starting set, and can thus escape local maxima or minima and enter new parameter spaces by itself. It is interesting that in the application of a GA, randomness of mutations plays an important role in obtaining a new solution. Furthermore, genetic algorithms are nondeterministic methods. It is neither possible to predict the number of generations the algorithm will produce until a "best" solution is reached, nor can anything be said about the solution itself.

Although there have already been many reports on the use of GAs in materials research, there are as many different algorithms. The choice of algorithms and the strategy applied to generate the offspring generations characterize each GA and are also responsible for success or failure. One application of genetic algorithms is for the design of diverse combinatorial libraries for high-throughput screening.[45–47] The first use of an evolutionary strategy for searching the optimal composition of catalytic materials was described by Baerns and co-workers.[37,48–51] Another evolutionary optimization approach combined with high-throughput synthesis and screening has been applied to the discovery of new catalysts for the oxidative dehydrogenation of ethane to ethylene.[52] Mirodatos and co-workers[53,54] used genetic algorithms in several ways: they developed a GA platform software called OptiCat that enables the user to construct custom-made workflows. They tested their approaches on a virtual benchmark test and on experimental response surfaces obtained from HT screening. The research group also studied the effects of genetic algorithm parameters on the optimization of heterogeneous catalysts, especially the influence of population sizes on the robustness and convergence speed.[54] Corma et al.[55] used a GA to optimize isomerization catalysts for light paraffins. The successful combination of GA and DoE led to the discovery of new paraffin isomerization catalysts (Figure 4).[56]

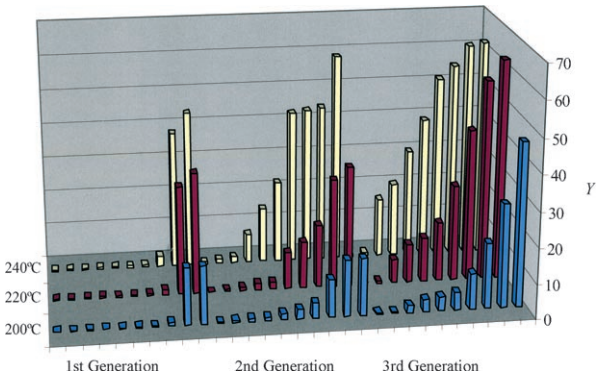

Figure 4. Catalyst development for pentane isomerization with the ten best ranked materials from three generations through the combination of GA with DoE (from Ref. [56]). $Y = n$-pentane conversion.

In a theoretical study, a combination of density functional theory (DFT) and genetic algorithms has been applied by Nørskov and co-workers to search for new stable alloys consisting of four components.[57] The research group identified several new alloys among the 192016 possible face-centered cubic (fcc) and body-centered cubic (bcc) alloys that can be constructed out of 32 different metals. The method has now been extended to the discovery of electrocatalytic materials for hydrogen evolution. Not only is the theoretical approach remarkable, but the authors also did not stop with the prediction but verified the validity of their study with experimental data. Starting with a screening for catalyst activity, the selection was refined by testing (theoretically) for segregation, island formation, and dissolution of the potential alloys. From a starting set of over 700 binary transition-metal alloys BiPt was identified as the most promising. It was synthesized and tested experimentally and, in agreement with the theoretical prediction, its hydrogen evolution activity was better than that of pure Pt.[58] The application of genetic algorithms to polymer design is illustrated in Ref. [59]. Giro et al. demonstrated how the application of a genetic algorithm can help to accelerate the development of new conducting polymer materials (binary up to quinternary disordered polymeric alloys).[60–62]

The evolutionary strategies (ESs) developed by Rechenberg are related to GAs.[63] Evolutionary strategies allow the use of continuously variable parameters, such as elemental composition, and have been applied to a large variety of problems, such as the design of an optimal cross-section for a

hypersound nozzle.[64] Evolutionary strategies, combined with GAs were used by Kirsten and Maier in a search for new oxidation catalysts.[65]

2.3. Artifical Neural Networks

Artificial neural networks (ANNs) are computing systems that are based on the concepts of neurons in biology. A neuron can be seen as an elementary signal processing unit that is either connected to other neurons or to the environment such that the transmission of signals can be realized. Input neurons receive signals from the environment, while output neurons can send signals to the environment. The neurons in between are called hidden neurons. The architecture of the networks gives the structure of the connections between input, output, and hidden neurons. The most important class of networks for applications are so-called feed-forward networks. Here, the set of neurons is partitioned into several layers such that signal transmission between neurons is only possible from a lower layer to a higher layer. So-called multilayer perceptrons are the most common networks of the feed-forward kind and, according to Ref. [37], all neural networks applied so far in materials research are of this type.[66–71] Figure 5 illustrates an example of a multilayer perceptron.

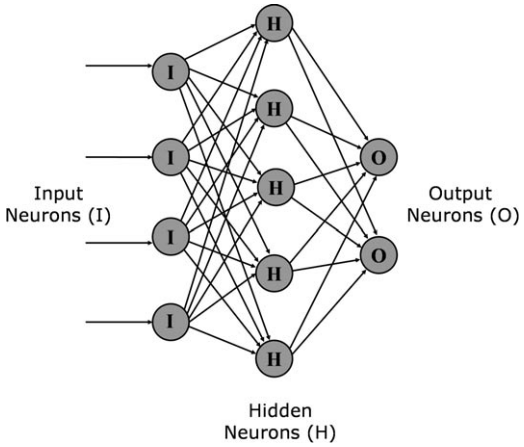

Figure 5. Example of a multilayer perceptron.

Multilayer perceptrons with applications in catalysis are described in detail in Ref. [66]. The approximation of complicated and general dependencies is one of the most remarkable features of feed-forward networks. These networks have been used to approximate relationships between catalytic performance and chemical composition, physical properties, and reaction conditions.[66–72]

Neural networks need to be trained first on a selected set of training data. Theoretically, there is no limitation to the number of parameters or connectivities. A main problem with neural networks is that the information used for learning does not extrapolate reliably to trained dependencies outside of the training data. It might happen that the approximation perfectly fits the training data and also the noise included. In this case, points outside the training set are quite irrelevant to the approximated dependence. This phenomenon is called "overfitting" and can be recognized by using a new data set (test data) that also possesses the approximated dependence but has not been used for the learning process. A detailed treatment of artificial neural networks can be found in Ref. [73,74] and a detailed overview on the application of neural networks in chemistry can be found in the cited books.[75,76] Within the last decade a review[77] and a book[78] have been published that cover the applications of neural networks in chemistry and science. Additional applications of ANNs to catalytic problems are described in Section 2.4.

2.4. Combination of GAs and ANNs

The search for the best material within a predefined parameter space is approached from different directions by GAs and ANNs. The combination of both methods has led to positive effects being noted, such as remarkable acceleration. A GA has been used to train an ANN in catalysis for parameter tuning of a three-way catalytic converter.[79] This strategy of integrating neural networks in GAs has been used to find the optimal composition of a catalyst for the ammoxidation of propane.[80] In this case, no experiments were performed and the network was trained with literature data. The same strategy has been used to find the optimal Cu:Zn:Al ratio in mixed oxide catalysts for the synthesis of methanol from syngas.[81] The process variables of the TS-1-catalyzed hydroxylation of benzene have been optimized by a similar strategy, and the predicted process variables were experimentally verified.[82]

Another approach is to use ANNs to simulate experimental feedback concerning the performance of proposed catalysts selected by a GA. The GA is run several times using different population sizes to study the influence of population size on the convergence behavior and decrease of population diversity. This approach allows an intensive study of the adjustable parameters in the GA and their influence on convergence speed and decrease in diversification. Parameter studies for GA have been described by Mirodatos and coworkers[54] as well as by Sundaram and Venkatasubramanian.[59] Corma et al. described several applications of ANNs and GAs for modeling the kinetics of catalytic reactions.[83,84] ANNs have been used to study the behavior of catalysts under different reaction conditions for the isomerization of *n*-octane. Based on the reactor conditions, the networks have been trained to predict the composition of new catalysts for the oxidative dehydrogenation of ethane.[85] Larachi[86] used modeling with ANNs to describe the coke burn-off on MnO_2/CeO_2 oxidation catalysts under wet conditions. Huang et al.[87] proposed another method for catalyst design based on the combination of artificial neural networks and genetic algorithms. They trained an ANN to model the relationship between catalyst components and catalytic performance. To enhance the efficiency of the designing process, a new hybrid genetic algorithm was developed to solve the global optimization problem. With this method, a multicomponent catalyst for the oxidative coupling of methane was developed that

exceeded the results previously reported for other catalysts. Mirodatos and co-workers[88] used ANNs to predict the performances of catalysts for the water-gas-shift reaction and also as a classification tool within an evolutionary approach (Figure 6). Roy et al. presented an approach of combining neural networks, genetic algorithms, and Markov chains to simulate polymer blends and predict the miscibility of unknown polymer systems.[89] Other applications also include the modeling of chemical reactors,[90] studies on soot formation in hydrocarbon flames,[91] and predictions of catalyst deactivation.[92]

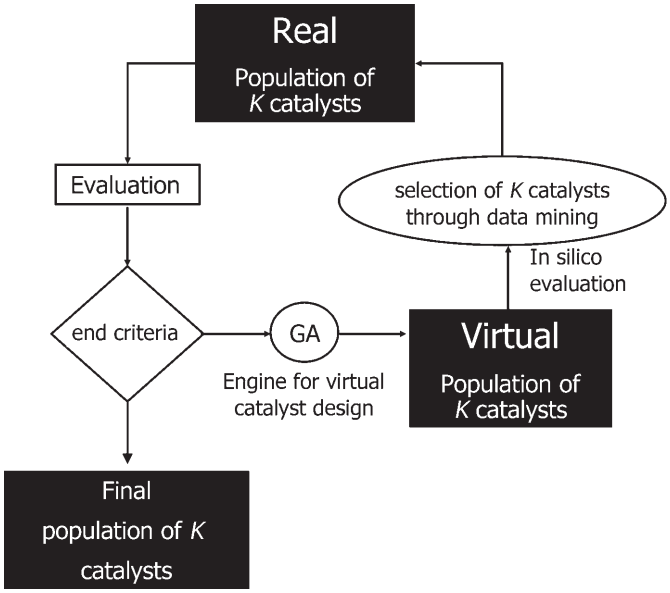

Figure 6. Scheme of the methodology proposed by Mirodatos and co-workers for boosting primary screening in heterogeneous catalysis.[88].

Another approach to multiparameter modeling and optimization is the holographic research strategy (HRS) developed by Margitfalvi and co-workers. The authors[93] compared the performance of a genetic algorithm approach to the HRS to find an optimal material composition in a multidimensional search space. Similar to GAs, HRSs can be used for library design, predictions in materials synthesis, and functional optimization. In elaborate studies, an HRS was combined with an ANN and compared to a GA in catalyst optimization for methane combustion at 350 °C, propane combustion at 150 °C, and oxidative coupling of methane at 800 °C. Catalysts composed of Pt, Pd, and Au on mixed oxide supports of Ce, Co, Zr, Cr, La, and Cu were used for the first two reactions and Na, S, W, P, Zr, and Mn on SiO_2 for the coupling reaction.[93–95] In all cases, very similar optimal catalysts were obtained, while the HRS is claimed to require only half the samples to converge to an optimum. HRS has so far only been used by the Margitfalvi research group. Support vector machines (SVMs) have been used by Baumes et al.[96] for the predictive modeling of heterogeneous catalysts for the isomerization of hydrocarbons and the epoxidation of olefins. SVMs belong to the machine-learning techniques. Instead of starting with assumptions about a problem, SVMs use tools to identify the correct model structure from the data available. Data sets therefore include a training data set and test samples to evaluate the accuracy of the derived models. SVMs have been applied to olefin epoxidation and isomerization catalysts.

2.5. Data Mining/Knowledge Discovery/Data Bases

The use of high-throughput experimentation generates lots of data and information within short time periods. These data are just information and only proper data analysis can turn the data into knowledge. The extraction of knowledge (knowledge discovery, KD) out of large data sets is not a trivial task and misleading conclusions readily result if data interpretation is not accompanied by proper statistical analysis.

A large variety of mathematical tools are available for data analysis. Important data-mining techniques used for knowledge discovery in large data sets are principal component analysis (PCA), clustering techniques (for example, hierarchical clustering, *k*-means clustering, etc.), ANNs, GAs, classification methods, regression methods, kernel methods (for example, SVM), decision trees, and self-organizing maps. Nearly all of these techniques require profound statistical and mathematical knowledge for proper application. For a detailed description of these data-mining tools we refer to adequate handbooks of multivariate statistics,[97] machine learning,[98] and data mining itself.[99]

Many new approaches have been published which combine HTE and mathematical data-mining techniques to speed up the development of new materials. Caruthers et al.[100] presented a new framework for designing catalysts that integrates HTE with computer-aided extraction of knowl edge. The current state of HTE is described and its speed and accuracy was illustrated using a FTIR imaging system for CO oxidation over metals. Furthermore, the authors show the performance of a "knowledge extraction (KE) engine" (with respect to robustness, automated model refinement, etc.) and its possibility to predict optimal catalyst composition using a forward and inverse model (Figure 7).

A hybrid evolutionary framework was also used that combines ANNs and GAs to solve the forward and inverse problem for the development of industrial products and which benefits from this synergistic approach.[101] Böcker et al.[102]

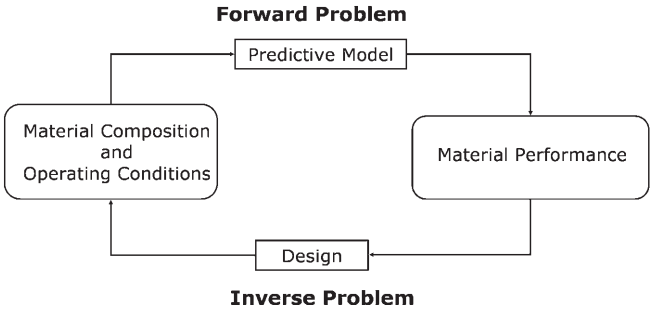

Figure 7. Schematic representation of the forward and inverse problem in materials design (from Ref. [100]).

published a review on data-mining approaches in HTS. The most frequently applied techniques are described, including kernel-based machine-learning tools. This review also provides a large bibliography for data mining in HTE, including textbooks that provide theoretical background. Ohrenberg et al.[103] have reported how data mining and evolutionary optimization can be used to increase the efficiency of material searches in high-dimensional parameter spaces. The authors used different data-mining techniques, such as clustering, correlation analysis, and decision trees, in combination with evolutionary strategies for materials optimization. As the most important result, the authors stress the importance of combining different techniques to gain significant advances in knowledge. The application of data-mining techniques in polymer science has been reported by Adams and Schubert.[104,105] The authors give an overview on the development of a detailed data-management system to handle high-throughput screening data and to derive knowledge out of these experiments. As a main focus of their work, they refer to an informatics infrastructure that was developed to support the experimental work and especially the analysis of screening data. Another application of a clustering method (sequential superparamagnetic clustering) has been applied by Ott et al.[106] to cluster chemical structures. The authors conclude that sequential clustering can also be of particular interest to chemical applications, such as combinatorial library design and hits analysis in HTS data. Saupe et al.[107,108] illustrated how the use of appropriate software tools in every single step of the HTE process helps to increase the speed of knowledge discovery. A modular approach to an HTE platform was presented which satisfies the required flexibility for the changing requirements of research. Farrusseng et al.[109] pointed out the main issues involved in data management for the discovery and development in heterogeneous catalysis, that is, for example, automated data acquisition, data storage, and data analysis together with the application of data-mining techniques. They also provide a methodology for facilitating data management for heterogeneous catalysis. The authors also presented a database linked to a powerful algorithm for the iterative discovery and optimization of catalytic samples. A more theoretical approach to data mining has been published by Clerc et al.[110] The authors show how optimization problems can be solved by hybridizing a classical GA with a KD system (for example, a learning process using k nearest neighbors) that extracts information from a database. A schematic flow chart is shown in Figure 8. This approach has been applied to a problem in the field of heterogeneous catalysis in which different possibilities for the hybridization of the GA with the KD according to robustness and optimization speed were compared.

Rajan and co-workers[111–114] applied data-mining methods, such as PCA, and predictive methods, such as partial least squares (PLS) to certain fields of materials science (zeolites, semiconductors, etc.). They connected conventional materials databases with experimental data sets in searches for correlations and patterns. One further possibility to design combinatorial libraries is by integrating data-mining techniques with physically robust multivariate data. In doing so,

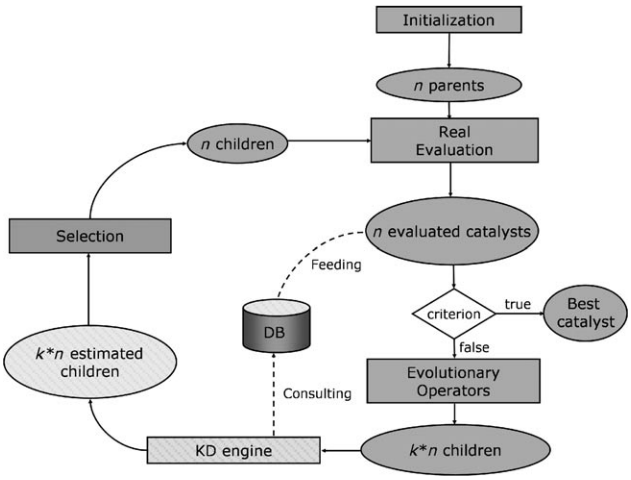

Figure 8. Hybrid GA with a KD System. The hatched blocks are the elements of the KD engine, the remainder are traditional elements of the GA (from Ref. [110]).

large data sets can be generated from relatively small amounts of experimentally and theoretically based information. During this process a strategical selection of appropriate physical parameters is necessary that can be analyzed in a multivariate manner. This "virtual" approach to combinatorial experimentation has been applied by several research groups. For example, Suh and Rajan[115] predicted the band gaps and lattice parameters of nearly 200 stoichiometries of new and yet to be synthesized semiconductors with chalcopyrite structure and tested the robustness of this approach by comparison with predictions of band gaps from theoretical studies on selected quaternary semiconductors covering a range of compositions. They applied the multivariate PLS technique to a training set of selected data from the literature. PLS has distinct advantages over classical multiple regression and principal component regression approaches. By using the PLS coefficients they completed their analysis of property prediction for over 200 compounds based on their initial combinatorial data input for training. In this way they presented an approach to develop combinatorial libraries, which can serve as an effective screening tool to guide combinatorial experimentation. Kubo, Miyamoto et al.[116] applied a combinatorial, computational-chemistry approach mainly based on static first-principles calculations to various catalyst and material systems. By determination of the formation energies of intermediates for a number of metal catalysts, such as Cu, Ru, Rh, Pd, Ag, Re, Os, Pt, and Au—in neutral as well as cationic form—by DFT calculations, they investigated the design of catalysts for the synthesis of methanol. Their calculations confirmed the Cu^+ ion as the active center in industrial $Cu/ZnO/Al_2O_3$ catalysts and predicted Ag^+ and Au^+ to be potential candidates for highly active catalysts for methanol synthesis. In an analogous way, they studied precious-metal catalysts for the deNO_x process by investigating the adsorption properties of small metal clusters for NO. It was demonstrated that the energetically most stable adsorption state of NO is on an Ir cluster, independent of both the structure and number of atoms

within the metal atom cluster.[117] Combinatorial computational chemistry (CCC) has also been used to find materials with novel properties in lithium battery applications. DFT calculations were performed on periodic models of $LiMO_2$ (M = 3d transition metal) with layered rocksalt superstructures to investigate the structural properties of $LiCoO_2$, $LiNiO_2$, and doped $LiNiO_2$. This study revealed that the poor cyclic charge-discharge reversibility of $LiNiO_2$ resulted from the large change in the structure because of the difference in the ionic radii of Ni^{3+} and Ni^{4+}.[118] Since Co^{3+} and Co^{4+} ions give almost the same metal–oxygen distances, the use of Co as a dopant reduces the structural changes of $LiNiO_2$ and improves the cycling stability of the material. This approach was recently extended from static first-principles calculations to high-speed simulations of chemical reaction dynamics based on quantum-chemical molecular dynamics (MD) calculations to realize an even more effective and efficient CCC screening. Improving the conventional performance speed by a factor of 5000 resulted in sufficient computational capacity to perform a high-throughput screening. The applicability and effectiveness of the method was demonstrated by investigating the atomistic mechanism of the methanol synthesis with the Cu/ZnO catalyst system at reaction temperatures and comparing it with the results of regular first-principles MD calculations; the HT screening potential of the method has still to be demonstrated by the authors.[119]

A critical issue remaining in high-throughput technology is the actual databases. Only limited information is available about software or database solutions in industry, academia, and research institutes. The lack of simple and versatile data bases for materials research means that Microsoft Excel sheets are still used for data collection in many laboratories. There have been several reports on the development of databases for combinatorial and high-throughput materials science. One example is the work by Frantzen, Sander et al.,[120] who developed a project-oriented Microsoft Access based database for data storage, visualization, and data mining in the search for new sensor materials. The concept satisfies the essential needs of high data compatibility and versatility together with convenient data import and export. Potyrailo and co-workers[121–123] presented a centralized data-management and storage system for their work on organic polymer and hybrid coatings. One important fact of their approach is the sharing of information from synthesis, testing, and evaluation by the database. Another example of a data-management system developed in a research institute is the StoCat database of Mirodatos and co-workers[109] for the acquisition of laboratory and experimental data for HTE. Commercial data bases are provided by high-throughput companies, such as Symyx Technologies, hte-AG, and Avantium.

A rather simple aspect of knowledge discovery is the mapping of any function against chemical composition, which was often studied in the early high-throughput experiments. This approach can be considered as a form of QCAR. Basic research in materials science and heterogeneous catalysis currently focuses on microstructure, oxidation states, surface polarity, pore size, porosity, or phases, but rarely on chemical composition. Through the search for defined phases responsible for performance, composition has been dominated by stoichiometry. It is not clear, whether there is a correlation between composition and catalytic performance. There is a wealth of catalytic literature based on amorphous systems, especially mixed oxides as well as all the mesoporous materials, whose pore walls are consistently amorphous. The search for defined phases still continues, but few studies are being carried out by the catalytic community in regard to the identification of active sites in amorphous catalysts. The reason is clear—there are few tools to solve such a task. Therefore, amorphous materials are accepted as catalysts, but not understood. However, such amorphous materials, to a first approximation, are free of stoichiometric restrictions and allow the sampling of continuous composition spaces. This is of fundamental importance for our desire to understand catalysis, since the chemical composition of catalysts can now be treated by continuous variables, and the catalytic performance can be mapped against chemical composition.

The first direct mapping of catalytic performance against chemical composition to our knowledge was reported in 1999 by the scientists at Symyx in their search for new catalysts for the oxidative dehydrogenation of ethane.[124] The map of the phase space (Figure 9a), which consists as a test on the reproducibility of two in the compositional range identical triangles, shows that the catalytic activity of these mixed oxides varies smoothly with composition and that there is a distinct maximum in the catalytic performance.

Paul et al. found in a study on the direct oxidation of isobutane with air on mixed oxide catalysts[125] that the formation of methacrolein is highest at a low V content (2%) and with about 10% Mo in Sb oxide (Figure 9b), while the parallel formation of isobutene is favored by the Mo-poor compositions with higher levels of V in the Sb oxide (Figure 9c). The undesired combustion to CO_2 is strongly favored by compositions with low levels of Sb and high levels of V relative to Mo (Figure 9d). This is an ideal example of catalytic performance, since here the selectivity can be tuned directly by the chemical composition of the catalyst.

Such a significant correlation of the catalytic selectivity with chemical composition is by no means general. In a related study with mixed oxides of V, Bi, and Sb, the activity for the formation of methacroleine, isobutene, and CO_2 were found to be located in the same range of composition.[126]

The mapping of the function of a material against composition has not yet become routine, but it has become increasingly common. In a study on a range of compositions prepared by co-deposition of thin films, the dielectric constant and stored charge density (Figure 10), for example, showed a smooth dependence on chemical composition.[127] The mapping of the catalytic activity–composition relationships for the dehydrogenation of ethane with Mo-Nb-V mixed oxides obtained by wafer technology compares very well with literature data obtained by traditional methods.[128]

The mapping of functions against chemical composition is by no means trivial. Materials functions such as catalytic selectivity or piezoelectric performance are critically dependent on the exact preparation conditions. To map a function against composition, therefore requires that all the materials within a composition range are prepared by identical

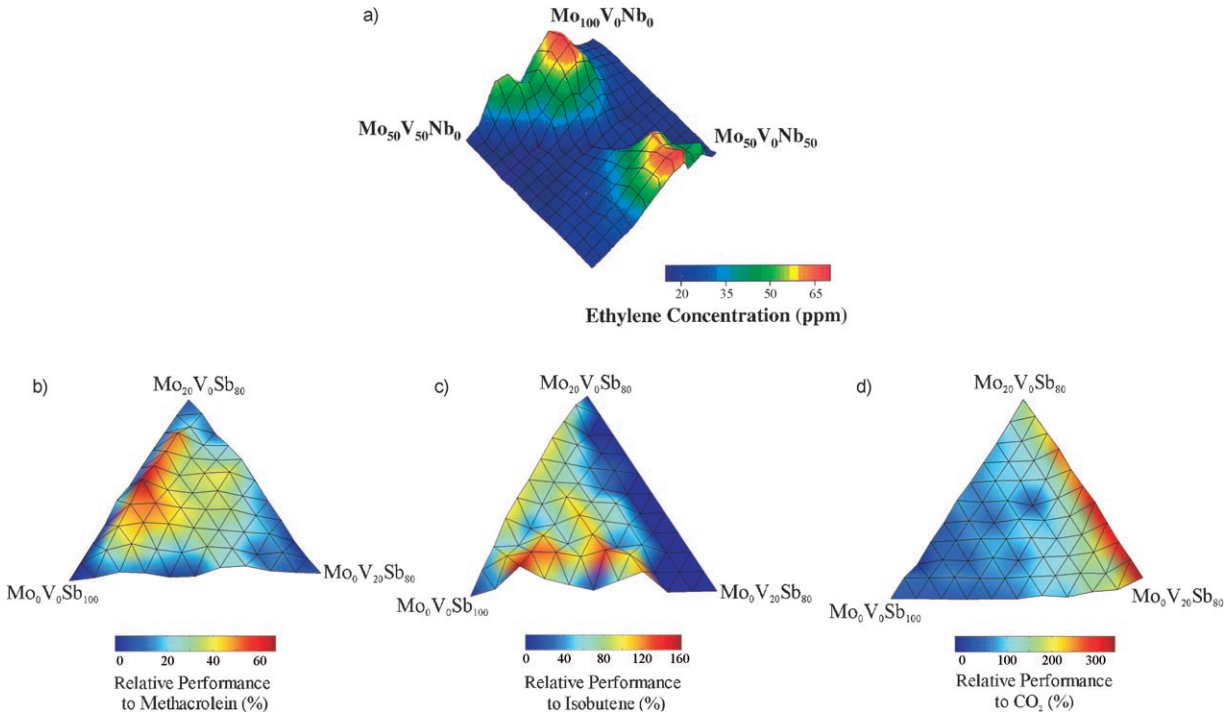

Figure 9. a) Mapping of the catalytic activity for the oxidative dehydrogenation of ethane against composition (from Ref. [124]); b–d): Dependence of the relative activity of the oxidation of isobutane to methacrolein (b), isobutene (c), and CO_2 (d) with air on the chemical composition of the mixed oxide catalysts indicated (from Ref. [125]).

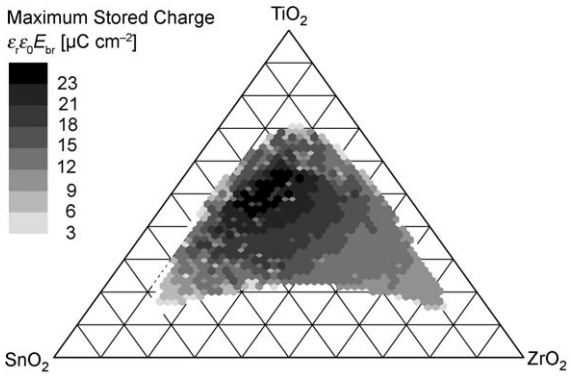

Figure 10. Stored charge densitiy of potential capacitors mapped against chemical composition (from Ref. [127])

procedures or recipes. This is relatively trivial in the cases of thin-film materials prepared by PVD, CVD, and related methods. It is not trivial, however, if the materials are prepared by liquid-phase or solid-phase procedures.

In comparison to conventional preparation and testing of individual samples, the preparation and testing of whole libraries has several advantages. All materials are tested at the same time and under identical conditions. This allows for the first time to reliably compare the performance of all the samples in a library. The use of an internal reference sample allows standardization of the relative performance data. The use of synthesis robots and computer-controlled synthesis and testing strongly increases the reproducibility of the data accumulated. Furthermore, if suitable data bases are used for data storage, and the mining and library preparation are automated, libraries can be reproduced easily. Outliers are easily recognized if their immediate neighbors show significantly different functional activity. If the materials of a composition library are statistically and randomly distributed over the library or array and subsequently ordered according to composition, a continuous smooth activity map is evident for comparable performance across the library.

Data sets obtained experimentally by the mapping of parameter spaces also provide the basis for the direct modeling of such QCARs.[129] Sieg et al. showed with quaternary composition spaces that the proper mathematical modeling of such relationships can be accomplished readily with the help of SVMs, multilevel B-splines, or Kriging (Figure 11).[130]

There have been significant developments in the use of IT tools for HTE. It has also been widely demonstrated that the huge data sets produced by HTE can be handled properly and beneficially by the IT tools already available. Unfortunately, the field has turned into a maze of individual solutions, and many laboratories are hesitant to implement the necessary information technology. Compatible data bases, the most essential prerequisites for a future data sharing and more advanced discovery of knowledge, have not yet entered many laboratories.

3. High-Throughput Syntheses

An ever increasing number of synthesis and screening methods have been developed in the field of HT materials science and catalysis. While HT techniques were originally

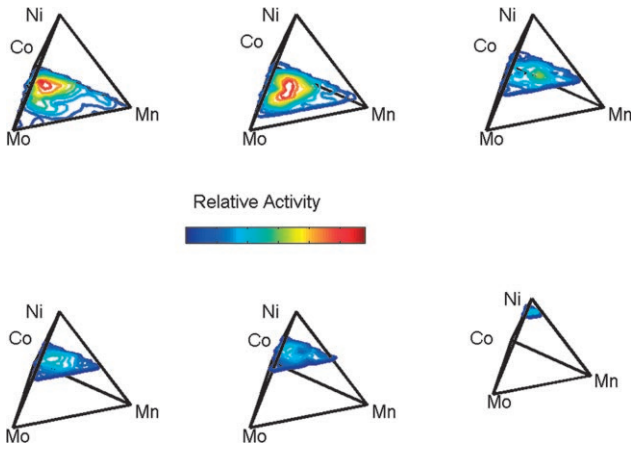

Figure 11. Tetrahedral visualization of the dependence of the relative activity for the oxidation of propene at 350 °C on the composition of quarternary mixed oxide catalysts (from Ref. [130]).

believed to be limited to the most simple materials, library preparation with complex materials, such as block copolymers, zeolites, supported catalysts, detergent or adhesive formulations, magnetic resists, and other complex materials, now dominates the field. Mapping, screening, and optimization experiments have different primary goals and therefore make different requirements in the planning of an experiment.[131] There is a large variety of preparation methods for materials. Many synthesis methods are not suitable for HTE, and alternative, HTE-suitable synthesis procedures need to be developed.

3.1. Thin-Film and Related Techniques

The so-called "diffusion-multiple approach" enables the generation of a large number of phases and compositions for the efficient mapping of phase diagrams, phase properties, and kinetics by the creation of composition gradients and intermetallic phases through the long-term annealing of junctions of three or more phases/alloys.[132] Not only phase diagrams, but also diffusion coefficients, precipitation kinetics, as well as solution-strengthening and precipitation-strengthening effects can be evaluated by this method. The method is based on the fundamental solid-state principle of counterdiffusion of the constitutional elements in diffusion couples made by placing two blocks of dissimilar materials in intimate contact with each other to give a well-defined and planar interface. The length scale of the product layers usually investigated by bulk diffusion couples is on the order of micrometers. According to the rules of Walser and Bené, the first compound nucleated in planar binary reaction couples is the most stable congruently melting compound adjacent to the lowest temperature eutectic on the bulk equilibrium phase diagram.[133] After nucleation, this first phase grows and thus two new diffusion couples (that of the crystallizing binary compound with either of the two constitutional elements) are generated. Consequently, as products of long reaction times, every thermodynamically stable binary compound in the phase diagram will nucleate and grow. Zhao et al.[132,134,135] extended this approach to more than two elements by using an assembly of three or more different metal blocks in intimate interfacial contact and subjecting this to high temperature to allow thermal interdiffusion to create solid-solution compositions and intermetallic compounds. In their investigations, the resulting library of intermetallic compounds was mapped for thermal conductivity with micrometer-scale resolution by time-domain thermoreflectance with a femtosecond pulsed laser (a method developed recently)[136] and also for Young's modulus by nanoindentation techniques. An example of the diffusion multiple mapping of the phase diagrams in the Pd-Pt-Rh-Ru-Cr system is shown in Figure 12.

The idea of synthesizing samples that show continuous phase diagrams (CPDs) or continuous composition spreads (CCSs) is rather widespread within the "thin-film community", where initial work using composition-spread thin films dates back to the mid-1960s. A detailed historical introduction to composition-spread approaches has been given by van Dover and Schneemeyer.[127] Here, we only mention the early work of Hanak, who in 1970 published a prescient declaration of the general potential of these high-throughput synthesis and evaluation techniques for materials investigations (entitled as "multisample concept") and provided details and examples for the particular case of multitarget sputtering.[6] The unique feature of these approaches is a synthetic technique in which material is deposited on a substrate simultaneously from two or more sources that are spatially separated and chemically different. In this way thin films are produced with an inherent composition gradient and intimate mixing of the constituents. As with the diffusion multiple approach mentioned above, complete multinary phase diagrams can be prepared in a single experiment. Hanak[6] already recognized the persistent problem of determining the film compositions efficiently, and identified the need for rapid automated testing to complement the parallel synthesis technique.

Two possibilities in principle exist for preparing continuous composition spreads: cosputtering and coevaporation. The critical challenge with both techniques is the ability to create a set of samples with the same properties when prepared under identical conditions, that is, the reproducibility of the synthesis, in situations where variations between runs could confound systematic trends. Even the smallest composition deviations arising from flux variations between different runs may alter the physical properties of materials significantly, as reported by Hanak.[6] Coevaporation is a much more challenging technique to implement successfully than cosputtering, since the evaporation rates of conventional evaporation sources are sensitive to the conditions of the evaporant source and depend exponentially on the input power, thus making it very difficult to maintain constant deposition rates during a number of experiments. For materials with low evaporation temperatures which can be deposited by effusion cells, as in molecular beam epitaxy (MBE), a careful control and stabilization of the source temperature is necessary. In contrast, for materials with high evaporation temperatures, for example, refractory materials,

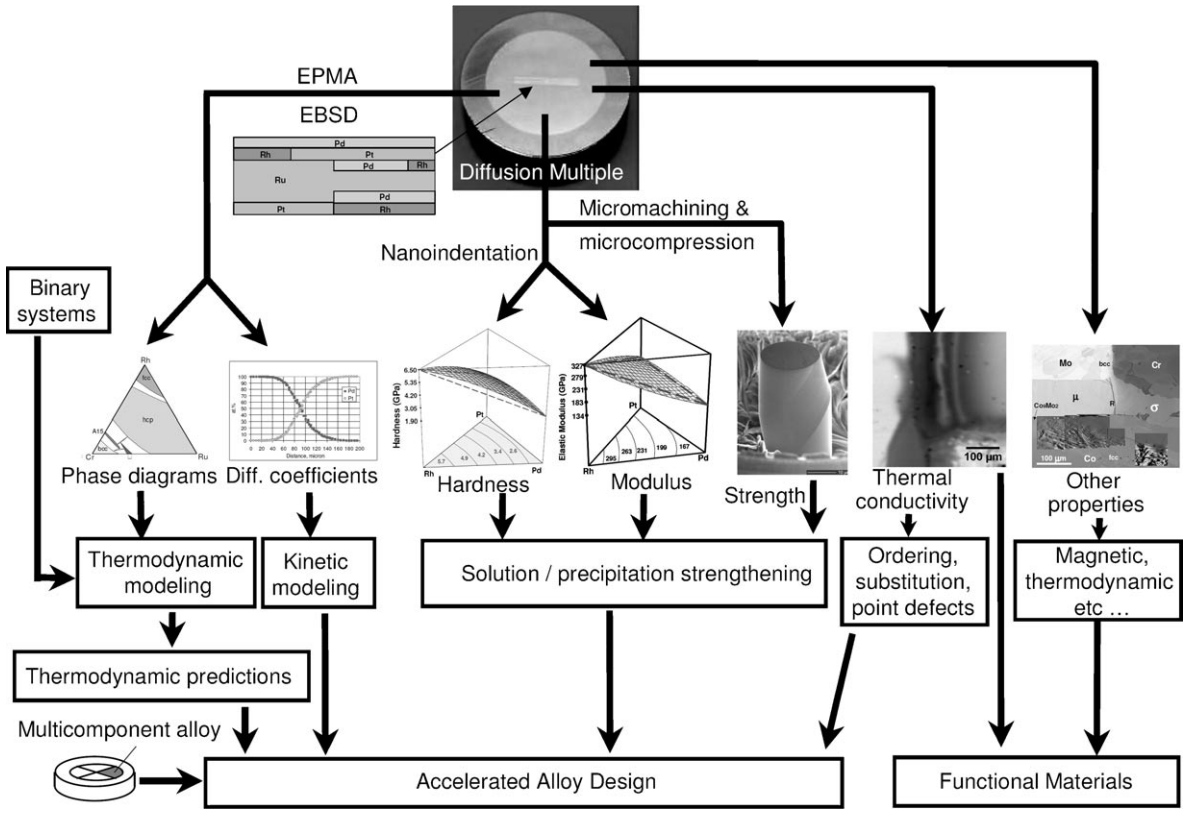

Figure 12. Diffusion multiple approach to high-throughput materials research (from Ref. [134]).

which have to be deposited by electron beam evaporation, control of the evaporation rate can only be achieved by feedback loops, for example, by employing ion gauge rate monitors and feedback algorithms. Only in this case can each constituent be controlled routinely to less than 1 mol %.

The co-deposition technique to obtain continuous compositions spreads has been used for the systematic exploration of known systems and also for the discovery of new materials in unknown phase systems. An example of the first case was reported by van Dover and Schneemeyer who described the systematic trends of crystallization in amorphous Zr-Si-O dielectrics.[127] Transition-metal oxides such as ZrO_2 and HfO_2 show a distinct tendency to crystallize at standard processing temperatures (1000 °C for 20 s to activate dopants). By adding a component with a much higher crystallization temperature, for example, Al_2O_3 or SiO_2, this tendency can be reduced to the detriment of the dielectric constant (ε_R: 9.0 and 3.9, respectively). By using this technique, the authors prepared a sample with a length of 5 cm and a composition of $Zr_{1-x}Si_xO_2$ ($0.1 < x < 0.8$), that is, the deposition gradient was roughly 1 mol % per mm. To simulate the effect of temperature during a standard processing procedure the sample was subjected to high-temperature annealing and X-ray data were collected at 5 mm intervals along the composition spread. Only when $x >$ 0.8 was the film found to remain amorphous with a dielectric constant of $\varepsilon_R \approx 6.9$, a value that is only marginally larger than that of the industrial standard, amorphous silica. As the Zr-Si-O system does not satisfy the requirement of a high ε_R value together with an amorphous state, the authors decided to start a systematic research for new solid-state materials in higher-dimensional phase space, for example, the Zr-Ti-Sn-O system, to find superior dielectric compounds that could be processed below 400 °C, a requirement that largely excludes the extensively investigated crystalline dielectric materials. For this they used a deposition chamber with three magnetron sputtering units, and deposited the CCS materials on Si substrates covered with metal base electrodes at slightly elevated temperatures of 200 °C. Traveling Hg probes or contacts of 0.2 mm radius made by deposition through a shadow mask were used as counterelectrodes for the capacitance mapping measurements. These measurements revealed that the optimum amorphous material has a composition in the vicinity of $Zr_{0.2}Sn_{0.2}Ti_{0.6}O_2$, whereas the commercially used crystalline microwave dielectric material has a composition close to $Zr_{0.45}Sn_{0.1}Ti_{0.45}O_2$ (see also Figure 10). It is extremely unlikely that this optimum amorphous composition would have been found by single-sample studies, which would certainly have concentrated on compositions closer to the important crystalline composition.

Besides the magnetron sputtering technique, pulsed-laser deposition (PLD) is also used for rapid, sequential submonolayer deposition of the constituents of the phase spread, with an intermixing of the constituents on the atomic scale during the growth process. Therefore, as for co-deposition, a pseudobinary or pseudoternary phase diagram can be generated without the requirement of a postannealing stage, thus

making this approach applicable to the non-equilibrium synthesis of metastable phases. Prerequisites for the perfection of CCS approaches are the submonolayer deposition of the constituents and intermixing without postannealing, as mentioned above, as well as an automation (very similar to that used in discrete composition spread approaches) that can continuously move masks. As with all moving-shield applications, CCS deposition also relies critically on the uniformity of the deposition zone across the entire substrate area, thus limiting the compositional spread in most cases to an area of less than 2 cm. Again the synthesis and analysis methods are intimately interwoven, as only sophisticated analysis techniques such as scanning probes (scanning microwave or SQUID microscopy) or simultaneous imaging by concurrent X-ray and optical methods are suitable. By applying a number of different "firing schemes" with synchronization between the laser firing and substrate translation behind a fixed-slit aperture, Christen et al.[137] were able to show that this method can be used to obtain controlled lateral variations in film thickness, film composition, and deposition temperature. In all cases, the resulting samples are sufficiently large for conventional characterization and measurement techniques, including ellipsometry, SQUID magnetometry, and temperature-dependent resistance measurements. The PLD technique has been applied in several studies, for example, to the investigation of electrooptic ($Sr_xBa_{1-x}Nb_2O_6$) and magnetic materials ($Sr_{1-x}Ca_xRuO_3$) as well as epitaxial heterostructures in the form of superlattices with alternating stacks of $SrTiO_3$ and $Sr_xBa_{1-x}ZrO_3$, where the parameter x varies continuously across the sample.[137–139] Similar approaches were also used by other authors, for example, in Ref. [140], for the growth of combinatorial libraries of thin films. Guerin and Hayden[141] reported a novel co-deposition method in which fixed shutters were combined with electron beam and Knudsen PVD sources to produce controlled libraries with a wide composition range. The insertion of fixed shutters to partially shadow the source can be optimized to produce fluxes which vary across the substrate, and this shadowing effect can be used to control the deposition profile. By modeling the finite PVD source, deposition has been simulated for a number of geometries for a single finite source site to establish the conditions required for optimal wedge growth. The modeled PVD profiles were subsequently compared with experiments and revealed good correlation between the simulated and experimental data. The combination of three sources with individual shutters enables co-deposition of metals at room temperature to provide large compositional ranges of alloy materials in a non-equilibrium state, thus allowing amorphous or microcrystalline mixed crystal systems to be obtained. Annealing the sample either during deposition or postdeposition induces the formation of thermodynamic phases and surface segregation. To demonstrate the methodology, ternary CCSs of Pd, Pt, and Au as well as Ge, Sb, and Te, each arranged in a threefold symmetry, were co-deposited, and the relative atomic percentage of the deposited elements determined by energy-dispersive spectroscopy (EDS).

A similar approach, but with different terminology, was applied by Xiang.[142–144] The difference between his "continuous phase diagram" (CPD) approach and the former ones is that in the ternary phase diagrams, three different precursors are deposited sequentially in the form of wedges, one on top of the other in opposite directions. Homogeneous mixing of the precursors is achieved by an appropriate postannealing process, the temperatures of which are highly dependent on the thickness of the individual elemental layer. It has been known since 1983 from experiments by Schwarz and Johnson[145] that in the case of very thin layer thicknesses, so-called ultrathin layers with thicknesses up to several hundred Å, multilayer composites interdiffuse at low temperatures to form a homogeneous, amorphous alloy. Interesting aspects of these solid-state reactions to generate an amorphous sample are the surprising stability of the amorphous alloy with respect to the crystalline, elemental components and the inability of the system to nucleate a compound from the amorphous intermediate. The stability of the amorphous alloy with respect to the elements has been attributed to the large negative heat of mixing of the elements, which originates from the observation that in many of the solid-state reactions investigated, the formation of an amorphous alloy produces the majority of the heat of formation of the final crystalline compound. Although the crystalline product is more stable than the amorphous alloy, it is thought not to form because of kinetic limitations resulting from the existence of a nucleation barrier. The formation of an amorphous intermediate therefore results from a competition between diffusion and nucleation. Xiang used this approach to discuss, as examples, the results of mapping optical, electrical, and magnetic properties of manganese oxides as a function of doping concentrations, ionic radii, etc. Surprisingly, evidence was found for various electronic phase transitions, such as spin–orbit orderings and smectic phase formation, in highly correlated electronic systems such as the CPDs of perovskite manganites of formula $RE_{1-x}AE_xMnO_3$ (with RE = rare earth and AE = alkaline-earth element).[144] The systematic experimental data presented in this study should help to identify new phenomena and elucidate the underlying physics of these complex systems. Continuously mapping the doping dependence of complex materials has distinct advantages compared to extrapolating over discrete doping points. A similar CPD approach has been used by Yoo and Tsui, but with the difference that the perovskite manganites were deposited epitaxially in the form of monolayers or submonolayers of individual precursors at elevated temperatures on an appropriate substrate.[146] The real-time epitaxial processes were monitored and controlled by using in situ MBE techniques, such as scanning reflection high-energy electron diffraction (RHEED). Control over the composition is achieved by the sequence in which different precursors are deposited as well as by the use of well-characterized flux gradients that are strategically positioned to produce the desired continuous composition spread across the substrate. Besides perovskites, magnetic alloys in the Co-Mn-Ge system have also been grown and the magnetic properties of these thin films investigated by the magnetooptic Kerr effect (MOKE) as well as scanning Hall probes.[147]

The multilayer technique has also been applied to isothermal sections of the Cr-Fe-Ni system grown on Al_2O_3-

(0001)-sapphire substrates by sequential deposition of layers of graded thickness followed by annealing to interdiffuse the elements. Maps of phase composition and lattice parameters as a function of composition for several annealing treatments were generated by rastering the film covering the Cr-Fe-Ni ternary system under a focused beam of synchrotron radiation while simultaneously measuring the diffraction pattern with a charge-coupled device (CCD) detector to determine crystallographic phases, texture, and lattice parameters and also measuring the X-ray fluorescence (XRF) with an energy-dispersive detector to determine the elemental composition.[148] A versatile ion beam sputtering technique has been described by Chikyow and co-workers to speed up the development of electronic components. Through deposition of binary and ternary metal films in a composition spread on a dielectric film and characterization by capacitance–voltage measurements, XRF, and XRD mapping, new multicomponent metal gate materials for CMOS transistor development were investigated.[149] Similarly, effects of composition and annealing temperature on the achievable coercive field to identify its maximum at low processing temperatures were studied by Ludwig et al. in the Fe-Pt system on multilayer thin films with a broad composition range.[150] Two types of multilayer systems were deposited, the first type was comprised of alternating opposing wedges, whereas the second type consisted of repeated uniform Fe and Pt layers interspersed periodically with wedge layers. It was found that coercive fields with $\mu_0 H_c > 0.7$ T can be achieved at annealing temperatures of 300 °C for both types of multilayers close to the composition FePt. Multilayers with additional Fe layers showed increased remanence but reduced coercive fields. An additional advantage in the deposition of thin films is the possibility to apply external fields during deposition to influence specific properties of the synthesized materials systematically. For example, films and multilayers with a defined magnetic anisotropy can be achieved by application of magnetic fields. This was shown for nanoscale-fabricated $Fe_{50}Co_{50}/Co_{80}B_{20}$ multilayers ($\mu_0 H_{ext} = 10$ mT) produced by magnetron sputtering, which resulted in a transition in the dependency of the anisotropic field H_K, and thus the ferromagnetic resonance frequency f_R, which was not observed before.[151] Even more promising, in view of unexpected properties of designed new materials, are specific features of multilayer stacks that differ from bulk materials of the same composition. It is known that Ti-BN multilayers generate ultrahard coatings with hardness values up to 6000 HV, which exceeds the hardness of TiB_2 with 3480 HV, at a concentration ratio Ti/B/N of 1:0.5:0.4 after a subsequent thermal treatment to induce a diffusion-activated mixing process between the Ti and BN layers and subsequent phase transformations.[152] The coating with this compositional ratio is assumed to comprise a mixture of two solid solutions of type $Ti(B_x,N_y)$ and $TiB_{1-x}N_y$. Another example is the first observation of a dramatic increase in hydrogen solubility in Nb-Ta superlattices, compared to what would be expected for bulk Ta or Nb, as a result of strain modulation in the multilayer induced by interstitially dissolved atomic hydrogen.[153] Multilayer thin films with compositional gradients can be synthesized to systematically investigate unexplored regions in phase space to discover new materials that reveal phenomena of this type. For example, by using HTE on thermoplastic shape memory alloys (SMA), a new composition region of Ti-rich SMA was identified by the research groups of Takeuchi and Ludwig.[154] From the relationship between the magnetic hysteresis and the transformation stretch tensor, the geometric nonlinear theory of the formation of martensite based solely on crystal symmetry and geometric compatibilities between the corresponding phases which predict a reversibility of structural phase transitions could be verified. Among these new materials, giant magnetorestriction and magnetic SMA are currently being studied for high-speed actuation in adaptive systems. A limitation in the application of these materials in actuators is the requirement large switching fields for actuation. In exchange-coupled geometries such as multilayers, the switching field might be reduced because of the so-called Kneller's exchange spring mechanism,[155] in which the average magnetization is increased and the average anisotropy of the multilayers decreased. This is achieved by sandwiching actuator thin films with high switching fields between high magnetization soft magnets such as Fe or $Fe_{50}Co_{50}$. Prerequisite for this is that the individual layer thickness is kept below the wall thickness of the domain to prevent formation of domain walls parallel to the interfaces, whose presence would otherwise lead to a substantial reduction in the observed magnetostriction and a more complex behavior. The microscopic nature of the Kneller exchange spring mechanism was investigated using TbFe/FeCo and FePd/Fe multilayers deposited by magnetron sputtering on Si(001) substrates.[156] In this approach the composition of the FePd films was varied either by sputtering a $Fe_{70}Pd_{30}$ target under varying powers and pressures, or by cosputtering $Fe_{50}Pd_{50}$ or $Fe_{70}Pd_{30}$ targets with a pure Fe target.

A disadvantage of the CCS approaches is the need for analytical methods with high lateral resolution to avoid information averaged over the spatial region analyzed. For example, only microfocused beams of synchrotron radiation scanning the surface of the composition spread are appropriate when using X-ray diffraction for characterization. When these analytical tools are not available, combinatorial masked deposition (CMD) has to be applied for the production of thin films with individual spots of homogeneous composition. Masking can be obtained either by physical shadow masks[157] or photolithographic lift-off systems.[151] In this context the study by Weinberg and co-workers has attracted a great deal of attention, in which they describe an automated combinatorial method for synthesizing and characterizing thin-film libraries of up to 25000 different materials on a substrate with a diameter of three inches as candidates for new phosphors.[10] These libraries were deposited as thin films by electron-beam evaporation from multiple graphite crucible target pockets using a stainless-steel primary mask consisting of 230 μm square elements spaced 420 μm apart. This enabled the authors to identify a new red phosphor $Y_{0.845}Al_{0.070}La_{0.060}Eu_{0.025}VO_4$ with superior quantum efficiency. The use of this combinatorial concept in conjunction with laser MBE is widespread, and is named combinatorial laser MBE (CLMBE). The research group of Koinuma has developed a CLMBE system which features a multitarget

holder and a disk plate consisting of eight distinctly patterned masking plates.[158] This approach, documented in a large number of manuscripts, was used, for example, for the synthesis of high-quality *c*-axis-oriented Mg-doped ZnO thin films on sapphire (0001) substrates,[158] 3d transition metal ion doped epitaxial ZnO films,[159,160] libraries of thin $(Ca_{1-x}Ba_x)_3Co_4O_9$ films on TiO_2 rutile (001) substrates,[160] and $SrTiO_3/BaTiO_3$ superlattices with equimolar ratios and different periodicities.[161] Epitaxial composition spreads of Sr-V-Cr-Ti oxides on two different single-crystal substrates, $LaAlO_3$ and Nb-doped $SrTiO_3$, have been evaluated for the photoreduction of Ag^+ to Ag. Photodeposition of Ag was enhanced in the region of $SrV_{0.05}Ti_{0.95}O_3$ only on the Nb-doped $SrTiO_3$.[162] However, the CMD method can only be effective when three conditions are satisfied: the mask-source distance has to be much larger than the mean free path of the deposition species, the mask–substrate distance much lower than the mean free path of the deposition species, and last but not least the sticking probability near 1. Under these conditions, the flying direction of the deposition species is randomized by sufficient gas-phase collisions in the space between the source and the mask and, therefore, the species passes through the hole at randomized angles. Deposition flux is another important factor that determines the structures of the vapor-deposited materials. Noda et al. investigated the effect of the deposition flux on the island structure, and developed a simple method to control the deposition flux and its spatial distribution.[163] Photolithographic techniques in combination with the production of thin films by magnetron sputtering were used by Whitacre et al., who developed a methodology for batch-fabricating hundreds of submillimeter thin-film solid-state batteries from $LiMn_2O_4$ and $LiNiO_2$ sputter sources.[164] Their process flow for the microfabrication of a Li metal anode is depicted in Figure 13.

Many other different evaporation techniques have been applied for the generation of thin-film libraries. For example, hot-wire chemical vapor deposition (HWCVD) has been used in a combinatorial approach to grow device-quality amorphous and microcrystalline thin Si films by decomposing SiH_4 at a tungsten wire at 2000 °C.[165,166] In this context, micro-

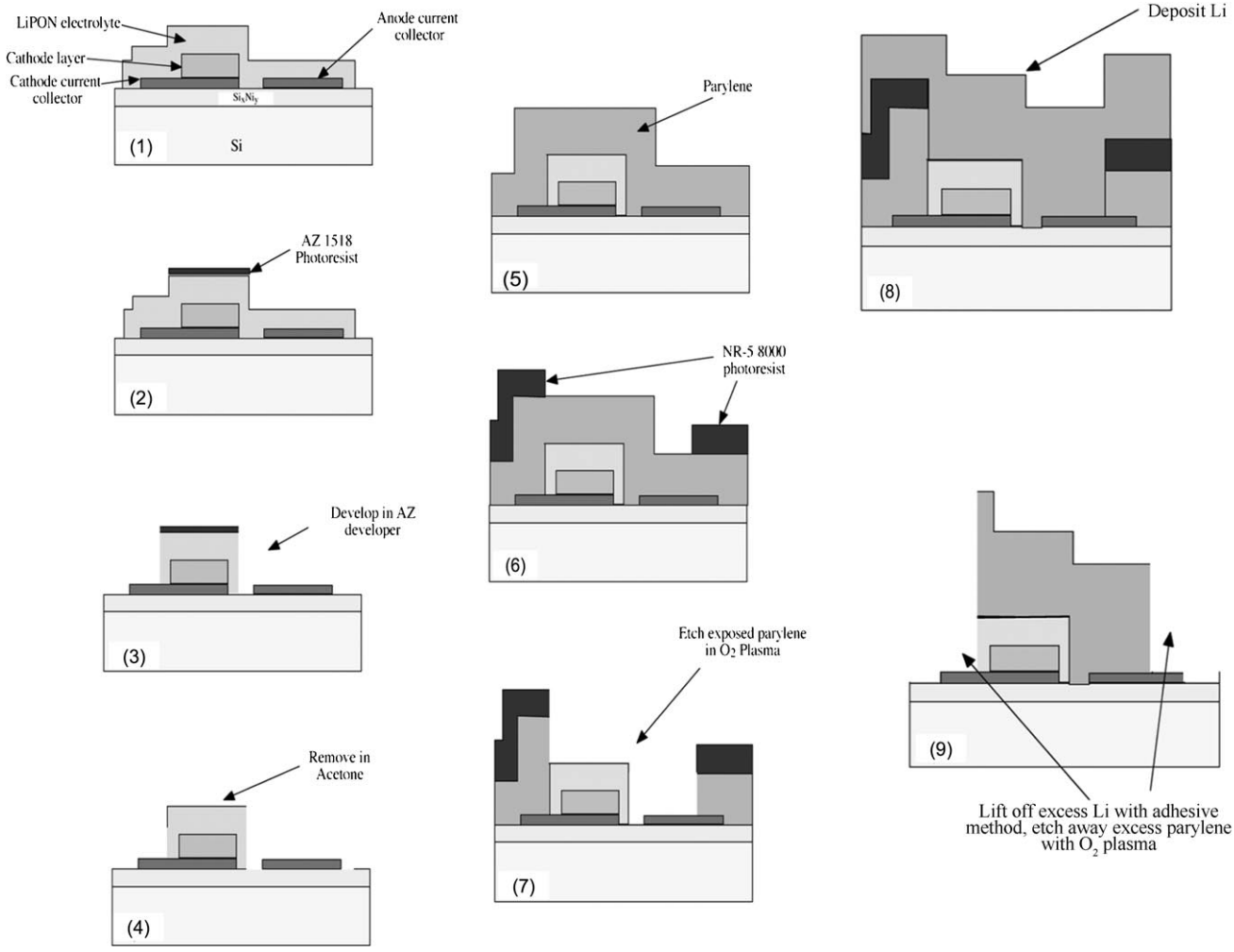

Figure 13. Process flow for the microfabrication of Li metal anodes (from Ref. [164]) which shows the processing steps involved in creating a microdimensional Li anode on an existing thin-film microbattery structure. These include masking with photoresists, exposure to UV light, removing excess photoresist, deposition of a lithium film, and removal of excess lithium (1–9). The last step is carried out by covering the entire area with adhesive kapton and slowly peeling it away. The processing is done in a dry room environment with less than 1% humidity.

electromechanical systems (MEMS) are powerful tools for the fabrication and processing of materials libraries. MEMS can be used for the parallel processing of materials, either as passive devices such as shadow-mask structures or as active devices such as micro-hotplates. Ludwig, Takeuchi et al. described the production of discrete arrays of micro-hotplates and the concepts for micromachined gradient heaters.[167] These are well suited as microdeposition substrates for materials research using CVD. To illustrate this approach, Taylor and Semancik deposited TiO_2 from Ti^{IV} nitrate and isopropoxide as precursors using micro-hotplates for developing metal oxide thin film gas sensors.[168]

Deposition of thin films by electrochemical methods has also been used for HTS and the screening of materials. Besides not needing an ultrahigh vacuum (UHV), electrochemical methods have the advantage that the synthesis can be directed in a way that the resulting thin films have a sufficient surface roughness to catalyze chemical reactions. With electrochemical methods, there are many synthesis variables under direct control, such as voltage, current density, and electrolyte. These can be changed readily using automated programmable systems, thereby resulting in a diverse range of structures and compositions. Baeck, McFarland, and co-workers developed an automated system for the electrochemical synthesis and HT screening of catalytic materials by using a well-plate-based assembly with up to 63 samples.[169,170] The library plate is sealed in this system beneath a perforated polypropylene block with an array of independent O rings underneath. Electrodeposition is achieved either serially using an *x*-*y*-*z* translatable counter and reference wire electrodes or in a parallel mode using an array of counterelectrodes multiplexed to a potentiostat. The authors characterized their system in a way that the parallel system had a higher throughput; however, the rapid serial method offers better control for each deposition.[171] This system was used to synthesize 2D arrays of gold nanoparticles on a thermally oxidized titanium dioxide substrate for the photoelectrochemical oxidation of water and electrooxidation of CO,[171] ZnO samples with varying concentration of the structure-directing agent (SDA) poly(ethyleneoxide)-*block*-poly(propylene oxide)-*block*-poly(ethylene oxide) EO_{20}-$PO_{70}EO_{20}$ ranging from 0–15 weight % for photocatalysis,[169] and WO_3-MoO_3 mixed-metal oxides on Ti foil with n-type behavior for photocatalytic activity measurements.[172] The activity screening was performed in the same device automatically by using a scanning photoelectrochemical cell that traverses the library, thereby illuminating each sample with a modulated light source.

Besides the electrodeposition of samples with discrete structure and composition, there is also a counterpart for continuous compositions spreads in electrochemistry: by using homemade, modified Hull cells with nonparallel electrodes that resulted in a current density gradient, Beattie and Dahn[173] performed the deposition of a 2D composition spread library of Sn-Zn alloys. A third element, Cu, was subsequently introduced in the composition spread library by dripped immersion plating (DIP), that is, by continuously increasing the amount of Cu sulfate solution in a beaker, in which the library was placed vertically, and with the composition gradient running parallel to the solution surface. As a result of the continuous dripping (by a Tsunami Blaster X water gun as a peristaltic pump!) of the Cu solution, the contact time of the library with the solution during electrodeposition and thus the vertical Cu content varies. The choice of the Sn-Zn system was not arbitrary, but it is well-known that Sn as well as Zn undergo ion exchange with aqueous Cu ions, as indicated by their relative standard hydrogen reference electrode (SHE) reduction potentials. Alloy systems such as Cu-Sn-Zn have been proposed as a replacement for graphitic cathodes in commercial lithium-ion batteries as a consequence of their high theoretical capacity and relatively good cyclability. Several other methods have been reported for the generation of composition gradients, including the novel gradient fabrication technique based on solution diffusion, followed by electrodeposition for the construction of highly dense libraries of samples of electrooxidation catalysts on indium tin oxide (ITO) substrates.[174] In this method, a surface gradient is created by controlled diffusion of precursor materials into a swollen polymer gel. In special cases a binary composition gradient is produced by diffusion of a solution containing the salt of a second metal into a gel containing a uniform concentration of a salt of the first metal in its matrix under controlled humidity conditions to avoid shrinkage of the gel. After diffusion, the metal ions are electrochemically reduced onto the surface of a conductive substrate. Removal of the gel leaves a composition gradient of the binary catalyst system on the substrate. A binary Pt_xRu_y composition gradient was constructed as a model system and screened for catalytic electrooxidation activity using a scanning electrochemical microscope (SECM). Instead of implantation into a gel, implantation into solid materials by nonelectrochemical methods has also been used to prepare combinatorial libraries. Stritzker and co-workers have built up an advanced apparatus for the combinatorial synthesis of densely packed, thin buried layers of semiconductor nanocrystals, such as CdSe, in thermally grown SiO_2 on Si.[175–177] In this approach, the combinatorial materials library was generated by sequential implantation of Cd^+ and Se^+ ions and the gradients generated by spatially moving selective shields inserted into the particle beam. In practice, this is achieved using a Freeman ion source loaded with CdSe material and selection of the isotope to be implanted by an electromagnetic isotope separator. A lateral pattern of well-defined distinct combinations of dose and isotope ratios of different sequentially implanted ion species is obtained by moving a precise and automated stainless-steel shield stepwise. Analogously, mixed cadmium sulfide selenides were ion-implanted and characterized by Rutherford backscattering analysis (RBSA), XRD, and Raman spectroscopy, which indicated the formation of the solid solutions CdS_xSe_{1-x} of the implanted ions in silica.[178] In a similar way, modifications of the structure and magnetic properties of magnetron-sputtered $Fe_{50}Co_{50}$ films induced by high dose Sm or Xe implantation have been achieved by combinatorial ion implantation.[179]

Solid thin films are usually not suitable for the study of catalytic properties because of mass-transport problems. HTE for catalytic applications therefore often relies on the synthesis of bulk materials by solution-based methods.

3.2. Solution-Based Methods

The application of combinatorial methods to materials synthesis in the field of solution chemistry generates a number of new challenges to be faced, such as issues of scalability and reproducibility, poorly defined and understood active sites, poorly understood links between activity and chemical process conditions, as well as the formation of metastable structures. Many new parameters, for example, particle morphology, may play just as important a role as composition in the performance of a catalyst. Compared to the deposition of thin films, especially electrodeposition and chemical vapor deposition methods, solution methods are very complex and are labor-intensive processes which are sensitive to handling procedures, such as, for example, experimental conditions, high temperatures or pressures, pH value, and nature of solvents, preparative procedures, for example, milling, mixing, and mixing order, as well as work-up procedures, for example, washing, filtering, and drying. The influence of all these parameters on the catalytic performance of a material necessitates the extension of high-throughput concepts into the even more demanding process of catalyst optimization. It is not only important to recognize all the parameters that affect catalytic performance, but also the complete documentation of these in a database in a reusable and mineable form is crucial, especially if quantitative structure–activity relationships (QSARs) need to be deduced.

Impregnation of porous support materials with active components, such as noble metals, is a common technology for catalyst preparation. It lends itself perfectly for HT applications and has thus been applied in many studies.[180–184] The automation of conventional precipitation reactions is less trivial. The parallel preparation of catalysts for libraries by precipitation remains a challenging problem because of the high dilution, necessity of temperature, and the need for pH control during precipitation, followed by filtration, washing, and calcination.[2] Hoffmann et al. used automated co-precipitation for the preparation of Au catalysts.[185] A typical example of the complexity of solution-based reactions and challenges which have to be faced is hydrothermal synthesis. A number of parallel hydrothermal crystallization configurations have been reported in the literature, one of the first being that of Akporiaye et al.,[186,187] Bein and co-workers,[188] and Klein et al.[189,190] The main focus of this method has been the parallel synthesis of meso- and microporous zeolites and aluminophosphates (AlPOs) by a multiclave concept, a term derived from the condensation of "multiple autoclaves". Historically, parallel experimentation has been the norm in the exploration of zeolite crystallization fields, but increasing the number of parallel reactors, achievement of sufficient control over physical parameters, and the development of analytical approaches that need much smaller product amounts still need to be addressed. Song et al. recently presented a strategy toward the rational synthesis of microporous materials by the combination of a computational and a combinatorial approach.[191] The templating abilities of various organic amines in the formation of the microporous aluminophosphate $AlPO_4$-21 have been evaluated by considering the nonbonding host–guest interaction energies simulated by molecular dynamics (MD) calculations using the Cerius package of MSI. On the basis of the predicted suitable templates, the use of a rational selection of amines such as ethanolamine, triethylamine, and *N*,*N*,*N*′,*N*′-tetramethylethylenediamine in the reaction system $Al(i\mathrm{OPr})_3/x\,H_3PO_4/y$ amine/$255\,H_2O$ resulted in the successful synthesis of $AlPO_4$-21. Characterization of the products was achieved by inductively coupled plasma (ICP) analysis, thermogravimetry (TG), as well as powder and single-crystal X-ray diffraction (XRD). The framework of $AlPO_4$-21 belongs to zeotype AWO, with eight-membered ring-shaped channels along the [001] direction.

Special attention has also been paid to the rational DoE in the synthesis of microporous materials. For this purpose, Newsam and co-workers developed a Monte Carlo approach based on the method of automated assembly of secondary building units (AASBU).[192] This method generates virtual libraries of viable inorganic structures by sampling the ways in which predefined secondary building units (SBUs) can be three-dimensionally interlinked. Knight and Lewis reported on a template-screening approach in which combinatorial methods were applied to investigate the structure-directing properties of the ethyltrimethylammonium (ETMA) template, both by itself and in combination with other structure-directing agents (SDAs) in the range Si/Al = 2–48.[193] The main topic addressed in this investigation was the decoupling of the role of the different components that strongly influence zeolite crystallization, that is, the silica, alumina, and hydroxide sources, from the sources of additional SDAs. This was accomplished by using ETMA aluminosilicate solutions, ETMAOH as the sole hydroxide source, and additional SDAs as salts. These experiments yielded the new zeolite species UZM-4, UZM-8, UZM-15, and UZM-17, and thus demonstrated the broad potential of a single organic template to synthesize materials with both small and large pores. The application of porous aluminosilicates has also been of considerable interest, for example, as matrices for the encapsulation of conducting organic polymers to stabilize these highly degradable and labile species. Atienzar et al. reported the first synthesis of oligo(*p*-phenylenevinylene)s (OPVs) encapsulated within zeolites by using a high-throughput system for the preparation and screening.[194] A 96-well sample library based on a $(2\times3^2\times5)$ factorial design was obtained after consideration of the following preparation factors (levels) in the synthesis of OPV@zeolite: different monomer loadings (2), synthesis temperatures (3), zeolite structures (3), as well as nature of the exchanged alkali-metal ions (5). High-throughput characterization of the library was achieved by operando photoluminescence spectroscopy, which revealed that the synthesis temperature and the nature of the alkali-metal ion present in the zeolite were the most important experimental parameters to be controlled in the synthesis.

A combinatorial hydrothermal synthesis methodology with variation and optimization of the pH value has also been applied for the characterization of 48 perovskite samples in the $(Pb,Ba,Sr)ZrO_3$ compositional field.[195] In a second series of 96 samples, the $(Pb,Ba)(Ti,Zr)O_3$ compositional field was also investigated combinatorially to control the crystallinity

and particle size. Both series revealed that combinatorial hydrothermal synthesis and characterization techniques are applicable to the perovskite family.

During the course of the continuous miniaturization of HT devices in the discovery and screening of new materials, a reduction of both the droplet size of the applied precursor solution during the synthesis and the complete reactor assembly to increase the sample density in combinatorial libraries has been explored. In regard to the amount of liquid applied, there is a continuous transition from micropipetting methods to ink-jet printing techniques associated with a continuous reduction in the droplet size. Whereas micropipetting is normally used to transfer liquids from stock solutions to discrete wells, ink-jet printing offers the possibility of reducing the dosing volumes to several magnitudes smaller than with micropipetting and thus offers the possibility of generating pseudocontinuous sample libraries. Ink-jet printing (Figure 14) has been successfully used in the last

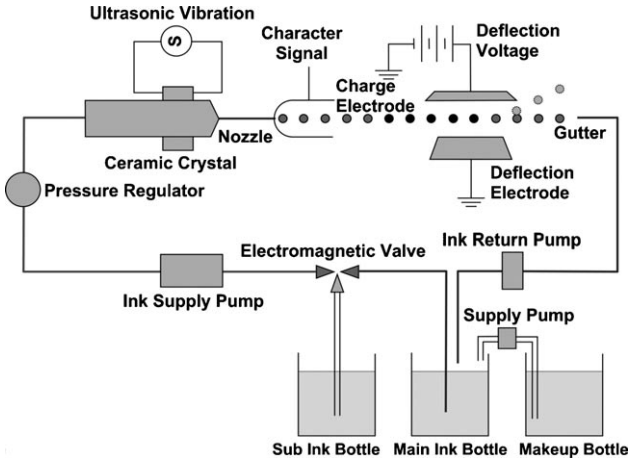

Figure 14. Principle of ink-jet printing.

decade for a number of new applications, such as the fabrication of organic light-emitting diodes (OLED), transistors and integrated circuits, ceramics, and a large number of polymer applications, which are not cited here in detail. For an overview, we recommend a special issue of the journal "Macromolecular Rapid Communications"[196] as well as a detailed review by Wallace and Grove.[197]

The inks to be deposited on substrate surfaces by ink-jet techniques have to meet very strict physicochemical properties, such as viscosity, surface tension, adhesion to a substrate etc., that is, parameters which are summarized in the ink formulation. The materials to be printed are either soluble or insoluble, so the ink is either a solution or a dispersion (solid in liquid) or even a microemulsion (liquid in liquid). A reduction of the particle or micelle size to 50 nm or less is expected to improve the image quality, resolution, and reliability of the printhead. Ink-jet techniques have been applied in combinatorial chemistry for the deposition of metallic nanoparticles and microemulsions.[198] Kamyshny et al. used aqueous dispersions of Ag nanoparticles stabilized by polyelectrolytes and surfactants for printing conducting patterns onto various substrates using standard ink cartridges. Wang et al. generated multiple compositions by combinatorial ink-jet printing of ceramics in the pseudoternary system $BaTiO_3$-Al_2O_3-ZrO_2.[199] Two different approaches were used: discharging variable compositions by mixing liquids within the printer with the help of pressurized reservoirs, electromagnetic valves, a micropump, and an associated mixing chamber, tubing, and nozzle, or well-plate reformatting by aspiration–dispersion action for the application of individual ceramic suspensions. Both approaches involve the mixing of ceramic suspensions such that diffusion distances during sintering are comparable to the particle or agglomerate dimensions, thereby achieving high compositional accuracy in both cases. The main difference between the two methods is that the mixing in front of the nozzle in the well-plate techniques enables mixtures with a large number of components to be made, which is limited only by the number of wells and nozzle dimensions, whereas in direct mixing, the number of components is limited by the number of printer lines available. Well-plate reformatting of ceramic inks was also the principle of operation of the London University Search Instrument (LUSI), which was commissioned to create and test combinatorial libraries of ceramic compositions.[200]

3.2.1. *Microfluidics*

Another miniaturization approach, which has the advantage of being able to handle nanoliters of fluid and to provide fast response times, is microfluidics. This is a rapidly developing technology that involves the handling of fluids in devices containing channels in the micrometer-size regime. Microfluidic technology is used in many applications in the life sciences and pharmaceutical industry as a quick and efficient method for performing biological assays on the nanoliter scale and for rapid chemical analysis of aqueous solutions. Beers and co-workers used rapid prototyping photolithography of a thiolene-based resin to fabricate microfluidic devices stable to aliphatic and aromatic organic solvents.[201] For this purpose, the thiolene-based adhesive NOA 81, which can be hardened with UV light, was spread between two glass slides and two identical photomasks aligned and placed on the top of the thiolene device. After precuring the sample under a UV lamp, the uncured resin was flushed from the channels with air and solvents. Droplets of hexane and toluene of uniform size were generated inside a water matrix containing SDS surfactant within the generated channels. The possibility of performing reactions within the organic phase were demonstrated by the bromination of alkenes within the droplets. Alternatively, microcapillaries with diameters as small as 0.5 μm have been drilled into PDMS microfluidic devices by using femtosecond laser pulses as a micromachining technique.[202] Laser-drilled microcapillaries were also used by the same research group to trap a polystyrene bead by suction and hold it against a shear flow. Symyx Technologies used a massively parallel microfluidic reactor system, which consisted of a microfluidic flow distribution system, a 256-element catalyst array, and colorimetric detection methodology to allow parallel reaction and parallel detection, for the high-throughput screening of catalysts for the gas-phase oxidation of ethane to acetic

acid,[203] the oxidative dehydrogenation of ethane to ethylene, the selective ammoxidation of propane to acrylonitrile,[204] as well as other heterogeneous catalytic liquid and gas-phase oxidation reactions.[205]

3.2.2. Approaches To Increase the Sampling Space (vHT)

As a consequence of increasing parallelization and the integration of reactor and analysis systems, the requirements for new synthesis methodologies include ever smaller amounts of samples, for example, different multicomponent mixed oxides in the mg or even μg range have to be prepared reproducibly and by a fully automated process. The need for automation brings experts of different skills together to fuse the challenges of robotics and automation with those of inorganic or organic synthesis. So-called split&pool (S&P) methods have been developed to achieve very high throughput (vHT) of highly diverse materials libraries in the range of 10^3–10^8 samples by a simple procedure to realize combinatorial chemistry in its intrinsic meaning, that is, the combinatorial permutation of element combinations or synthesis parameters. Based on the pioneering work by Houghton[206] as well as by Geysen et al.[207] on multiple peptide synthesis, Furka et al. presented a novel concept at a conference[208] in which some characteristics of the former methods were merged. Common synonyms for the S&P synthesis are "mix&split", "split&combine", "one bead—one compound" and "selectide process".[209] The process is depicted schematically in Figure 15: a batch of porous spherical beads, originally made from resin in peptide chemistry, but in inorganic S&P synthesis made from an inert support material such as Al_2O_3, SiO_2, etc., prepared with a homogeneous size and loading capacity is divided ("split") into a number of aliquots of equal size. A different monomer (A, B, C) is coupled to each portion, or a different metal precursor solution (A, B, C) is impregnated in each portion.

After completion of the coupling, excess reagent is removed by washing, the aliquots are combined again and mixed ("pool"). As shown in Figure 15, a library with three precursors A, B, C consists after three cycles of $3^3 = 27$ members, after four cycles of $3^4 = 81$ members, and so on; in general 3^S library elements will result after S split cycles. If the number of precursors is denoted as M, the total number of library elements N is calculated as $N = M^S$. The S&P technique can be used to evaluate a large number of compounds with very little effort. The practical limit of the library size depends strongly on the number of beads which can be handled and screened with a corresponding assay. The problem with the S&P technique is that, due to the mixing steps, the composition of each bead is unknown and has to be determined in a separate step, for example, by μ-XRF techniques. Another solution to this problem is to arrange the beads in a two-dimensional array so that each library member is spatially addressable by its position in the array or to tag the beads by labels for identification. Klein et al.[209] developed a powerful enhancement of this synthesis tool in the form of a "single-bead reactor" (SBR), which allows efficient testing of the libraries created by the split&pool methodology.

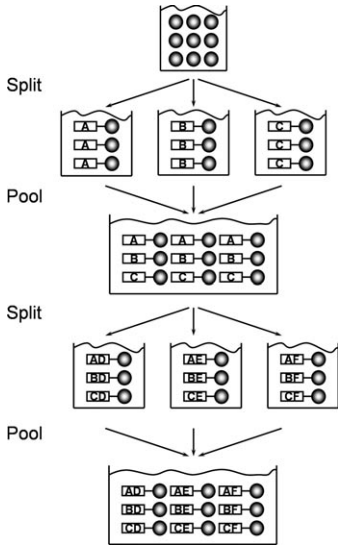

Figure 15. Schematic representation of the split&pool principle (from Ref. [209]).

Nanosphere lithography is an inexpensive alternative technique if not the composition but the size of the individual library members has to be varied. This technique offers the possibility of inherent parallelization, high throughput, and the relatively unlimited preparation of accessible materials for well-ordered 2D periodic arrays of nanoparticles.[210,211] In this technique, the self-assembly of spherical beads is used as the shadow mask for the physical vapor deposition (PVD) of materials, such as Ag nanoparticles. The nanosphere lithography masks were created by spin-coating suspensions of polystyrene nanospheres of different sizes (165, 264, 401, 542 nm) in water together with a surfactant to assist the solutions in wetting onto the substrate of interest. Thin films of Ag were deposited whilst varying the in-plane diameter of the nanoparticles from 26 to 126 nm, and similarly the out-of-plane height by variation of the mass thickness of the Ag overlayer. The experimental determination of these parameters after deposition was carried out by AFM measurements. These studies revealed that the dimensions of the nanoparticles accurately correspond after correction for convolution of the AFM tip to predictions based on the mask geometry of the nanospheres. Furthermore, the authors established that nanosphere lithography can fabricate nanoparticles that contain only approximately 4×10^4 atoms (in-plane diameter: 21 nm, out-of-plane diameter: 4 ± 1 nm), that is, in the size-range of surface-confined clusters. Additional compositional variation may be achieved within this approach by sputtering gradients, multilayers, or codeposition of different elements, that is, topics, which have already been addressed in more detail above.

The two extreme cases in the broad field of sample preparation for HT applications are: the combining of all the samples in one pool and the synthesizing of a large number of individual samples with different properties in a parallel manner. Between these two extremes there is a continuous transition, which opens up the possibility of various intermediate approaches, such as, for example, the single-sample concept (SSC) proposed by Hulliger and Awan.[212,213] In this

approach, a single sample of approximately 1 cm^3 is prepared by treating N randomly mixed starting materials by solid-state reactions. Whereas in traditional ceramic synthesis only a small number of components (usually 2–4) are reacted by thermal treatment, which results in one stable product at nearly any place within the sample—at least after a long reaction time—a large number of starting materials N each randomly constituted in a neighborhood of grains, which leads to a so-called local configuration C of different elements and corresponding masses, may lead in principle to a new multicomponent compound. However, experience shows that the thermodynamic stability of a multicomponent compound decreases with the number of constituents, and that important material properties may be obtained even by a limited number q of constitutional elements ($q \approx 6$) in solid-state compounds. Consequently, as the available number of starting grains within the 1 cm^3 sample exceeds realistic estimations for the number of phases present in the phase diagrams, the SSC concept can provide access to all existing compounds in a high-dimensional phase space in one single preparation step. The experimental implementation of the concept was demonstrated by the authors by the synthesis of a library of ferri- and ferromagnetic oxides. After milling the reactant mixture to reduce the size of the grains, surfactants were added to obtain a suspension, by passing the emulsion through a separation column, and then a magnetic-field gradient was used to extract the magnetic particles. Analyses of single grains by scanning electron microscopy (SEM) revealed a library consisting of individual grains of magnetic Fe oxides.[212] As calculations show, the number of reactions performed in parallel in a single sample can be orders of magnitude higher than achieved by present 2D approaches. Furthermore, this concept is not restricted to inorganic chemistry, but also has a counterpart in organic or molecular chemistry in the form of branched architectures of functionalized monomers that lead to the formation of unique, asymmetric dendritic species with multiple functionalities.[214]

4. High-Throughput Analysis and Characterization

Every high-throughput synthesis technique automatically generates the need for a corresponding and appropriate high-throughput characterization method for testing the generated sample libraries for desired properties (functions). As already stated in Section 3.1, not only may the throughput become the bottleneck, but also the spatial resolution of the analytical method may be limiting if very high sample "densities" are produced by continuous composition spread techniques.

In principle the HTS tools to be applied for the evaluation of libraries of combinatorially developed materials can be divided according to the different sampling methods into in situ (or even operando) and post-reaction methods, or alternatively according to the measurement mode used in serial and parallel techniques, as classified by Potyrailo.[215,216] The development process is depicted schematically in Figure 16. The first step in this development process is the identification of the analytical problem, by using well-established criteria for the analysis capabilities to select the adequate method. The factors to be specified are, for example, the analysis turnaround, sample size, quantification precision and accuracy, need for the availability of samples for further characterization, etc. If the analytical method has not been used previously in HTS for this particular analytical problem, an appropriate conventional technique using larger sample sizes or other required parameters should be chosen as a reference technique for validation of the new method.

Among the truly parallel methods for library screening developed so far, a number of methods immediately attracted general interest, such as resonance-enhanced multiphoton ionization (REMPI),[217] emission-corrected IR thermography (ecIRT),[218] as well as laser-induced fluorescence imaging (LIFI).[219] Each technique has its field of application; for example, IR imaging is a powerful tool for the detection of heats of reactions, such as catalytic activities or heats of absorptions, in combinatorial libraries. The use of ecIRT enables temperature differences down to 0.02 K to be detected and the heat evolution identified from catalyzed gas-phase reactions with small catalyst amounts (< 20 mg). Reactions have been observed at temperatures up to 650 °C, thereby indicating that the method can be applied over a wide temperature range.[220,221] Quantification of ecIRT data through integration of the heat spots on an image has also been described.[221] However, ecIRT cannot differentiate between desired and undesired reactions. Rapid, sequential HT mass spectrometry was applied early on by several research groups for the screening of catalyst activities and selectivities.[222–225] The use of gas chromatography in HTE

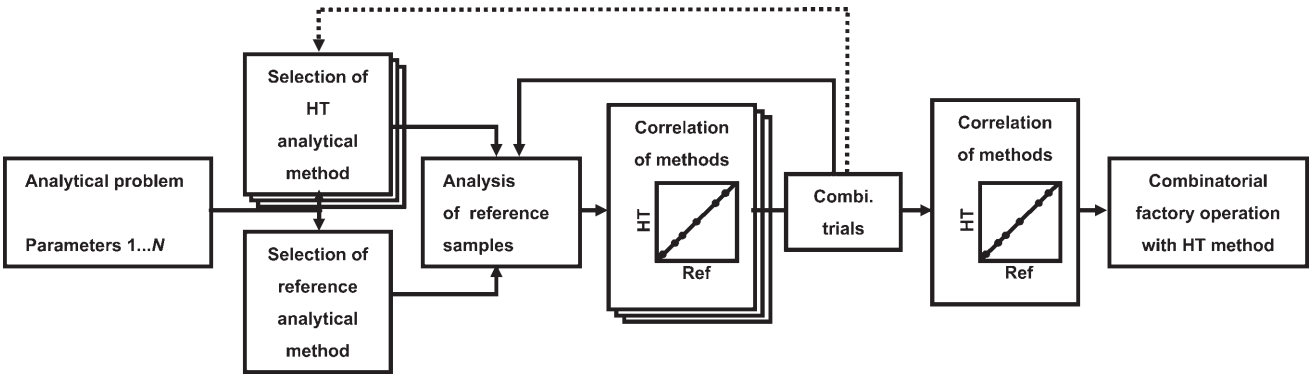

Figure 16. Strategies for the development of new high-throughput screening methods (from Ref. [216]).

was described early on in catalysis research.[124,226] The use of HT-GC and HT-MS on larger libraries was described in detail by Weiss et al.[227] Here, the authors made use of the short MS analysis times of conventional instruments, which can collect large numbers of MS scans within seconds, and interfaced a regular MS instrument through a capillary with an open reactor system. The problems, such as sources of error and data-storage considerations as well as the handling of the measured data when using such a sequential MS analysis approach with libraries have been described in detail.[228,229]

The screening of enantioselectivity has been problematic, since the usual times for analysis with conventional chiral columns in GC or HPLC applications is much too long for sequential applications in HT experiments. A variety of methods, such as UV/Vis analysis, fluorescence analysis, IR-thermographic assays, circular dichroism assays, chromatographic assays, parallel capillary electrophoresis, mass spectrometric assays, radioactivity assays, NMR, and IR assays were developed within only a few years for the rapid screening of enantioselective catalysis. The methods have been reviewed by Reetz,[230] and most of them have also been developed by his research group. The most rapid (more than 7000 *ee* determinations per day) and most versatile method for the analysis of chiral products of HTE appears to be parallel capillary electrophoresis.[231]

Among the techniques with potential to be parallelized, spectroscopic methods are most promising, because a number of 2D detectors have been developed which dramatically accelerate sampling and allow for the direct imaging of a sample so that the spatial distribution of different components of the library can be obtained simultaneously in a single measurement. This approach is different to conventional microscopy as it maps a specimen by running a series of spectra in a 1D row or in a 2D grid thereby allowing comparison of any one point with surrounding points.[232] The photoluminescence of the 25000 materials library mentioned before was investigated after UV excitation (at 254 nm) using optical imaging with a CCD.[10] Sun described how phosphor libraries can be made in both thin-film and powder form by using masking strategies and liquid-dispensing systems, respectively.[233] After annealing the libraries at a high-temperature, photoluminescence images were taken under UV (254 nm) illumination, and revealed some interesting tricolor UV phosphors. Measurement of the photoluminescence images under a spatially uniform X-ray field of 12 keV generated from a synchrotron radiation source provided a few leads for efficient X-ray scintillators. In fact, the human eye is so sensitive that it can in most cases pick up the phosphor lead of interest directly from the library under irradiation, but a scientific CCD camera in combination with a spectrophotometer has been set up to perform high-speed spectral acquisition and calculation.

An impressive variety of image analyses for materials properties have been developed at the US National Institute of Standards and Technology (NIST). These analyses can be used to visualize such complex phenomena as polymer dewetting, adhesion measurements, or cell-materials interactions in HTE.[234] A typical example is shown in Figure 17. The multilens contact adhesion test (MCAT) has been developed

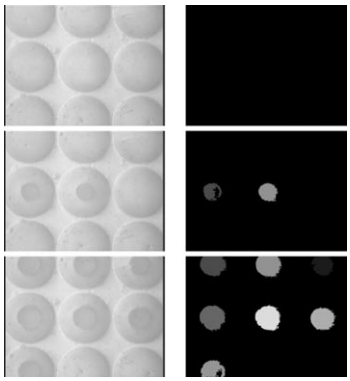

Figure 17. Multilens contact adhesion test (MCAT), monitored by a CCD camera (left side) and false color (here in gray) images (right side). The brightest spot indicates the longest contact and thus best adhesion (from Ref. [234]).

to measure adhesion reliably in HT. In this test, an array of over 1000 microlenses (here polydimethylsiloxanes) is brought into contact with a complementary substrate. The contact area and displacement of each microlens are monitored by a CCD camera and 820 images are collected to record the entire process of interface formation and failure. The adhesion of each lens is calculated automatically and displayed by false colors (here in gray). Figure 17 shows three images of the contact process of nine microlenses—from top to bottom: no contact, contact of two lenses, and contact of seven lenses. In the associated false colors the brightest images had the longest contact and thus the best adhesion.

Laser-induced fluorescence imaging (LIFI) has been used by Su and Yeung to screen for heterogeneous catalysts. The method relies on the change in fluorescence properties upon bond breaking and bond formation, processes typical for catalysis. It has been used to screen for new mixed-oxide catalysts for the selective oxidation of naphthalene and the coupling of benzene and phthalic anhydride to anthraquinone.[235]

The optical imaging approach with a CCD was extended to the combinatorial screening and optimization of organic light-emitting diodes (OLEDs), that is, devices that will find application in the next generation of flat-panel-display technology.[236] In a neighboring spectral region, a wide variety of infrared-based techniques have also been investigated for high-throughput analyses of samples interfaced to an infrared beam of light. Although microbead analysis by an IR beam has been extensively used as a characterization tool in the pharmaceutical industry, Lauterbach and co-workers demonstrated a major improvement in the characterization of catalytic activity by using FTIR imaging approaches.[237–239] In principle, FTIR measurements can be performed either in the transmission mode for transparent substrates or in the reflectance mode for nontransparent ones. In the latter case, there are potentially severe problems with regard to optical interference fringes produced in the spectra from thin, flat films on a reflective surface,[240] which can only be avoided by catalytic systems with enough surface roughness to give a diffuse scattering of the IR beam. The feasibility of FTIR imaging to study gaseous or solid-state reactions was demon-

strated in several transmission cells.[237,241] By using attenuated total-reflection (ATR) imaging Chan and Kazarian studied samples under a broad range of humidities and applied high-throughput testing to pharmaceutical formulations.[242] Their FTIR imaging system consisted of a step-scan spectrometer coupled with a macrochamber extension and a 64×64 focal plane array (FPA) detector with a size of $3.8 \times 3.8\ mm^2$. Images were acquired through an inverted ZnSe pyramid crystal not originally designed for imaging purposes. The aspect ratio meant that the size of the imaging area was $3.8 \times 5.3\ mm^2$. By using a device that can deliver microliter-sized droplets, that is, an ink-jet printing technique, and dispensing 10 droplets at each location, they were able to form samples on the ATR crystal with a diameter of 200–250 μm. Multivariate and univariate analyses of IR imaging data were also used to study NH_3 decomposition as well as NO_x storage and reduction (NSR) catalysts.[243,244] Their optical set-up consisted of a spectrometer, several refractive optical elements, a gas-phase array (GPA) sampling accessory, and a mercury cadmium telluride (MCT) FPA detector with a size of 64×64 pixel. This arrangement is shown schematically in Figure 18.

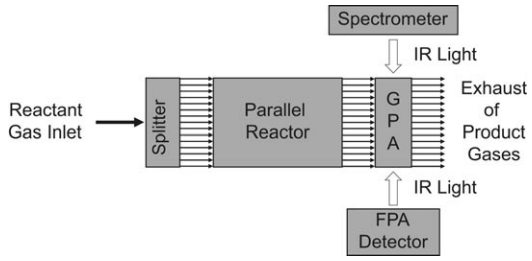

Figure 18. Experimental set-up used by Lauterbach and co-workers to analyze the reaction products of 16 heterogeneous catalysts in parallel by FTIR imaging.[243]

The GPA is based on an array of 16 stainless-steel tubes, capped by barium fluoride windows on each end. Each tube had a separate inlet and outlet to maintain separation of the products being analyzed. The effects of the number of co-added mirror scans of the spectrometer used in the data collection together with the number of factors used in the data analysis on the predictive ability of the multivariate approach were characterized by using three multivariate factor based models of PCR and PLS. Another development of parallel real-time detection systems for the analysis of the products of heterogeneously catalyzed gas-phase reactions is based on the photoacoustic effect.[245] This method relies on the detection of pressure pulses, which are generated by exciting a selected type of molecule with a laser pulse. Prerequisite for this technique is that the molecule to be analyzed has an absorption band in a frequency range which can be excited by the wavelength of a laser. The absorbed energy is radiationlessly converted into molecular translation, so that it produces, because of the pulsed or modulated laser beam, a pressure pulse which is detected by a microphone. The intensity of the pressure pulse is directly correlated to the product concentration. Spatial resolution is achieved because of the fact that the time taken for the acoustic pulse to reach the microphone is different for each channel. The detection method has to be changed for molecules with very low extinction coefficients, which can not be detected by microphones. The sensitivity can be increased by amplifying the signals from each channel by the use of resonance tubes integrated at the end of each tunnel in the gas outlet. With cylindrical resonance chambers, these tubes can be arranged in a parallel arrangement and therefore are suitable for quasiparallel operation without complex guidance of the laser beam. The laser modulation frequency must fulfil the resonance conditions of the tubes. The standing wave amplified by a lock-in technique operated in the phase-dependent mode is detected by simple electret microphones. To ensure that the lock-in amplifier amplifies only the signal of one channel at one time, a multiplexer is used for switching within the single channels, thus giving up spatial resolution and truly parallel detection, which requires good time resolution. Analytical evaluation of the systems and catalytic testing of the prepared materials was performed for CO oxidation and oxidative dehydrogenation (ODH) of ethane.

To ensure a complete parallel combinatorial workflow in the discovery of new thin-film photocatalysts, an HT evaluation method was developed by Nakayma et al. for screening photocatalytic activity by using a 2D pH imaging method.[246] First they generated thin-film libraries of Co-doped TiO_2 by using a laser MBE technique combined with a masking system. Control of the composition was achieved by 2D X-ray fluorescence (XRF) analysis. Subsequently, a thin liquid film of ferric sulfate was placed on the library and then irradiated with visible light. Electrons of photogenerated electron-hole pairs reduce iron(III) to iron(II) ions and simultaneously holes oxidize water molecules to oxygen. The resulting increase in the proton concentration in the thin liquid film was measured using a light addressable potentiometric sensor (LAPS) developed by Hafeman et al.[247] A LAPS is an insulated semiconductor device that responds to changes in surface potential at solid–electrolyte interfaces through the effect of such a potential on the electric field within the semiconductor. It is composed of a silicon substrate, a silica thin-film, a silicon nitride insulator, and an electrolyte containing an agar gel. The readout of the sensor at each point is the photocurrent generated by a laser beam. The photocurrent intensity depends not only on the proton concentration at the irradiated area, but also on the applied bias voltage. This bias is selected to show the highest sensitivity to pH changes. For pH measurements, the photocatalyst library is simply placed top-down on the agar gel, so that the proton can diffuse through the gel onto the silicon nitride surface where they are absorbed. Electrochromic counterelectrodes (CE) have also been used to monitor pH changes in electrochemical cells. Here, a WO_3-coated conducting glass acts as an ion-insertion electrode, which intercalates protons from the background electrolyte to balance the charge passed by the working electrode. Owen and Hayden used this method as a parallel optical screen for analysis of the electrochemical oxidation of methanol on Pt-based electrode arrays.

The rapid development of biological and pharmaceutical technology has posed a challenge for high-throughput analytical methods. For example, multiplexed high-performance liquid chromatography (HPLC) and capillary array electrophoresis (CAE) have been used for the combinatorial screening of homogeneous catalysts, but achieving a high degree of multiplexing, such as 96 capillaries in CAE, is not trivial.[248,249] Thus, many attempts to find new methods for library screening focus on the development of scanning methods with rapid serial measurements of physical properties instead of parallel testing. In particular, the more complex the technique and the smaller the scale on which the method operates are, the more likely the serial measurement will be used.

To date, a variety of screening techniques and instrumentation using scanning-probe techniques have been developed for the rapid characterization of structural, compositional, optical, electrical, and magnetic properties. In particular, scanning superconducting quantum interference device (SQUID) microscopes (SSM) have been employed for the rapid screening of magnetic properties in libraries, thereby detecting the magnetic field emanating from the sample. The SSM is equipped with a miniature SQUID ring of 10 μm diameter near an edge of an atomic force microscope (AFM) cantilever to sense local magnetic fields perpendicular to the film surface without the need of an external field.[250,251] In this device, the sample is set on a variable-temperature stage and mechanically scanned against the SQUID sensor with a scanning range of 10 mm × 10 mm whilst keeping the distance between the tip and the sample constant at 5 μm. The sample temperature has been controlled in the range 3–100 K using a heater surrounding the sample stage. The field sensitivity and spatial resolution are 50 pT in the direct current mode and 5 μm, respectively. Hasegawa et al.[251] have performed HT SSM measurements on composition spreads of the manganite perovskites $La_{1-x}Ca_xMnO_3$ and $Nd_{1-x}Sr_xMnO_3$ obtained after annealing a gradient system deposited at room temperature from three precursor sources by PLD in a high vacuum deposition system. In both types of films, SSM successfully observed spatial variations of the magnetic field, which corresponds to magnetic phase transitions with respect to chemical composition. This approach was later extended to combinatorial studies of other transition-metal oxides such as Co-doped TiO_2, Ge-based magnetic semiconductors, and Heusler alloys.[252] Another development in the field of magnetic thin-film analysis uses the magnetooptic Kerr effect (MOKE) for characterization. The magnetooptic Kerr effect as well as the Faraday effect correspond to a change in the intensity or polarization state of the light either reflected from (Kerr) or transmitted through (Faraday) a magnetic material. Since the change in the polarization state or intensity is proportional to the local magnetization of the material, it is possible to use these two effects to examine magnetic properties. There are three principal modes of operation for MOKE: longitudinal, transverse, and polar MOKE. The measurements mentioned above are based on a new method for MOKE microscopy described by Silva and Kos[253] with which it is not necessary to apply an external magnetic field for the extraction of the magnetic-contrast image. All previously developed longitudinal MOKE microscopy methods perturb the magnetic structure of the sample with an applied magnetic field. An alternative method is scanning Kerr effect microscopy SKEM, in which the sample is excited with an AC magnetic field while the MOKE signal is extracted from an optical detector with phase-sensitive lock-in detection. Scanning MOKE microscopy has been used intensively to study the magnetic properties of complex systems by utilizing the approach of continuous phase diagramming CPD,[146] as described previously. For example, the alloy system $Co_xMn_yGe_{1-x-y}$ grown epitaxially on Ge(001) substrates by MBE was chosen by Tsui and Ryan because a novel half-metallic ferromagnetism had been predicted for this system.[147,254] Similarly, high-resolution scanning Hall probe microscopy (SHPM) was used for real-time imaging of local magnetic fields near the surface of a sample. It is characterized by both high magnetic field sensitivity (ca. 2.9×10^{-8} T $\sqrt{\text{Hz}}$ at 77 K) and high spatial resolution (ca. 0.85 μm). The technique involves scanning a μm-sized Hall probe manufactured in a $GaAs/Al_{0.3}Ga_{0.7}As$ heterostructure with two-dimensional electron gas. Sampling was successful at low temperatures just 0.5 μm above the surface of the sample. The Hall probe was microfabricated by optical lithography.[255] This technique has been applied to several problems in the area of superconductivity for the characterization of thin films.[256]

Many microscale methods can be used to study different materials phenomena. In a similar way that SKEM and SHPM can be applied to the study of the magnetic properties of thin films, microscale thermal conductivity measurements can give new insights into order–disorder transformations and crystallographic site preferences in intermetallic compounds, the effect of solid–solution formation on conductivity, and compositional point defect propensity. Both elemental substitution and the formation of point defects decrease the thermal conductivity, since both increase the scattering of the free electrons in metals and intermetallic compounds. On the other hand, ordering in crystals decreases the electron scattering and thus increases the thermal conductivity. In materials with free electrons, thermal conductivity is correlated to electrical conductivity through the Wiedemann–Franz law, so it can be used to estimate electrical conductivity. For insulating materials, thermal conductivity is carried by phonons and the Wiedemann–Franz law no longer holds. In this case, thermal conductivity can be used to study lattice vibrations. Zhao et al.[134,136] developed an accurate method for mapping the thermal conductivity with micrometer-scale resolution by using time-domain thermoreflectance with a femtosecond pulsed laser. For this type of measurement, a 100-nm thin Al film is first sputter-coated onto a sample acting as a transducer by absorption of the laser pulse, thus enabling a sensitive measurement of temperature changes. At the wavelength of a Ti:sapphire laser ($\lambda = 770$ nm) used for sensing, the optical reflectivity of Al shows a strong temperature dependence as a result of a special band-structure feature. The femtosecond pulsed laser beam is split into two parts, a pump and a probe beam, to measure thermoreflectance. The two beams are modulated at different frequencies to reduce possible interference. The pump beam is used to

heat the sample, whereas the probe beam monitors the decay of the temperature increase introduced by the pump beam. The thermal properties of the sample are subsequently evaluated by matching the temperature decay observed from the experiment with those from theoretical calculations on the basis of heat flow models.

The formation of thermal conductivity on the μm scale was applied, for example, in the study of ordering phenomena in the Cr-Pt and Ni-Al binary diffusion couples, and revealed increased thermal conductivity in regions where ordering, that is, phase formation occurs. This finding means the method is well-suited to discover and locate new compounds in phase diagrams, especially in continuous composition libraries or continuous phase diagram approaches.

Thermoreflectance measurements are well-supplemented by the localized mapping of Young's modulus using instrumented nanoindentation. During nanoindentation experiments the load and displacement of well-defined indentation probes—usually trigonal pyramid-shaped diamonds—are recorded continuously while they are pushed into a sample in a controlled manner. Indentation hardness is determined by analyzing the unloading segment of the force–displacement curve usually by using the Oliver–Pharr[257] method, irrespective of the choice of indenter geometry. Several corrections have been implemented into commercial nanoindentation systems to account for friction, compliance between the indenter and mechanical system, exact contact area, etc. Nanoindentation imposes a complex stress field within the sample, but over the years much has been learned in regard to correlating the results with those obtained by classical forms of mechanical property testing, so that Young's modulus data measured by nanoindentation and those from handbooks now show good agreement. Mapping of the Young's modulus of the Pd-Pt-Rh ternary system as part of the Cr-Pd-Pt-Ru diffusion multiple has been used for testing the capabilities of the technique.[134] The modulus follows a linear relationship for Pd-rich compositions, but deviates positively from a linear rule-of-mixtures modulus for Pt-rich compositions, which shows there is a more complex behavior than expected from simple mixing rules. The results are, however, consistent with first principles calculations of the modulus for the binary system, again proving the usefulness of the diffusion-multiple approach on the validation of fundamental models of alloying.[134] The use of nanoindentation for screening combinatorial libraries of thin films is currently still in its infancy. For a more detailed review we recommend the recent report by Warren and Wyrobek.[258]

The number of studies combining combinatorial and nanoindentation specialities is expected to grow considerably in the near future, because many high-technology industries, especially the microelectronics industry, face serious integration issues related to the mechanical integrity of small amounts of materials. Considerable work in the area of nanoindentation has also been performed on thin films with low dielectric constants k which play an important role as gate materials in the fabrication of silicon chips. Alternatively, high-throughput characterization of electric properties such as the dielectric constant and loss tangent required that the discovery and design of new dielectric materials can be performed in the radio or microwave frequency region by using scanning microwave microscopy (SμM),[259] also called scanning evanescent microwave microscopy (SEMM).[260] The implementation of SμM can be formally divided into two categories according to the style of the resonator probe: one is the coaxial cavity resonator probe[260] and the other is the LC (where L stands for inductance and C capacitance) lumped-constant resonator probe.[259] In both methods the linear dielectric constant beneath the probe needle is detected as a shift of the resonance frequency; the advantage of the coaxial resonator is its stability and the high quality of the measured data. The lumped-constant resonator method has predominantly been used to probe the nonlinear dielectric constant by applying an additional low-frequency voltage to the sample; the advantage of this method is the extremely small probe size which results in a high lateral resolution and a simpler principle of operation, thus making practical operations easier. A combination of the LC resonator probe with an atomic force microscope AFM is also feasible for facilitating the simultaneous measurement of sample morphology and dielectric constant.[261] Several quantitative measurements of the dielectric constant, tangent loss, and surface conductivity have been reported in the characterization of combinatorial library samples with SμM. Okazaki et al. have performed SμM scans on $Ba_xSr_{1-x}TiO_3$ thin film libraries deposited on Nb-doped $SrTiO_3$ and showed the dielectric constant was affected by the lattice strain.[259] In contrast, Lippma et al. observed compositional variations at the cell edges of combinatorial perovskite thin film libraries generated by PLD with a carousel design and linear movable masks.[140]

The analysis techniques for the screening of combinatorial libraries mentioned above focus on the characterization of magnetic, electrical, and mechanical properties of materials. Low-temperature fuel cells such as the hydrogen polymer electrolyte membrane fuel cell (PEMFC) or direct methanol fuel cell (DMFC) have attracted much interest in the search for new competitive alternative energy sources. They have also created the need for new electrooxidation catalysts with high efficiency as a result of the inability of existing anode catalysts to oxidize fuels other than hydrogen at sufficient levels. Typically, Pt-Ru alloys are used because the addition of Ru reduces the extent of Pt deactivation caused by the presence of CO in the fuel, which can exist either as a by-product from upstream reforming or be formed as a partial oxidation product during the direct oxidation of liquid fuels. Scanning electrochemical microscopy (SECM) has been employed for the characterization of electrochemical activity in the search for new electrooxidation catalysts. SECM has already been reviewed,[262] and the method has been used for a number of combinatorial characterizations of fuel-cell catalysts.[174,263–265] In an SECM, a fine electrode is placed near a surface by an x-y-z positioning system to measure the electrochemical current between the tip and substrate while using the H^+/H_2 redox couple to provide the potential at the microscope tip. During the scans, the tip potential is varied to yield conditions where protons are reduced at a diffusion-controlled rate. Variations in the tip current are monitored to characterize the relative reactivity of the substrate in the

applied conditions, that is, electrolyte, bias voltage, temperature, etc. The diffusion-limited current obtained by using ultra-microelectrodes (UMEs) with a tip radius of 1 μm in a 1 mM solution of a typical redox species is approximately 200 pA; thus, typical SECM is highly sensitive.[262] The operation of an SECM can be fully automated, but the reliable evaluation of materials libraries with SECM is not trivial. A more detailed description of these can be found in Ref. [263]. SECM has become a routine analytical technique that can perform a range of analyses, including topographic imaging of conductors and insulators.

To characterize interfaces in layered systems, as for example, in dielectric multilayer devices, to obtain important information on interface structures and stoichiometries, it is necessary to perform high-resolution transmission electron microscopy (HRTEM). The problem in combinatorial material synthesis is the time needed to fabricate the individual HRTEM specimen from a library with a large number of members. To solve this critical problem, Chikyow et al. employed for the first time a "microsampling method" involving micromanipulation techniques together with thinning in a focused ion beam (FIB) to enable HRTEM sample preparation to be applied as a semi-automated characterization tool.[266] Figure 19 shows schematically the workflow for sample preparation (top) as well as an example for an interface structure of the dielectric material $SrTiO_3$ grown on an As-terminated Si(100) surface at 200 °C (bottom).

To understand the phenomena at the $SrTiO_3$/Si interface, a temperature-gradient sample-heating system consisting of an Nd:YAG laser point heating and thermal diffusion was attached to the preparation chamber. The $SrTiO_3$ layer becomes amorphous at 200 °C with a black line running at the interface with Si, which is indicative of arsenic, which also diffuses into the Si substrate. Crystallization of $SrTiO_3$ occurs above 550 °C, but still with an amorphous interface region of varying thickness. It is interesting to note that the thickness of the amorphous layer again increases above 600 °C.

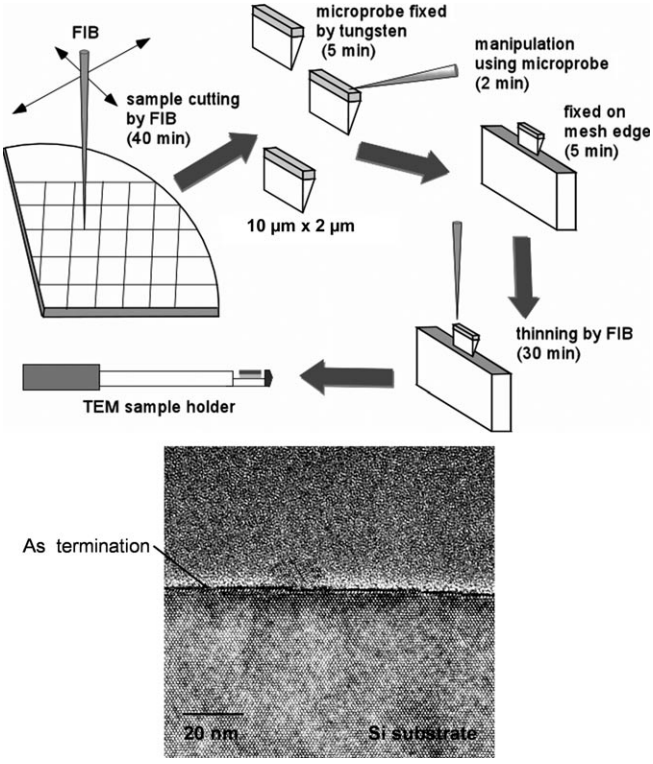

Figure 19. Top: Schematic illustration of the "microsampling method" for the preparation of HRTEM samples. Bottom: HRTEM image of the interface structure of $SrTiO_3$ on As-terminated Si(100) grown at 200 °C which reveals amorphous $SrTiO_3$ (from Ref. [266]).

Apart from the scanning probe microscopic techniques described above, there are a number of other mapping methods, such as scanning X-ray fluorescence (XRF) microscopy for compositional analyses, and scanning X-ray diffraction (XRD) measurements for structural characterizations of materials libraries, both of which use microfocused synchrotron X-ray beams. Since these have now become standard characterization techniques that are available commercially, we refer the reader to the literature.[267,268]

5. HT Applications and Discoveries

5.1. Luminescent Materials

Phosphors, and more generally luminescent materials, are key materials in fluorescent lighting, flat-panel displays, X-ray scintillators, and other applications. Today, most commercially viable white-light-emitting diodes (LEDs) are prepared as phosphor-converted LEDs (pc-LEDs) through a combination of a material emitting blue light at 460 nm and a yellow phosphor, with the blue-light-emitting material based on the wide band gap semiconductors gallium nitride or indium gallium nitride and the yellow phosphor on the YAG:Ce system. With the exception of the YAG:Ce phosphor and some organic luminescent materials, there have been no reports for a long time on yellow phosphors as down-conversion materials that have significant emission in the 450–470 nm emission range. Since the life-time of organic dyes is often too short, and some inorganic phosphors under consideration pose some environmental problems both in their preparation and in their use as they contain toxic elements, the development of new phosphors with high quantum yields and stability, as well as no environmental hazards is still challenging. This is especially true for the generation of a warm white light, as YAG:Ce emits only a greenish-yellow color that is not warm. This problem can only be solved if the yellow phosphor is combined with another red-emitting phosphor to give two-phosphor blends or by developing a novel long-wavelength yellow phosphor.

With a combinatorial chemistry approach Park et al.[269] found a new yellow phosphor based on silicate materials that emitted light in the 450–470 nm excitation range. In contrast to former investigations, for example, as in Refs. [10,233], quaternary libraries can also be obtained as bulk materials by solution-based combinatorial syntheses by using a computer-programmed liquid-dosing system instead of thin films by evaporation techniques. After performing "finer screenings", the two-phosphor blend of Ba^{2+}- and Mg^{2+}-co-doped Sr_2SiO_4:Eu and Sr_3SiO_5:Eu was found to emit broad bands in the green and yellow spectral range. Although the quantum

efficiency of the Sr_3SiO_5:Eu was not higher than commercial phosphors (82% compared to 100% for the YAG:Ce system), the luminescence yield of the InGaN-based two-phosphor blend was slightly higher than that of the commercial InGaN-based YAG:Ce (930 mcd compared to 910 mcd for YAG:Ce) with also slightly different CIE chromaticity points, and good enough for many practical applications.

Still another approach for realizing white-light diodes consists of using a soft UV-light-emitting material on excitation at 400 nm and RGB phosphors that result in tricolor or three-band white LEDs. Inorganic oxides are the best candidates for the RGB phosphors for three-band white LEDs, even though their luminescence is inferior to that of either organic dyes or other inorganic phosphors, such as sulfides. However, as mentioned above, organic dyes have problems in regard to their life-time stability, and sulfides pose some problems in use because sulfur tends to soak into the InGaN material, which is then followed by erosion. The research group of Sohn employed an evolutionary optimization process involving a genetic algorithm and combinatorial chemistry (GACC) for the development of new red[270] and green[271] phosphors suitable for tricolor white LEDs. They developed a solution-based combinatorial chemistry method that allows a 54-membered library to be generated per generation in only 2–3 days. In the first generation, the GACC starts with 54 randomly chosen compositions. A large number of zero elements were introduced to reduce the composition dimensionality. Evolutionary operations such as elitism, selection, crossover, and mutation were then applied by using the actually measured luminescence intensities of all members in the library to generate the subsequent generation. The selection, cross-over, and mutation rates were all set at 100%. After ten generations, the luminescence of the green phosphors was improved by a factor of about six during the GACC process, an improvement that has, according to the authors, never been reported before either in the case of phosphors or catalysts.[271] Recently, a strong red and green luminescence was also found in rare-earth-calcium oxyborate systems. A strong dependence of the luminescence intensity on chemical composition was found in amorphous, thin CCS film libraries composed of Y-Ca-B and Eu-Ca-B mixed oxides prepared by combinatorial pulsed laser deposition.[272]

Despite the life-time problems of OLEDs, they have undergone tremendous progress over the last decade because they may find application in the next generation of flat-panel-display technology. The disadvantages are balanced by a number of advantages, that is, their relatively low power consumption, wide viewing angle, ease of fabrication, color tenability, and their ability to be made on plastic substrates.[236] A typical OLED consists of a hole-transport layer (HTL) and an electron-transport layer (ETL) sandwiched between two electrodes, one metallic and one made from a conducting glass to allow the transmission of light. The performance of OLEDs can be increased considerably if luminescent organic dyes are incorporated as dopants into either the HTL or ETL layer, or both, during fabrication. Many factors, including dopant level, placement of the doped layer(s) in the device structure, dopant concentration, host–guest compatibility, thickness of the individual layers, electrode materials, and interfaces between them, influence the performance of the OLED, thus offering a wide field for combinatorial optimization with high-throughput methods. Sun and Jabbour[236] used spin-coating from solution to deposit HTLs of polycarbonate (PC) as the host for rubrene dye (5,6,11,12-tetraphenylnaphthacene) molecules. In the ETL, the green-light-emitting material 8-trishydroxychinoline aluminium (Alq_3) was incorporated by vacuum deposition and the layer thickness varied by a sliding-shutter mechanism moving in a stepwise fashion at a deposition rate of 0.8 Å s^{-1}. A maximum of the external quantum efficiency of 1.2% at 10.8 V applied electric field was found at an Alq_3 thickness of 60 nm. The authors proved the usefulness of HTTs for the fabrication of OLEDs by optimizing the dopant profile in a given host, in this case they focused on the red-light-emitting material 4-(dicyanomethylene)-2-*tert*-butyl-6(1,1,7,7-tetramethyljulolidyl-9-enyl)-4*H*-pyran (DCJTB) in an Alq_3 host material. The device structure as well as the quantum yield results revealed a significant improvement over the rubrene OLEDs (Figure 20). In a similar approach, Schmidt and co-workers described a combinatorial vapor deposition technique to

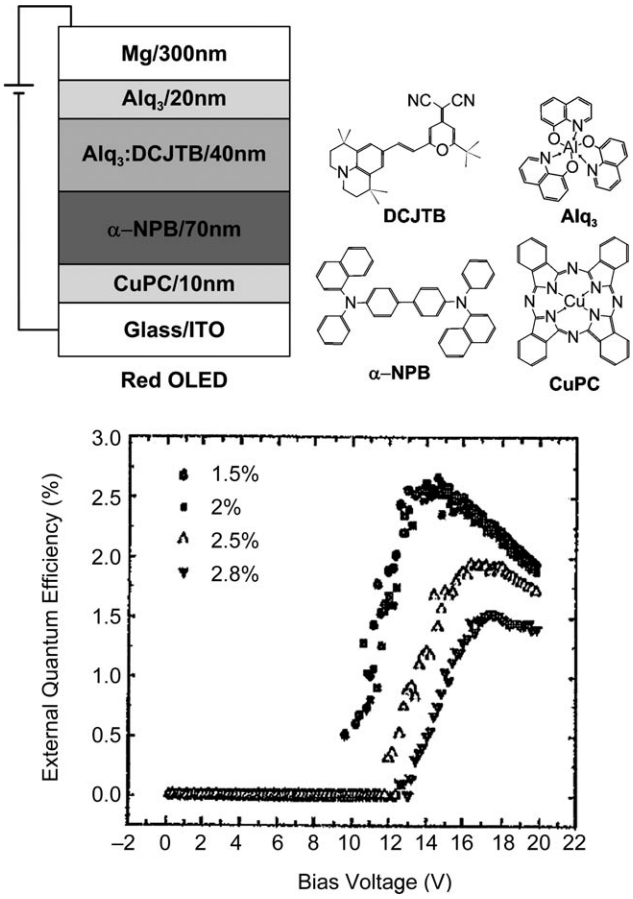

Figure 20. Top: Typical structure of a red-emitting OLED with the chemical structures of the molecules used for device fabrication. Bottom: External quantum efficiency versus bias voltage for OLEDs having 1.5%, 2%, 2.5%, and 2.8% DCJBT in an Alq_3 host (from Ref. [236]).

efficiently screen new materials and configurations in thin film multilayer OLEDs.[273]

Besides organic dyes, other phosphors based on inorganic oxides have also been tested in regard to their use in flat-panel displays, such as field-emission displays (FEDs) and plasma display panels (PDPs). Thus, borophosphate phosphor libraries doped with rare-earth elements have been generated by a scanning multi-inkjet delivery system for solution-based combinatorial syntheses followed by parallel screening of the synthesized libraries for VUV photoluminescence on a home-designed cathode gas Xe/He or Xe/Ne discharge lamp.[274] New ZnO-based phosphors have been discovered and optimized by using combinatorial methods to fabricate libraries of thin films by PLD on sapphire or Pt-coated silicon wafers as substrates.[275] ZnO has been doped with the elements (Y,Eu), V, W, (W,Mg) in such amounts that it has to be assumed that almost every ternary or quarternary compound of the phase diagrams is observed as a mixture with other phases in the phosphors despite the fact that, for example, X-ray diffraction experiments did not allow a positive identification of particular vanadate phases because of the low crystallinity of the samples. The authors found that the new phosphors had high low-voltage cathodoluminescence efficiency that potentially will allow their use in flat-panel display and lighting applications.

5.2. Other Optically Functional Oxides

ZnO has been used quite commonly as a base material in a number of combinatorial investigations that aimed to discover and optimize new transparent conducting oxides (TCOs). TCOs play a critical role in many current and emerging optoelectronic devices such as OLEDs (see previous section). The unique combination of high transparency in the visible region of the solar spectrum (typical transmittance $>85\,\%$) together with high electronic conductivity (typically $>1000\ \Omega^{-1}\,cm^{-1}$) also makes them ideal for applications such as transparent electrodes in liquid-crystal displays (LCDs) and solar cells. Commercially, the TCO market is dominated by Al-doped ZnO (AZO), the system In_2O_3/SnO_2 (ITO), and F-doped SnO_2, with ITO offering the best combination of high optical transparency together with high electrical conductivity. As the displays get larger and larger and the reaction times have to be faster and faster, the need for new materials has to be met by improved formulations—again offering combinatorial high-throughput methods the possibility of an accelerated investigation of the large TCO parameter space. Taylor et al. have grown compositionally graded, combinatorial libraries of indium-doped ZnO (IZO) by cosputtering ZnO and In_2O_3 on glass at 100 °C with an In content ranging from 5 to 50 %.[276] They were able to cover almost 50 % of the ZnO-In_2O_3 phase space with only three depositions. The highest conductivity was found in samples with 48 % In. Quite high electron mobilities of greater than $25\ cm^2\,V^{-1}\,s^{-1}$ and optical transmittances greater than 80 % were found for the samples with a high In content, as well as a distinct jump in mobility between 20–25 % In. The authors considered these properties sufficient for incorporation into the flat-panel displays. Glass materials have also been studied to evaluate time-temperature-transfer (T-T-T) diagrams by using a combinatorial evaluation system developed by Inoue et al.[277,278] By using a CCD camera (together with a computer system compiling the glass-forming regions) to analyze the crystallized area in the glass sample libraries annealed simultaneously in a furnace with a temperature gradient, they were able to reduce considerably the laborious routine work for the preparation and screening, relative to a conventional method. The effect of post-processing steps such as plasma treatment on sol–gel-derived semiconductor libraries were studied by Rantala et al.[279] By doping the SnO_2 with Sb as well as treatment with a radio-frequency argon plasma, they were able to increase the conductivity of the layered glassy SnO_2 films considerably. A sol–gel route has also been used to produce arrays of Al-doped ZnO as potential TCOs through hydrolysis of a zinc acetate/ethylene glycol precursor in aluminum nitrate solutions.[280] Potential dielectric materials have been synthesized automatically by sol–gel procedures, and the sols deposited on Si libraries with a pipetting robot. After calcination, the libraries were analyzed by automated AFM in the ultrasonic piezo mode.[281]

5.3. Dielectric and Ferroelectric Materials

A systematic approach for the discovery of new dielectric materials has already been discussed in the investigation of the crystallization in amorphous Zr-Si-O dielectric compounds by using the co-deposited continuous composition spread approach.[127] A "generalized" CCS approach that allows the simultaneous study of the combined effects of two parameters, which are imposed as spatial variations along two different orientations of a planar substrate (such as chemical composition, film thickness, growth temperature) was applied by Christen et al. for the epitaxial growth of libraries of the electrooptic materials $Sr_xBa_{1-x}Nb_2O_6$ (SBN) on Mg(001) by PLD.[137] SBN is an attractive ferroelectric material, because it shows an exceptionally large electrooptic coefficient r_{33}, thus making it a potential material of choice for miniaturized electrooptic modulators, real-time holography applications, and information-storage technologies. By changing the Sr to Ba ratio in SBN, the r_{33} coefficient can be varied, and values 30–40 times larger are reached than are observed for the congruently melting $LiNbO_3$, the current industry standard. They clearly observed variations in the optical and structural properties as a function of growth temperature for a series of $Sr_{0.5}Ba_{0.5}Nb_2O_6$ thin films on MgO(001) substrates deposited at different growth temperatures spanning a range of 500 °C. The same research group extended the CCS approach to the growth of epitaxial heterostructures, that is, superlattices consisting of repeated stacking of $SrTiO_3$ and $Sr_xBa_{1-x}ZrO_3$ layers, where the parameter x varied continuously across the sample. The periodicity was chosen to be 200 Å, with superlattice peaks in the X-ray scans clearly proving the formation of the desired structure. The corresponding titanate $Sr_xBa_{1-x}TiO_3$ was at the center of interest in the investigations performed by Xiang, who developed a strategy to lower the leakage current in next-generation integrated capacitors by

engineering Schottky barriers at the interfaces between both the electrodes and the dielectric material. However, the incorporation of Schottky barriers could degrade other important device performances, such as charging time. So the best approach for a reduction in the leakage current is to directly reduce the conductivity in the dielectric material itself.[282] To construct a capacitor device library Xiang deposited a 100–200-nm-thick amorphous layer of $La_{0.5}Sr_{0.5}CoO_3$ (LSCO) from a stoichiometric target at room temperature using PLD. After annealing the sample at 850 °C to form an epitaxial LSCO bottom electrode, the substrate was remounted in the PLD chamber to deposit different host–dopant combinations in three different host regions ($BaTiO_3$, $Ba_{0.7}Sr_{0.3}TiO_3$, and $Ba_{0.5}Sr_{0.5}TiO_3$) using 2D high-precision deposition masks. In the orthogonal direction, the substrate was divided into separate Ce, Y, La, and W dopant regions, each containing 0–3 % dopant added as a gradient to each host. In a complex sandwich structure with dopant layers embedded between pure and identical host layers, Pt counterelectrodes were deposited with a lithographic mask after a high-temperature ex situ annealing to interdiffuse the dopants and to ensure epitaxial growth. The resulting library was subsequently characterized by Rutherford back scattering (RBS), to evaluate the degree of interdiffusion, and by scanning evanescent microwave microscopy (SEMM), to determine the dielectric constants.[142] The HT screening of the dielectric constant and loss of the dielectric constant of a single phase strip is shown in Figure 21.

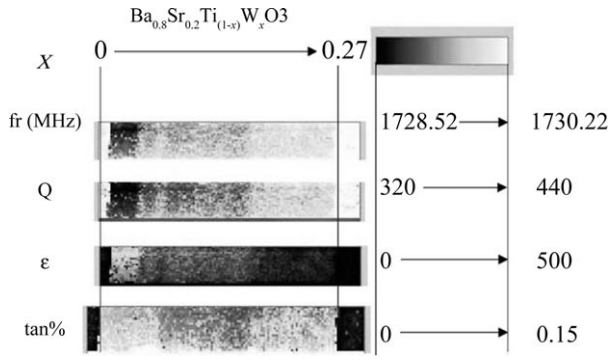

Figure 21. High-throughput screening of the dielectric constant and dielectric loss from a single strip from a 5500-member dielectric materials library (from Ref. [142]).

5.4. Battery Materials

Systems containing TiO_2 were not only investigated as dielectric or ferroelectric materials, but also in combination with lithium oxide as a component for solid-state battery applications. Fujimoto, Takada et al. prepared pseudoternary compounds of the Li_2O-X-TiO_2 system (with $X = Fe_2O_3$, Cr_2O_3, and NiO) by using a fully automatic combinatorial robot system that enables a complete combinatorial workflow.[283] Either aqueous salt solutions (Li, Cr, Ni) or slurries of nanoparticles suspended in water (Fe, Ti) were used as starting materials. The robotic arm of the system was programmed to perform weighing, pipetting, and mixing of the starting materials with the help of the corresponding auxiliary tools. After drying and calcination, the products were characterized by means of X-ray diffraction by using a combinatorial X-ray diffractometer developed for HTS and equipped with a position-sensitive proportional counter (PSPC) as well as a movable *x*,*y* translation stage. Powder XRD data revealed that the products were single or multiphase and represented up to six different crystal structures: spinel solid solutions $LiFe_5O_8$-$Li_4Ti_5O_{12}$, ramsdellite solid solutions $Li_2Ti_3O_7$, pseudobrookite Fe_2TiO_5, rocksalt-type solid solutions between $LiFeO_2$ and Li_2TiO_3, and rutile TiO_2. As reported by other authors, ramsdellite-type $Li_2Ti_3O_7$ shows excellent charge and discharge cycling performance when used as an electrode material in lithium batteries. A Cr-doped variant of the same structure type reveals reversible deintercalation and intercalation of Li ions. To date, there are no reports of Li-Ni-Ti oxides with a ramsdellite structure. Alternatively, the robotic system mentioned above was connected to a combinatorial electrode array of 16 current collectors, to which counterelectrodes were attached.[284] Two multichannel potentiogalvanostats, each of which had eight channels, were used as current sources, and all the cells operated simultaneously at constant current. The system was used to characterize $LiCoO_2$ libraries prepared from aqueous LiOH solutions and aqueous CoO particle suspensions by the robotic system measuring charge–discharge curves. An overview of the electrochemical characterization system is given in Figure 22.

$LiCoO_2$ was also the subject of a combinatorial approach called "combinatorial computational chemistry", which was proposed by Miyamoto and co-workers.[118] They investigated the structural properties of lithium transition metal oxides

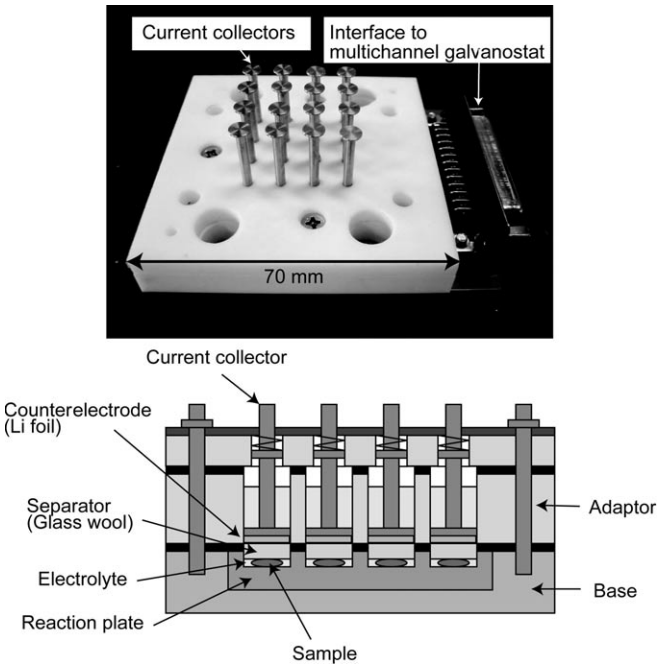

Figure 22. Combinatorial electrode array for testing electrode materials for batteries (top) and schematic cross-section (bottom; from Ref. [284]).

$LiMO_2$ (M = 3d transition metal) with a layered rocksalt-type structure, which revealed a poor reversibility of the charge–discharge cycle of $LiNiO_2$ because of large structural changes resulting from significant differences in the ionic radii of Ni^{3+} and Ni^{4+}. This effect can be reduced through doping of $LiNiO_2$ with other 3d transition metals, such as Mn. Whitacre et al.[164] described a methodology for batch-fabricating hundreds of submillimeter-sized thin-film solid-state batteries with spinel-type $Li_yMn_xNi_{2-x}O_4$ cathodes, sputtered lithium phosphorous oxynitride LiPON as the electrolyte, and evaporated, micropatterned Li metal as the anode layer. The process flow for Li anode fabrication has already been shown in Figure 16. It was found that the microfabricated battery assemblies had similar electrochemical performance parameters as bulk-fabricated powder electrodes with comparable composition ranges. Dahn et al. have applied HT methods to study thin-film alloy libraries of Sn, Co, and Cu for potential applications as anode materials in Li ion batteries by electrochemical methods and XRD. Amorphous phases seem to be associated with a good performance. The addition of carbon was found to positively affect the charge–discharge cycling and stability.[285]

5.5. Magnetic Materials

Perovskite manganites are highly correlated electronic systems that reveal a number of interesting optical, electrical, and magnetic properties as a function of the doping concentration, ionic radii, and other parameters which are accompanied by electronic phase transitions such as spin-orbital ordering and smectic phase formation. Xiang also applied his CPD approach to rare-earth perovskite manganites of the formula $RE_{1-x}A_xMnO_3$, where RE = La, Nd, Eu, Gd, Tb, Er, Tm, and Yb, A = Ca, Sr, and Ba, and $x = 0$–1.[144] Several different continuous phase diagrams were generated on 15 mm × 15 mm large single-crystal substrates ($SrTiO_3$(100) or $NdGaO_2$(110)) by using an eight-target carousel and a high precision in situ linear shutter system for gradient depositions of the precursors. The electronic and magnetic properties of the postannealed film were characterized by SEMM[144] and SSM,[251] respectively. The SSM was equipped with a minature SQUID ring with an outer diameter of 10 μm near an edge of an AFM cantilever to sense the local magnetic field B_z perpendicular to the film surface with and without a magnetic field. Figure 23 shows 2D magnetic images observed by SSM at 3 K within a scanning range of 300 μm × 300 μm of a composition spread of $La_{1-x}Ca_xMnO_3$ films with various values of x. In general, a ferromagnetic material is divided into domains with different magnetic axes instead of being homogeneously polarized. In thin films, the magnetic moments tend to lie parallel to the film surface because this reduces the magnetostatic energy. In this case the domain boundaries emit or absorb magnetic fields, which is detected in SSM as positive or negative B_z and indicated as white or black regions. Regions inside the domains are, in contrast, gray colored.

If one observes experimentally both the magnetic domain width d as well as the maximum field $B_z^{max} \equiv B_z(0;h)$ at a probe–sample distance h and at the domain boundary $d = 0$, the saturation magnetization M_z can be calculated. From the measurements it is evident that M_s shows a local minimum at $x = 0.2$, which is equivalent to a phase boundary between ferromagnetic insulator (FI) and ferromagnetic metal (FM) states and is consistent with the magnetic properties of bulk materials in this compositional range. In contrast, the SSM results differ remarkably from those of bulk studies for $x > 0.5$, with the SSM measurements strongly indicating that a phase separation into ferromagnetic and charge-order nonmagnetic phases occurs in this compositional range.[251]

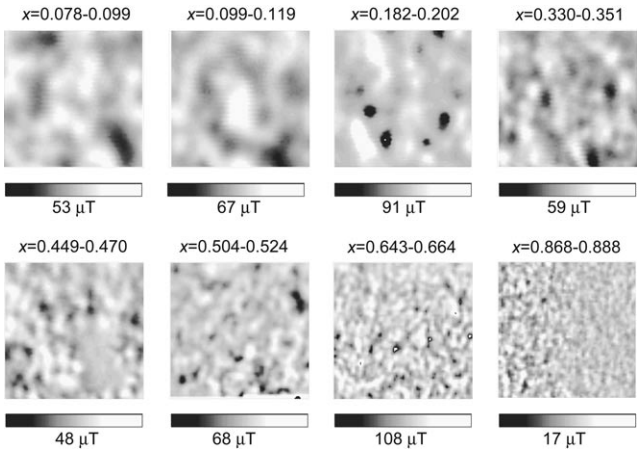

Figure 23. 2D magnetic images of a compositions spread library of $La_{1-x}Ca_xMnO_3$ (LCMO, with $x = 0.078$–0.888) thin films observed by SSM at 3 K and different magnetic fields B_z. Scanning areas are 300 μm × 300 μm for all images (from Ref. [251]).

Apart from manganites, alloy systems in particular have received much attention in the development of new magnetic materials by combinatorial synthesis because of the ease of evaporation of metallic elements in PVD deposition chambers by every kind of evaporation source, that is, Knudsen cells, e-beam evaporators, as well as magnetron sputtering systems. Specht et al. developed a technique based on synchrotron radiation that allows for the rapid structural and chemical characterization of ternary alloys over a wide range of composition by XRD and fluorescence measurements.[148] By this technique they were able to construct the phase diagrams and contour maps of lattice parameters from isothermal sections by examination of 2500 compositions of the ternary metallic alloy system Fe-Ni-Cr in a single experiment that took about 4 h. By using a high-flux synchrotron beamline, diffraction patterns were recorded with a 1024 × 1024 pixel X-ray CCD camera with a pixel pitch of 60 μm that was located 10 cm behind the sample. Typical measured phase diagrams of libraries annealed at different temperatures (samples A, B) and generated with different depositions sequences (samples A, C) are shown in Figure 24. Each layer was grown with a linear layer thickness gradient by a sliding shutter driven by a stepping motor and rotated by 120° after each layer for deposition of the next layer, thereby resulting in a triangular arrangement of the three elements in the phase diagram. Interdiffusion of the elements and phase formation was achieved by a postannealing step. As samples A and C

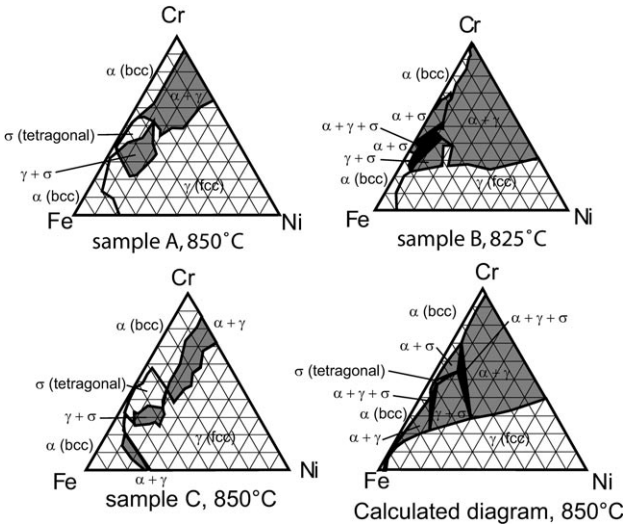

Figure 24. Measured phase diagrams of the ternary system Fe-Ni-Cr at different annealing temperatures (samples A, B) and for different deposition sequences (samples A, C; from Ref.[148]).

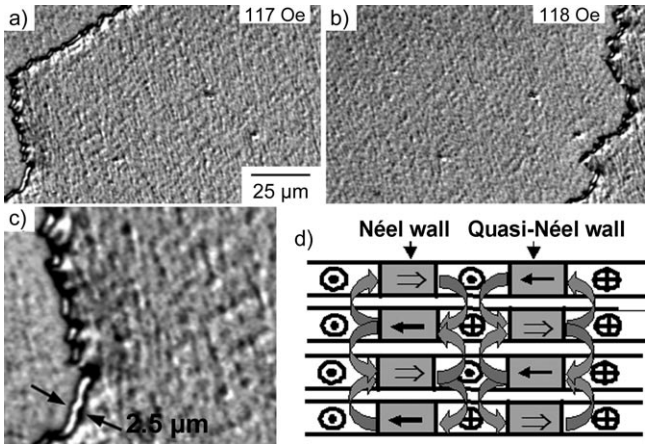

Figure 25. a,b) Motion of twin-domain walls in $(TbFe/FeCo)_{N=2}$ bilayer stacks as a function of the field. c) Magnified view of the twin walls. d) Schematic view of the magnetostatic coupling between stray fields of the domain walls in different layers (from Ref. [156]).

were deposited with different layer sequences, but the diffraction data reveal similar phase diagram sections in Figure 24, equilibrium data were obtained.

"Giant" magnetostriction alloys such as $TbFe_2$ (terfenol) or $Tb_{0.3}Dy_{0.7}Fe_2$ (terfenol-D) can reach strains of 0.1–0.2%, while those of shape-memory alloys (SMAs) can easily exceed 1%. As already mentioned before, the exchange-spring mechanism of Kneller and Hawig describes how the switching fields can be reduced and strain susceptibility enhanced.[155] Ludwig and co-workers deposited TbFe/FeCo and FePd/Fe multilayers by magnetron sputtering on Si(100) substrates to study the role of magnetostatic and magnetoelastic interactions in exchange-spring multilayers to understand the microscopic details of the exchange spring.[156] The systematic investigation of the multilayers as a function of the number N of bilayers showed that in the case of $(TbFe/FeCo)_N$ bilayer stacks, the coercivity of the films drops abruptly with increasing number of bilayers to a saturation value of about 60 Oe when the number of bilayers is greater than 10. Compared to a single FeCo film with a coercivity of about 168 Oe, the coercivity of 112 Oe of a multilayer with just two bilayers $(TbFe/FeCo)_{N=2}$ is significantly lower. The authors explained this by considering the field-dependent micromagnetic structure of the bilayer stack, as depicted in Figure 25. With saturation in the negative direction, the reversal of the magnetization in the multilayer occurs by nucleation of "twin" domain walls (Figure 25a). As the field strength increases (from 117 up to 118 Oe), the reversal proceeds by lock-step motion of the twin wall across the entire sample (Figure 25b). A magnified view of the twin domain walls clearly shows its complex nature in the form of Néel wall and quasi Néel wall combinations with a sandwich structure (Figure 25c). The solid arrows in Figure 25d, which reveal schematically the magnetostatic coupling between stray fields of domain walls in different layers, denote the rotation of the magnetization within a domain wall, whereas unfilled arrows indicate the stray field emanating out of the Néel walls that causes a fluctuation of the magnetization in the adjacent layers, thus giving rise to quasi-Néel walls. The formation of such twin walls leads to an overall decrease in the wall energy and thus coercivity. Multilayer thin-film libraries prepared by combinatorial deposition have also been used for the investigation of hard magnetic properties in the Fe-Pt system.[150] Additionally, $Fe_{50}Co_{50}/Co_{80}B_{20}$ multilayers with various FeCo layer thicknesses have been studied for their applicability in microsensors and high-frequency devices.[151]

Tsui and Ryan compared the deposition and co-deposition of multilayers by using combinatorial MBE techniques to generate continuous phase diagrams (CPDs) by considering the Co-Mn-Ge system as an example.[147] For this purpose, multilayers containing monolayers and submonolayers of Ge, Mn, and Co were deposited sequentially by using a combination of shadow masks, sample rotation, and pneumatic source shutters to obtain alloys by so-called artificial alloying and sequencing by interdiffusion of the elements. The multilayer approach also has special advantages in the production of metastable alloys, in particular, to impose an artificial stacking sequence along the growth direction, which can be critical for setting up desired properties such as half-metallic behavior. Half-metallic behavior together with a structural compatibility for epitaxial growth on Si, Ge, and GaAs substrates has been predicted for Heusler alloys,[286] such as Co_2MnGe, which is an interesting material for spintronic applications. Films of complete ternary combinatorial libraries (for example, $Co_xMn_yGe_{1-x-y}$) or two-variable libraries sliced through the ternary system (for example, $(Co_{1-x}Mn_x)_{1-a}Ge_a$) have been produced with 25-Å thick capping layers for ex situ measurements.[147] Scanning RHEED was used to track the structural evolution of the libraries in situ and Rutherford back scattering spectroscopy used to measure the compositions ex situ. Additionally, magnetooptic Kerr effect (MOKE) imaging and scanning SQUID magnetometry was applied to study magnetic properties. A room-temperature magnetic phase diagram of a 250-Å-thick combinatorial Co-Mn-Ge library grown on Ge(001)

by MBE, illustrated as the differential scanning MOKE intensity at ± 5 kOe (that is, $\Delta I = I(5\text{ kOe}) - I(-5\text{ kOe})$), is shown in Figure 26. Yellow and red areas correspond to the magnetic regions. The directions of the magnetic field and light polarization were vertical and the horizontal, respectively. The inset in the right section of Figure 26 gives more detailed information on the indicated section. The color scale bar represents the coercive field strength in Oe. Other Ga-containing phase diagrams, that is, Ni-Mn-Ga, Co-Mn-Ga, and Co-Ni-Ga, were investigated by Matsumoto and co-workers by using a combinatorial strategy to quickly survey the vast compositional landscape of Heusler alloys and related compounds by co-deposition of different elements in a triangular configuration.[252]

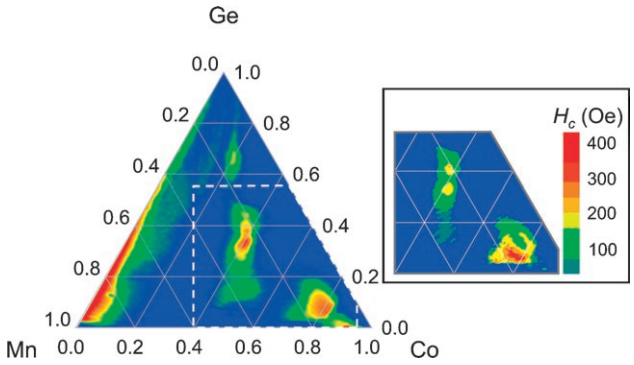

Figure 26. Magnetic phase diagram of a 250-Å-thick combinatorial library of Co-Mn-Ge measured at a differential scanning MOKE intensity at ± 5 kOe (from Ref. [287]).

5.6. Fuel-Cell Materials

Polymer electrolyte membrane fuel cells (PEMFCs, often also called proton exchange membrane fuel cells) have enormous potential as stand-alone power sources. The energy conversion efficiency of a standard fuel cell is directly governed by the activity of the anodic and cathodic materials, which are targets for development in PEMFC technology. Combinatorial approaches are attracting increasing attention as a novel and powerful methodology for the high-speed survey and optimization of new functional materials for fuel-cell technology.

Among the PEMFC catalysts examined so far, a high performance can frequently be achieved by the catalytic synergism of noble metal/base metal oxide combinations or precious metal alloys. For example, support metal oxides are often selected to suppress carbon deposition during hydrocarbon reforming, a feature which can be related to the acid–base properties of the oxides. The selectivity for the formation of hydrogen in the product is also strongly affected by the metal oxide support. The strong acidic and corrosive conditions generated by the nafion polymer electrolyte also limits the materials that can be used in PEMFCs. PtRu alloys usually show the highest performance among the electrocatalysts examined to date. Improvement in the CO tolerance of the Pt metal was also attempted through combination of Pt with oxides such as WO_3 and MoO_3.[288] Several explanations have been proposed for the origin of the synergism in the noble metal/base metal oxide system:[289] 1) the bifunctional activation of carbon monoxide and oxygen or water molecules on adjacent, but different active sites, 2) the creation of a new site for the activation of CO at the interface, 3) the relaxation of the strong CO-Pt adsorption through an electronic interaction. Furthermore, for example, three different aspects can be considered for the electronic interaction: formation of a Schottky junction; electron exchange with donor and acceptor surface states; and modification of the redox properties of the supported metal cluster by the acid–base properties of the oxide support. Kobayashi et al. proposed that not only a comparison of the catalysts in one reaction, but also the comparison of interrelated reactions with a common catalyst library generates important information for elucidating the catalytic synergism.[289] They therefore studied the effect of a given set of catalysts in one library consisting of 5 different noble metals and 12 different base metal oxides on both the water gas shift reaction and the steam reforming of methanol, and compared the results. Their findings of the first screening stage are summarized in Figure 27. The high activity of Pd/MnO_2 for both reactions

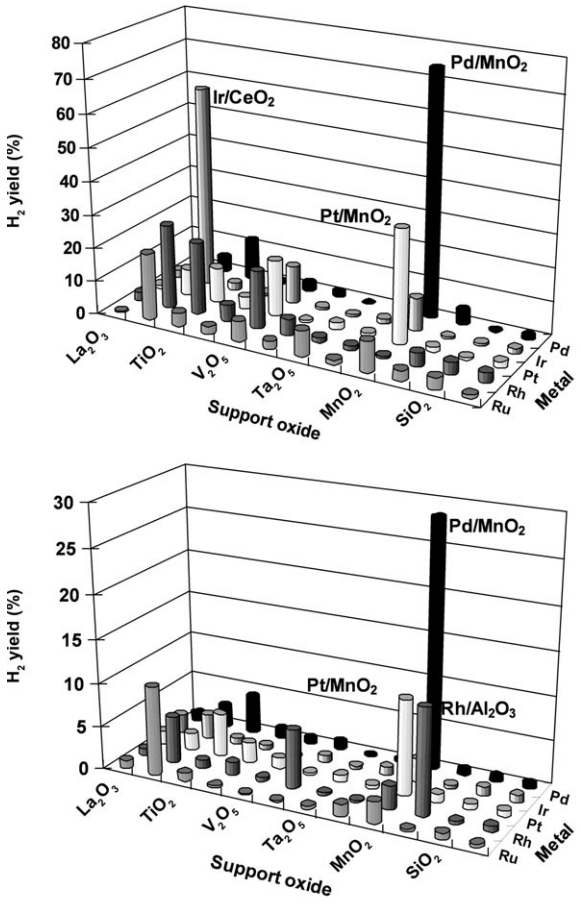

Figure 27. Hydrogen production from the water gas shift reaction (top) and methanol steam reforming (bottom) measured on a library of precious metal/metal oxide combinations (from Ref. [289]).

is noticeable, whereas the second best catalyst system is different for the two reactions: Ir/CeO_2 for the water gas shift reaction and Ru/CeO_2 for the methanol steam reformation. On the basis of these results, the authors concluded that the catalytic synergism is not a simple reflection of the physical structure of the catalyst but that the catalytic reaction also contributes to the synergism. If the elementary steps in the water gas shift reaction and methanol steam reformation are considered, it can be seen that the activation of water, the oxidation of a carbonyl group, and hydrogen recombination are involved in both reactions. One difference, however, is that the water gas shift reaction does not involve the C–H dissociation step. Thus, analogies and differences between related reactions with common elementary steps can offer the chance to elucidate the synergistic mechanism.

Other authors have reported on the application of the scanning electrochemical microscope (SECM) for spatially mapping the kinetics of heterogeneous electron-transfer reactions to enable screening measurements to be performed for combinatorial studies on electrooxidation catalysts.[265] For this Jayaraman and Hillier used multielement band electrodes containing various compositions of binary Pt_xRu_y and ternary $Pt_xRu_yMo_z$ alloys deposited by pulsed electrochemical deposition onto patterned substrates. After verification of the catalyst compositions through a combination of Auger electron spectroscopy and energy-dispersive X-ray spectroscopy, the activity in regard to the hydrogen oxidation reaction was probed in sulfuric acid solutions using a scanning microelectrode tip placed in proximity to the catalyst surface and recording the cyclic voltammograms at selected points on the band electrodes. Interestingly, the cyclic voltammetry curves of the $Pt_xRu_yMo_z$ electrodes differ from those of pure Pt, pure Ru, and pure Pt_xRu_y electrodes. The addition of Mo produces an additional electrochemical current in the potential range between 0.3 and 0.6 V. This observation suggests that the Mo component is undergoing an oxidation/reduction process. The Pourbaix diagram for Mo indicates that a stable oxide with a composition of MoO_2 or MoO_3 (including the Magneli phase region) will form in this pH range. The authors thus speculated that these Mo-containing electrodes would be able to dissociate water and provide hydroxide or oxide surface species with the ability to oxidize carbon monoxide at low potentials. This finding needs to be highlighted, particularly in view of the catalytic synergism discussed above. The authors are currently extending their methodology to examine additional regions of composition space in the $Pt_xRu_yMo_z$ system as well as multicomponent electrodes with additional metals that exhibit stable oxide formation at low potentials. Catalysts based on Pt-WO_3 were also prepared by McFarland and co-workers by using automated systems for high-throughput electrochemical synthesis and then screened for their applicability as fuel-cell electrooxidation catalysts, particularly as DMFC catalysts.[290] The same research group investigated Au nanoparticulate electrocatalysts on TiO_2 substrates for the electrooxidation of CO by using a 96-well polypropylene reactor block assembly, as mentioned before.[171]

Low-temperature fuel cells typically rely on platinum alloy catalysts, such as Pt-Ru. Despite their comparitively high complexity, high-throughput methods for the search of alternative electrode materials were developed early on in the field.[291] Mallouk, Smotkin, and co-workers have recently compared four of the HT electrochemical methods (linear sweep voltammetry (LSV), optical screening, array fuel cell testing, and single fuel cell testing) developed for DMFC applications through a ranking of the anode catalysts. They came to the conclusion that the LSV of disk electrodes is most reliable in applications at 60 °C.[292]

Guerin and co-workers developed both hardware and software for the fast sequential measurement of cyclic voltammetric and steady-state currents in 64-element half-cell arrays.[293] It is interesting to note that the 64-cell array uses only one reference and one counterelectrode (Figure 28). This setup allows the parallel screening of all 64 electrodes and catalysts deposited on these electrodes for various fuel-cell applications. Peak potentials, currents, and charges can be measured in a single experiment.

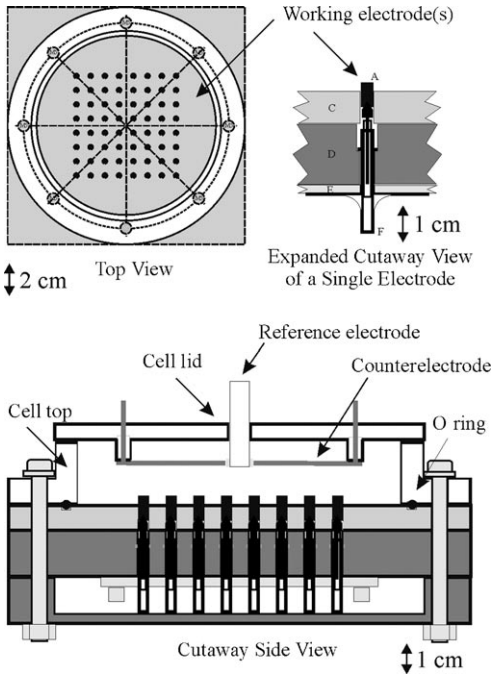

Figure 28. Electrochemical 64-cell arrangement with a single reference and counterelectrode (from Ref. [141]).

The use of array fuel cells for precise HTS of libraries of membrane electrodes for hydrogen cathode catalysts for PEMFCs as well as for DMFC anode catalysts has been described by Smotkin et al.[294] The libraries were prepared by ink-jet delivery of metal salts on carbon paper, and subsequently reduced by borohydride solutions. The authors also emphasized the potential problems and pit falls in HT searches for fuel-cell electrodes. On arrays of 100 electrodes Hayden and co-workers studied particle size effects of Au on TiO_2 catalysts for electrocatalysis (oxygen reduction). The HT data were validated with measurements on rotating disk electrodes (RDE) and the Au particle size distribution was determined by TEM measurements. The best electrocatalytic

performance was achieved with particle sizes in the range of 2.5–3 nm.[295]

5.7. Coating Materials

There are several different classes of coatings, but combinatorial approaches have been applied primarily either to hard coatings or coatings based on polymeric materials.

The variety of process parameters during the PVD of metastable hard coatings make a conventional approach for the development of new coatings time-consuming and expensive, while the increasing complexity of modern coatings has led to the demand for a cost-effective method in the development of new products for the advanced materials industry. These two factors have generated the need for the adaptation of combinatorial techniques to the specific requirements of the coatings industry. Hard coatings in the form of 1D or 2D laterally graded coatings such as (Ti,Al)N, (Ti,Al,Hf)N, or (Ti,Al,Si)N, which were deposited by means of reactive magnetron sputtering and plasma-enhanced chemical vapor deposition (PECVD) by using a composition-spread approach, were investigated with respect to the relationship between structure, composition, and the desired material properties by the research group of Cremer and Neuschütz.[268,296–298] A combination of electron-probe microanalysis (EMPA) and scanning X-ray diffraction was employed as a fast and reliable way of investigating the composition, crystal structure, and texture of the material libraries. Based on these investigations, the influence of Hf and Si additions on the structure, texture, and grain size of (Ti,Al)N hard coatings was determined.

Besides hard and polymeric coatings, metallic overlayers on substrates have also attracted attention for special applications. An HT concept for studying and optimizing the composition and thickness of potential switchable mirror materials (for example, Pd on Mg-Ni) was introduced by Borgschulte et al.[299] Switchable mirrors are shiny metal alloy films on glass, which become transparent upon exposure to hydrogen. Potential applications include windows for buildings and vehicles or visors for helmets. The studies revealed strong metal–support interactions as the origin of the observed thickness dependence of the switchability and reversibility.

5.8. Membranes

Vankelecom, Jacobs, and co-workers have successfully developed a 16-fold HTT to screen for potential membrane materials.[300] In the validation experiments, a membrane development was carried over four generations. Genetic algorithms were used to drive the development of polyimide-based nanofiltration membranes by variation of eight parameters (polyimide, NMP, CH_2Cl_2, THF, 1-hexanol, acetone, water, 2-propanol) comprising the membrane casting solution. The performance of the membrane was tested at a pressure of 10 bar with a methyl orange indicator in 2-propanol. After a total of only 192 membrane preparations in 4 generations, several new membranes outperformed all 3 commercial reference membranes (Starmem 120 and 240, MPF-50) in terms of permeance and retention.[300,301] With the help of genetic algorithms, novel polyimide-based solvent-resistant nanofiltration membranes have also been developed by HT techniques.[302]

5.9. Polymers

Polymeric materials, polymerization catalysts, and polymer blends belong to the group of complex materials originally believed not to be suitable for HTT. This original assumption was not without reason, since polymer properties depend, among other things, also on the molecular weight, and measurements of molecular weight distributions used to take hours. Many organometallic polymerization catalysts as well as many polymerization processes are highly sensitive to impurities, oxygen, and moisture. The reproducible screening of many catalysts or polymerization processes was viewed to be technically impossible. Many mechanical or optical polymer properties, such as scratch resistance, hardness, elasticity, transmittance, and reflectivity, are bulk properties, which are highly dependent on the blend composition and temperature treatment, which do not lend themselves easily to tiny samples on libraries. Despite these problems, the development of HT techniques for polymer research has been very successful and has led to the first commercial applications. Today HT techniques are applied in many fields of polymer research.

5.9.1. Polymerization Catalysts for Polyolefins

The application of HT techniques to the identification of polymerization catalysts began early on in the field. The scientists at Symyx built the first parallel polymerization reactor and reported in 1998 the discovery of new ethylene polymerization catalysts based on Ni- and Pd-diimine complexes.[303] The use of a fully integrated HTT for primary and secondary screening as well as rapid polymer characterization was reported in 2003 and led to the discovery of Hf complexes for the polymerization of higher olefins.[303–305] Müllen and co-workers reported the development of a split&pool concept for the development of catalysts for olefin copolymerization reactions, where fluorescence microscopy was used to screen for the polymerization activity of immobilized Zr catalysts on silica beads tagged with rylene dyes.[306] A new family of Cr catalysts for ethylene polymerization was discovered by Maddox and co-workers using HTT.[307] They found very active catalysts in the ligand parameter space of salicylaldimine with bulky *o*-phenoxy groups and small imine substituents. Catalytic activities of 7000 $g\,mmol^{-1}\,h^{-1}\,bar^{-1}$ with M_w of 1100 $g\,mol^{-1}$ and activites of 95 $g\,mmol^{-1}\,h^{-1}\,bar^{-1}$ with M_w of 0.93×10^6 $g\,mol^{-1}$ were reported. Figure 29 and Figure 30 show the screening results and the ligand structure of one of the best catalysts.

In a collaboration between British Petroleum and Imperial College, HTS was applied to the search for new Cr

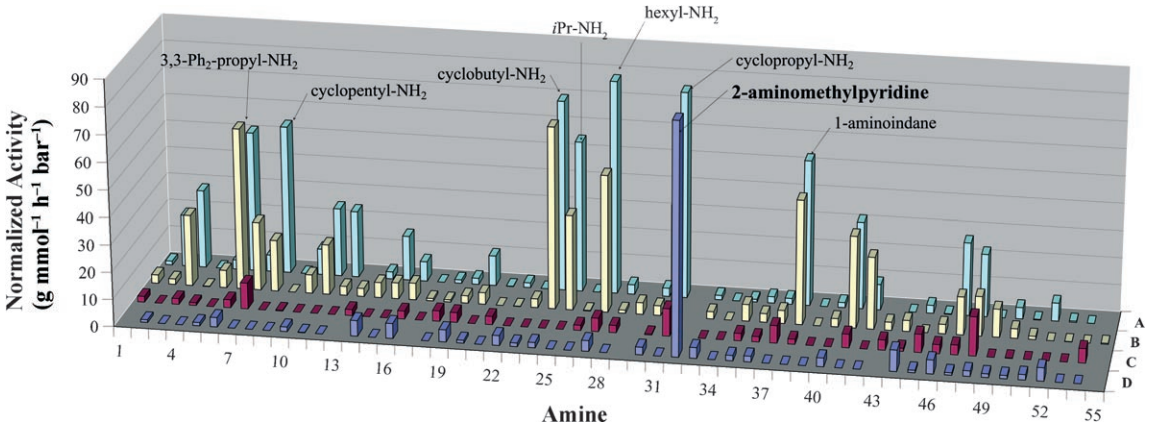

Figure 29. HTS results for ethylene polymerization (from Ref. [307], reproduced with permission from The Royal Society of Chemistry).

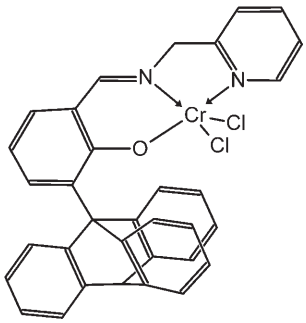

Figure 30. Typical polymerization catalyst with a bulky triptycenyl substituent (from Ref. [307], reproduced with permission from The Royal Society of Chemistry).

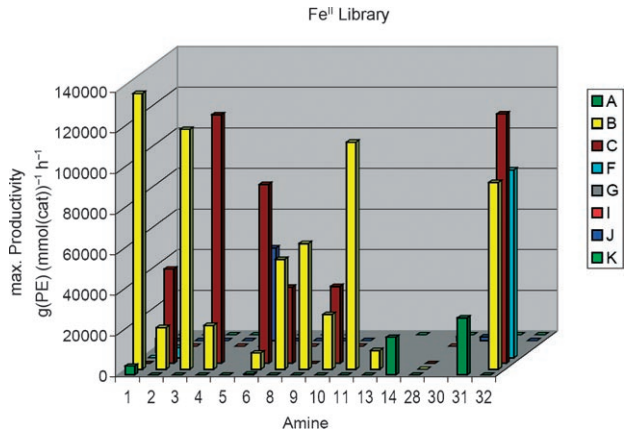

Figure 31. Activities of Fe^{II} catalysts with diimine or diiminopyridine ligands in the polymerization of ethylene (from Ref. [310]).

catalysts for ethylene polymerization.[308] The study was based on the above discovery of salicylaldimine ligands. In the primary screening, a library of 205 such Cr catalysts was tested in a 24-well reactor under standard polymerization conditions. Subsequent libraries were used to amplify leads and the hits were validated under conventional conditions. Linear high molecular weight polyethylene with catalytic activities of 3000 $g\,mmol^{-1}\,h^{-1}\,bar^{-1}$ was obtained by using bidentate 6-anthracenylsalicylaldiminato systems with alkylimino donors. A new class of tridentate *o*-tryptycenyl-substituted salicylaldimine ligands were discovered, which are thermally robust and oligomerize ethylene with catalytic activities of 10000 $g\,mmol^{-1}\,h^{-1}\,bar^{-1}$ to provide linear α-olefins.

Adams et al. reported on the discovery of new imidotitanium catalysts for the polymerization of ethylene.[309] The catalysts were prepared by semi-automated parallel syntheses from 50 commercially available amines. While details on the polymers and catalysts are given, no details on the high-throughput polymerization screening methods used are provided. At 100 °C and 7 bar ethylene, activities of up to 10000 $mol\,mmol^{-1}\,h\,bar$ (M_w 274000 $g\,mol^{-1}$) or M_w of 1.5×10^6 $g\,mol^{-1}$ at an activity of 4800 were reported.

A robust system for the synthesis and testing of ethylene polymerization catalysts has been described by Schunk and co-workers.[310] Catalysts based on Fe, Ni, and Cr were prepared through combinatorial ligand variations with the help of a synthesis robot (Figure 31). Polymerizations were carried out in a multiclave reactor (8×30 mL) at 50 °C and 10 bar, and the resulting polymers were characterized by GPC and DSC. The best catalysts provide activities of nearly 140 $kg(PE)\,mmol^{-1}\,h$ with an M_w value of > 20 kDA. An Hf-based metallocene-free catalyst for the production of highly isotactic polypropylene has also been discovered through the application of HT techniques.[311]

HTTs have been developed to screen for mixtures of three catalysts for ethylene polymerization.[312] Unusual catalysts mixtures were discovered, which produce branched polyethylene, which is not obtainable with single or two-component catalysts. The properties of the new polymers were dependent on the catalyst ratios.

5.9.2. *HT Studies on the Formation of Polymers*

Vapor deposition polymerization (VDP) in combination with masking has been used to generate libraries of aromatic polyimides on PTFE surfaces. FTIR measurements were performed to characterize the films, and UV as well as polarized light microscopy were used to investigate the complex interplay between evaporation and orientation behavior before, during, and after thermal imidization.[313]

The screening of the molecular weight of polymers, which usually requires hours per sample by conventional methods, can now be carried out in minutes in an automated fashion on short GPC columns with the help of robotics.[312] Pasch et al. have shown how size-exclusion chromatography (SEC) and high-pressure liquid chromatography (HPLC) can be accelerated for HTS applications to provide relative molecular weight distributions of a variety of polymers (PEG, PEO, epoxy resins) in 2–6 minutes per sample.[314]

In the HT development of pressure-sensitive adhesives, Mehrabi and co-workers used the absorbance of visible light in conjunction with a dye for the determination of film thicknesses. The adhesive properties of thin films in 48 arrays, prepared with a liquid dispenser, were measured automatically by recording force–displacement curves with a spherical probe adhesive tester in combination with an *x*-*y* stage. Profile parameters related to tack, peel, and shear were obtained for evaluation of each potential adhesive.[315]

A high-throughput method for screening moisture vapor transmission rates (MVTR) of polymeric barrier films has been developed that is based on a nafion-crystal violet (CVN) sensor that changes color from yellow to green upon absorption of water. HTS was demonstrated by depositing 20 emulsion-based PVC films of varying thicknesses onto the CVN sensor film and aging them at 40 °C and 90 % relative humidity for 72 h. MVTR values were accurately determined to a level of 0.9 $g\,m^{-2}\,day^{-1}$.[316]

Weathering is another important problem of materials in outdoor applications which is very time consuming and usually costly to determine. Potyrailo et al. successfully applied fluorescence imaging and spectroscopy to quantify photodegradation in arrays of materials after short exposure times.[317] The fluorescence methods detect trace amounts of degradation products arising from weathering and are much more sensitive and faster than the conventional yellowness index, with which a good correlation was found. It has been reported that the screening throughput can be increased by a factor of 150–800 compared to the conventional determination of color change and reduction in gloss.[317]

The deposition of polymer films with continuous gradients in temperature, thickness, or composition has been perfected by researchers at NIST to optimize beneficial properties.[318] Thickness gradient films were prepared by spreading a polymer solution by a knife edge with a constant acceleration of the edge movement. Composition gradient libraries were prepared quite cleverly by continually introducing and withdrawing polymer solutions A and B to and from a vial, while at the same time a syringe continually extracted solution from this vial. The syringe content was then deposited as a line on the substrate and orthogonally spread with a knife edge coater (Figure 32). Such composition gradient libraries lend themselves to efficient studies of polymer blends, which represent about a quarter of all polymers used.

Temperature gradient libraries can be obtained by placing a library on top of an aluminium block, on one side of which is a heat source and on the other a heat sink to generate a linear temperature gradient across the surface. Typical ranges are 70–160 °C over a length of 4 cm. In combination with composition (*c*) and thickness (*d*) libraries, *T*-*c*- and *T*-*d*-

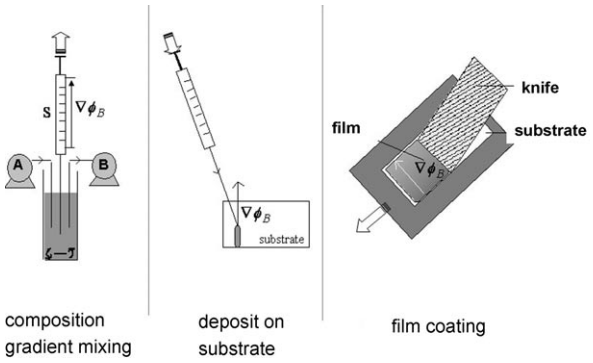

Figure 32. Deposition of composition gradient polymer films (from Ref. [318]).

dependent phenomena, such as dewetting, phase transition, and disorder have been studied very effectively. Thickness- and temperature-gradient libraries were mapped automatically by optical microscopy to investigate dewetting behavior.[319] Simon et al. have used an automated nanoindentation technique to determine the dependence of the indentation modulus on the blend composition (PLLA-PDLLA).[320] A cold-plasma reactor was developed to prepare combinatorial gradient libraries of copolymers of CO_2 with ethylene.[321]

Another important property of polymers is wettability, which is widely used to predict adhesion properties, surface wetting, and to control surface cleanliness. Bradley and co-workers have presented a simple and effective method to determine contact angles in an automated fashion in parallel by dispensing liquid droplets automatically and recording the droplet areas by imaging. The contact angles can be calculated automatically from the known relationship between the volume and droplet areas.[322]

Amis, Karim, and co-workers have reported the combinatorial mapping of surface energies of libraries of diblock copolymers.[323] After depositing a self-assembled monolayer (SAM) of octyldimethylchlorosilane on the surface of a clean Si wafer, a surface energy gradient was generated by a gradient of UV/ozone radiation. The induced change in the surface energy was characterized by contact angle measurements on water and diiodomethane droplets. Thin films of PS-PMMA block copolymers with three different molecular weights were cast on top of the SAM with a thickness gradient. The orthogonal gradients of surface energy and thickness create a library with a vast number of combinations of the test conditions. The optical image shows regions of cloudiness (islands and holes, which scatter light) and clear areas, where the color change is associated with the change in thickness (40–100 nm). The films are characterized by AFM imaging. The clear areas are attributed to ordering of the block copolymers (Figure 33).

The determination of the mechanical properties of polymers is important and nontrivial. Van Vliet and co-workers have developed a nanomechanical profiling of copolymer arrays with material volumes on the nanoliter scale.[324] The library of 1728 materials, consisting of 576 discrete polymers in triplicate (Figure 34), was printed on a standard glass slide in less than 24 h by a robotic fluid

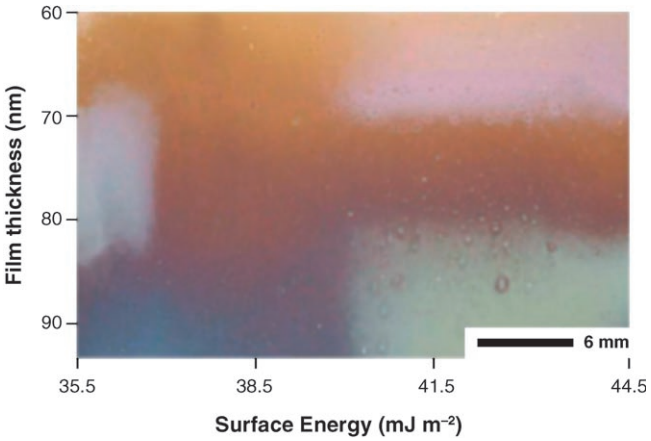

Figure 33. Optical photograph of a combinatorial gradient library showing the morphology of the thin-film block copolymer as a function of film thickness and surface energy. Islands and holes (not desired) on the surface scatter light causing the film to appear cloudy (lighter in color). The darker areas do not have surface features and do not scatter light (from Ref. [323]).

handling system. The library, the spot size, and the monomers used are shown in Figure 34. The whole library was characterized in 24 h by continuous automated acquisition and analysis of the nanoindentation. Measurement errors were less than 7.5% of the maximum elastic modulus measured.[324]

The chemical properties of polymers determine their applicability in different fields and need to be investigated for potential applications. An HTS method for the parallel evaluation of the solvent resistance of polymers was introduced by Potyrailo et al.[325] The authors used a 24-channel acoustic wave sensor system to map the solvent resistance of polycarbonate copolymers. The study of the relationship between the copolymer composition and solvent resistance led to a cubic model that quantitatively describes structure–property relationships.

Conventional quality control of thermoset resins (used for adhesives, composites, coatings) involves destructive mechanical testing as well as NIR and fluorescence spectroscopy. Eidelman et al.[326] have reported the use of FTIR microspectroscopy, confocal microscopy, and axisymmetric adhesion testing to study discrete epoxy samples cured at different temperatures and to follow curing across continuous gradient combinatorial libraries. Together, these techniques provide a comprehensive picture of the changes in the chemical and physical properties within the prepared libraries.

An instrument for the parallel measurement of the thermomechanical properties of polymers in libraries with up to 96 samples was reported by Hajduk and co-workers at Symyx Technologies.[327] Force sensors record the forces applied oscillatorily by a pin array as a function of time, environmental conditions, and motion of the translation. This method allows the determination of the modulus and loss tangent of the samples as a function of time or temperature.

Combinatorial near-edge X-ray absorption fine structure (NEXAFS) has been developed by Genzer and co-workers at NIST for the mapping of the bonding and molecular orientation of self-assembled monolayer gradients in polymer films.[328] Measurements at the C and N edges were used to map the surface density and molecular orientation of stressed gradient layers of fluorinated polymers as well as gold nanoparticles in gradients of amine-terminated organosilane films.

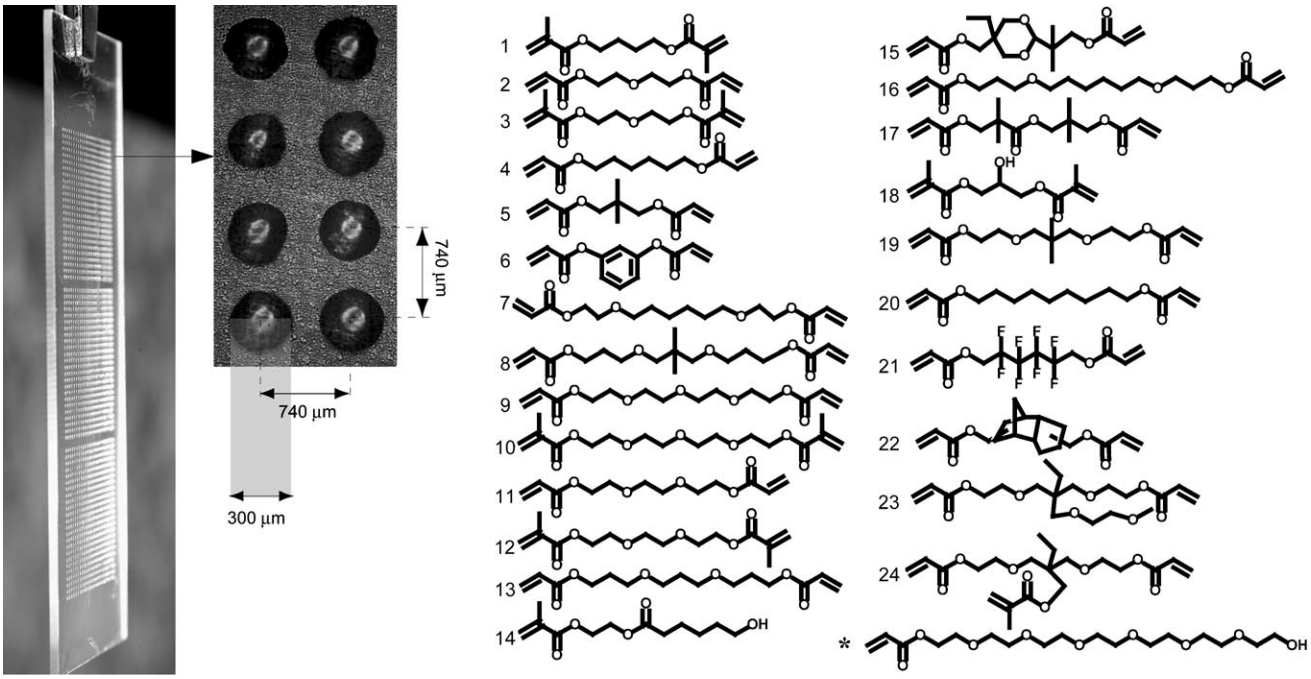

Figure 34. Discrete polymer library. Left: pairwise combinations of 24 monomers printed as 576 spot arrays in triplicate on a standard glass slide; middle: differential interference contrast image showing spots with diameters of 300 µm and thicknesses of 15 µm; right: monomer structures (from Ref. [324]).

Chemometric calibration of Raman spectra has been used to obtain the elastic modulus, stress data, density, methyl group content, and 1-hexene content from copolymer libraries of ethylene with 1-hexene.[329] The accuracy of the calibration is sufficient for screening applications, and can be used for predictions. This simple approach employs the full power of HTE in an application where conventional measurements are difficult and time consuming.

Potyrailo et al. have prepared one-dimensional libraries of polymer composites with the help of a microextruder.[330] The application was tested with bisphenol A polycarbonate in combination with TiO_2 pigments and various UV absorbers. The additives were varied systematically and the one-dimensional library was extruded as a continuous strand with a diameter of 1 mm. Reproducible step changes in the composition could be generated every 30 s. Figure 35a shows the

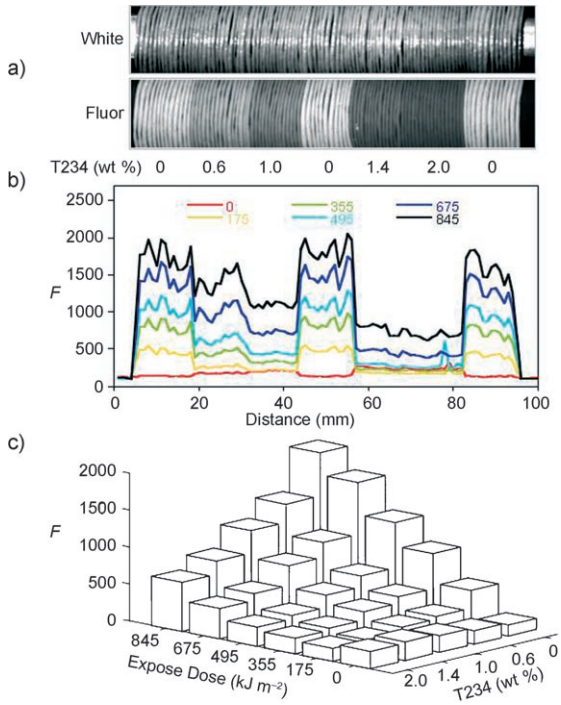

Figure 35. Performance testing of a 1D library of polymer compositions. a) White light and fluorescence images of a 1D library after irradiation at 845 kJ m^{-2}, b) spatially resolved fluorescence profiles of the 1D library at increasing levels of weathering exposure (dose: 0, 175, 355, 495, 675, and 845 kJ m^{-2}), c) weathering response of the 1D library of polymeric compositions containing increasing amounts of the UV absorber T234 at increasing levels of weathering exposure (from Ref. [330]).

library as a coil. The fluorescence image shows the spacing of the members. Weathering studies in Figure 35c show the effect of the UV absorber on the stability. The large advantage of such an approach is the realistic preparation conditions, which improve the transferability of the HT data to the performance of real polymer composites.

While various commercial synthesis robots suitable for studies of polymerization have been available for quite a while, the identification of final properties has been a bottleneck. In a valuable overview, Mülhaupt and co-workers described how the limiting factors can be overcome to allow efficient HT screening of copolymer materials.[331] A typical 5 h per sample HR NMR analysis could be replaced by 40 samples per hour by ATR-FTIR measurements. The authors point out that, for many practical applications, moderate throughput under conditions close to those of real life is advisable. Copolymers can be prepared in an automated fashion on a gram scale in vial arrays at a rate of about 100 per day. Emphasis has focused on providing a large variety of characterization data. The application of multivariate analysis with NIR has led to the determination of branching, melting points, and molecular weights.[331]

5.10. Gas Sensors

Sensors are a growing market in which there are increasing demands on selectivity and sensitivity. The properties of good sensor materials—rapid response, high selectivity, and stability as well as rapid regeneration—result to a large extent from the chemical composition and microstructure. Several HTTs have been developed, which allow extensive screening of parameters for various types of sensor materials. Vapor deposition was used early on to prepare 64 materials in an electrode array on Si wafers.[332] Such an approach is limited, since porosity, microstructure and homogeneous doping, which affect sensing properties, cannot be controlled properly.

5.10.1. Resistive Gas Sensors

Simon et al. used the wet synthesis of mixed oxides in combination with a ceramic library on an Al_2O_3 library plate with 64 printed Pt electrodes for the development of resistive sensors.[333] Application of sol–gel synthesis by the use of a special reactor allowed parallel measurement of temperature effects and resistance during exposure to pollutants.[334] The effect of various doping elements on a tungsten oxide containing 0.5% Ta was monitored by a completely automated determination of the sensor signals with HT impedance spectroscopy (in the frequency range of 10–10^7 Hz).[335]

The complete set up for HT impedance screening for gas-sensing materials has been described by Simon et al.,[336] who used doped In oxides as potential sensor materials for hydrogen. The layout of the electrode array is shown in Figure 36.

The gas-sensing properties of nanocrystalline La-doped $CoTiO_3$ for the detection of low ppm levels of propane and ethanol were discovered by Siemons and Simon using HT impedance spectroscopy (Figure 37).[337] The experimental setup and HT analysis with impressive visualization in the screening of sensor properties on application of a sequence of pollutants has been reported by Koplin et al.[338]

HT screening with gas sensor systems has also been explored in various applications by the research group of Yamada. They combined, for example, different gas-sensing semiconductors for the rapid analysis of benzene derivatives.[339] The composition of a variety of potential electro-

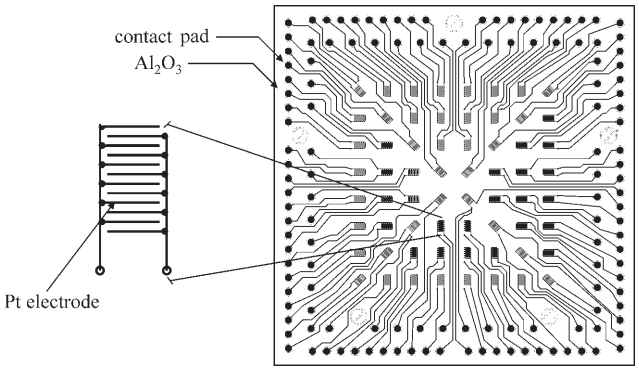

Figure 36. Layout of an 8×8 electrode array for sensor development (from Ref. [336]).

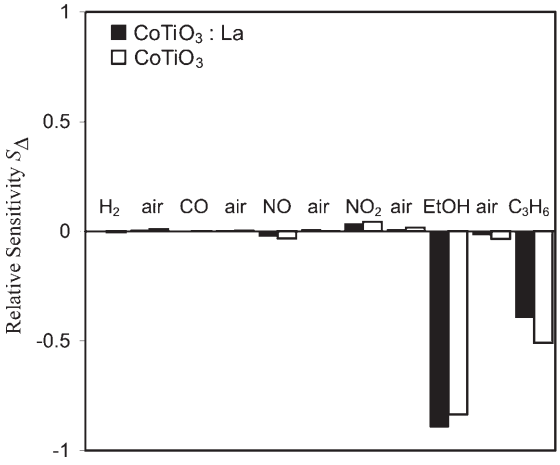

Figure 37. Response behavior of doped $CoTiO_3$ samples at 475 °C to a sequence of pollutants with the normalized sensitivity as the target quantity (from Ref. [337]).

chemical sensor materials for H_2, Co, NO, NO_2, and propene, discovered by HT techniques, has been reported by the research groups of Maier and Simon.[340] The authors used automated liquid-phase synthesis for the preparation of porous thick-film sensor materials on 64 electrode arrays. They used HT impedance spectroscopy to study the effects of doped SnO_2, WO_3, ZrO_2, CeO_2, In_2O_3, and Bi_2O_3 materials on the reponse towards the test gases.

5.10.2. *Polymeric Sensor Materials*

Polymeric sensor materials have the desirable properties for the detection of chemical and biological agents in gases and liquids. The combination of HTE with micro- and nanofabrication and microfluidics is leading to innovative sensor solutions. Modern sensing concepts cover ion-selective electrodes, optochemical sensors for ions, composite resistor polymeric films for vapors, biosensors from conducting polymers, and polymeric biosensors. The field has developed rapidly, as documented in a recent review by Potyrailo.[341]

Wolfbeis and co-workers[342] used an 8×12 microarray (Figure 38) to deposit polymers by electrochemical synthesis,

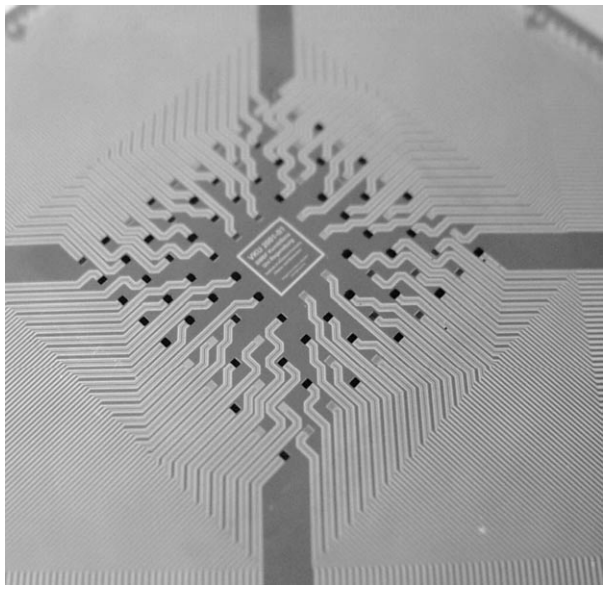

Figure 38. Sensor microarrays prepared by electrochemical polymerization on platinum electrodes. The detection of HCl with co-polymers of aniline and 3-aminobenzosulfonic acid is described as an application (from Ref. [342]).

followed by HT characterization of their chemosensitive properties to gases. The response time, recovery time, reversibility, reproducibility, sensitivity, and linearity could be studied in such adsorption–desorption cycles.

Optical sensor materials respond to analytes with a change in their optical properties, such as absorption, reflectivity, luminescence, or optical decay. A typical example of the development of such sensors by HT methods is provided by Apostolidis et al., who described the automated selection of the most suitable combinations of polymer types and indicators with plasticizers for the detection of O_2.[343]

5.11. *Heterogeneous Catalysis*

Catalysts can be differentiated by their phase of application (heterogeneous and homogeneous catalysts) or by field of application, such as biocatalysts, polymerization catalysts, petrochemical, and fine chemical catalysts. HT techniques have been developed in all these areas.

The application of HT techniques for the development of petrochemicals and fine chemicals has been reviewed recently by Corma and Serra.[344] The same authors reported on the successful use of semi-automated evolutionary strategies (ES) to optimize a selective epoxidation catalyst for cyclohexene (Figure 39)[345] as well as the strategy and results of a search for a new catalyst for the isomerization of light olefins. This latter study was driven by a genetic algorithm (GA) and resulted in interesting conclusions on the effect of calcination temperatures on the formation of tungsten-based acid sites and the disappearance of sulfur-based acid sites in mixed WO_x/ZrO_2 systems.

In 2001 scientists at UOP had already developed a combinatorial multiclave which could be used to explore

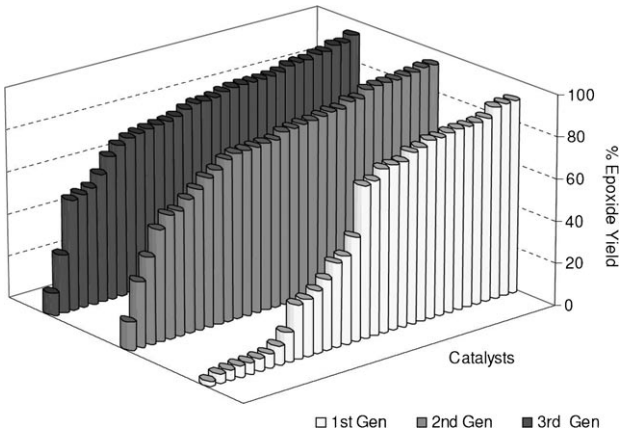

Figure 39. Development of Ti-MCM-41 catalysts by using genetic algorithums for the epoxidation of cyclohexene (from Ref. [346]).

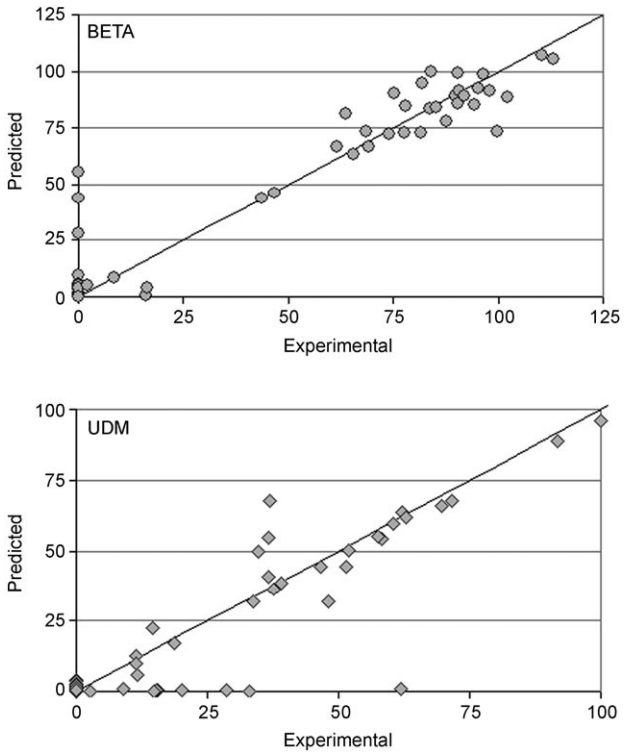

Figure 40. Quality of the predicted formations of beta and UDM zeolites by neural networks (from Ref. [352]).

hydrothermal space efficiently and effectively.[347] The setup has been used for both the discovery and scale-up of microporous solids. A noble-metal-free dehydrogenation catalyst has, for example, been developed successfully by HT techniques and commercialized.[348] A catalyst for the dehydrogenation of methylcyclohexane to toluene was developed, starting with four non-noble metals of different proportions and four different supports (alumina, titania, zirconia, and silica) prepared in different ways and then applying a statistical DoE for optimization.

An optical method for the parallel evaluation of hydrodesulfurization (HDS) catalysts was developed by Staiger et al., who proposed using binaphthothiophene as a dye for the parallel screening of HDS activity. The UV/Vis band at 353 nm was used as a direct measure of the catalytic activity.[349] Impregnation of ZSM-5 zeolites with transition metals was used in HT experiments in a search for new catalysts for the coupling of methane with CO. The screening was carried out in a 40-tube gas-phase reactor. Benzene and naphthalene on Zn/ZSM-5 were the main hydrocarbon products at temperatures as low as 500 °C, although the yield was significantly lower than that of traditional methane dehydrogenation catalysts.[350]

The new large-pore zeolite ITQ30 was discovered by the research group of Corma with the help of HT techniques.[351] The strategy applied involved the variation of selected synthesis parameters, automated synthesis of all samples, and HT characterization by XRD. Data-mining techniques (Pareto analyses) were used to extract useful knowledge. Corma and co-workers also used artificial neural networks to guide the HT synthesis of zeolites. This strategy allowed synthesis regimes to be predicted, which differentiated clearly between the formation of beta and UDM zeolites (Figure 40).[352]

Serra et al. applied an evolutionary strategy to optimize zeolite catalysts for the conversion of toluene and methanol to styrene and ethylbenzene, respectively. Within three generations, the best catalyst systems outperformed the reference system.[353] The synthesis of new IWR zeolithe polymorphs was accelerated by combining the experimental design of structure-directing agents, high-throughput, and data-mining techniques. Pure silica ITQ24 as well as borosilicate polymorphs have thus become accessible.[354] The synthesis of zeolites with pore sizes larger than 14-membered rings was believed to be hindered by the required O-Si-O bond angles. HT techniques has led the research group of Corma to identifying the untypical synthesis conditions for the generation of a new silicogermanate (ITQ33) large-pore zeolite with stable, linear 18-membered-ring channels.[355]

In a series of manuscripts, scientists at Symxy Technologies reported the development of various catalyst systems for the oxidative dehydrogenation of ethane to ethylene.[124,356] The Ni-Ta-Nb and Ni-Co-Nb systems provide catalysts which dramatically outperform the state of the art Mo-V systems. At only 300 °C, ethane conversions of over 20 % at selectivities of over 86 % are reported for $Ni_{62}Ta_{10}Nb_{28}O_x$.[128,357] Urschey et al. reported the discovery of novel butane dehydrogenation catalysts by HTE. Emission-corrected IR thermography combined with conventional gas-phase validations led to the identification of $Hf_3Y_3Ti_{94}O_x$ as a promising catalyst for the oxidative dehydrogenation of *n*-butane to *n*-butene at 450 °C (63 % selectivity for butene at 32 % conversion of *n*-butane).[358]

An HT technique has been reported by Hancu et al. for the chlorination of aromatic hydrocarbons.[359] The chlorination of *o*-xylene with zeolites was carried out in a 48-well array reactor and product analysis was performed afterwards by conventional GC. The selective formation of 4-Cl-*o*-xylene was found to be affected by the nature of the zeolite, the

bifunctional co-catalyst, and the operating temperature. The reaction can also be carried out in the absence of solvents. The highest selectivity was obtained with the H-beta zeolite.

The production of hydrogen from water and hydrocarbons (steam reforming) is of fundamental importance for the development of fuel cells. The activity of present noble-metal-free catalysts, such as CuZn or FeCr, is not sufficient. Research groups from Symyx and Honda reported results from a fully automated HT technique for primary and secondary screening in the search for improved catalysts for the production of hydrogen.[360] The best Pt-free catalysts (Ni-Mn-In-Sn) operated in the temperature range 250–450 °C, while the best low-Pt catalysts (for example, PtCeCoVMo-FeNa) operate at 200–350 °C.[361] Copper-free catalysts have been developed for the water gas shift reaction by application of evolutionary algorithms and HTE. The best catalysts are based on Cr and Fe on ZrO_2 as support materials.[362] In an HT search for coking-resistant and noble-metal-free catalysts for the dry reforming of methane, Kim and Maier identified Ni-Ce mixed oxide as the most promising catalyst from the more than 5000 formulations studied. After doping the catalysts with Zr or Al, they showed high catalytic activity, without the need for preactivation, as well as high coking resistance and excellent long-time stability.[363] Mechanistic studies on this new catalyst material revealed the solid solution of Ni in CeO_2 as the dominating microstructure responsible for the unusual catalytic behavior.[364] In situ detection of the formation of syngas through the optical read-out of Cu reduction has been applied by Omata et al. for HTS of catalysts for oxidative methane reforming under pressure.[365]

Uniformly sized, multimetallic catalyst nanoparticles deposited onto different substrates (for example, γ-Al_2O_3, CeO_2, TiO_2, SiO_2, or Y-ZrO_2) can be prepared by high-throughput through pulsed laser ablation (HT-PLA). The method was developed by Senkan et al., and its use was demonstrated in a search for catalysts for the selective oxidation of propylene.[366] Borade et al. have reported the development and scale-up of catalysts by HT techniques for the selective oxidation of alcohols in the liquid phase by air and H_2O_2.[367] Redox molecular sieves based on vanadium were identified as superior catalysts. IR thermography was used by Schuyten and Wolf to identify the most active catalysts for the selective oxidation of methanol to CO_2 and H_2 from libraries of catalysts with composition variation. Validation of the hits was performed in conventional flow reactors. The best catalysts within the Cu/Zn/Pd system provided, after promotion with 10 % Zr, a 95 % H_2 selectivity at quantitative MeOH conversion.[368] Noble-metal-free Co-Mn catalysts for the selective low-temperature oxidation of CO with air have been discovered with the help of HTE by Saalfrank and Maier.[369] The authors applied a directed evolutionary strategy, best described as hit selection from the starting library, followed by compositional sequential optimization, and doping to generate the subsequent libraries.[370] Doping of the optimized ternary catalyst with Pt resulted in a moisture-stable, selective catalyst for the oxidation of CO.[371] The direct, selective methanation of CO has been developed for gas purification of hydrogen for ammonia synthesis and is also of interest for fuel-cell applications. An HT technique has been presented by Yaccato et al. which allows the efficient search for new catalysts to competitively convert CO and CO_2 into methane. Ru, Rh, and Ni appear to promote methanation, while Pt tends to catalyze the reverse water gas shift reaction.[372]

Co, Ce, and In impregnated H-ZSM-5 catalyst libraries have been studied for the reduction of NO with methane. A multichannel UV-adsorption setup was developed to evaluate the catalyst performance. The best catalyst identified contained a 1:1 ratio of Ce/In at a loading of 2 % on the zeolite.[373] A five factor, two-level full factorial design was used by Schmitz et al. to develop supported Pt catalysts for the oxidation of NO in an HT approach that was composed of automated synthesis, screening, and statistical analysis. The relative order of influence of the factors at an optimal reaction temperature of 200 °C was: support > pretreatment > loading > calcination atmosphere > calcination temperature > precursor salt.[374]

Noda et al. presented a simple method to rapidly screen for catalysts capable of growing vertically aligned single-walled carbon nanotubes (SWCTs). The best catalysts discovered are based on Mo-Co material on silica supports.[375] Automated thermogravimetric analysis (TGA) has been used to examine libraries of alkali-metal-doped mixed oxides for their relative activity to combust diesel soot.[376] The strong influence of alkali-metal ions on the activity of diesel soot combustion catalysts was also confirmed by studies by Olong et al.[377] In this investigation, HTS was performed by ecIRT, and only selected hits were further characterized by TGA. In an interesting study on the HT search for low-temperature combustion catalysts for air pollutants, the authors noted a strong dependence of catalytic performance on the nature of the model pollutants used (dimethylamine DMA, benzene, and dimethylsulfide). The best catalyst ($Rb_3Co_{10}Cu_{48}Mn_{39}O_x$) combusts DMA at 150 °C. The authors also found several catalysts, such as $Co_{20}Cu_{50}Mn_{30}O_x$, which significantly reduced the formation of NO_x during quantitative DMA combustion at 250 °C.[378]

5.11.1. Formulations

Formulations are the backbone of many product developments in industry, and combinatorial or HT approaches are perfect means to accelerate their developments. Typical examples of materials based on formulations are paints, detergents, coatings, adhesives, and composites. As a consequence of their systematic, but somewhat empirical nature, formulation developments are centered in industrial research & development departments. The following example from BASF is an illustration of a typical formulations problem. Polymer coatings are affected by a large number of parameters, as illustrated in Figure 41.

Robotic systems are used to vary parameters and identify optimal formulations. Figure 42 shows flow curves of 30 combinations of thickener (A–F), solvent, and binder for paint formulations. The results of microindentation measurements as a function of acrylate binder and amount of isocyanate cross-linker are shown in Figure 43.[379] Clearly, the materials generally become softer with increasing elas-

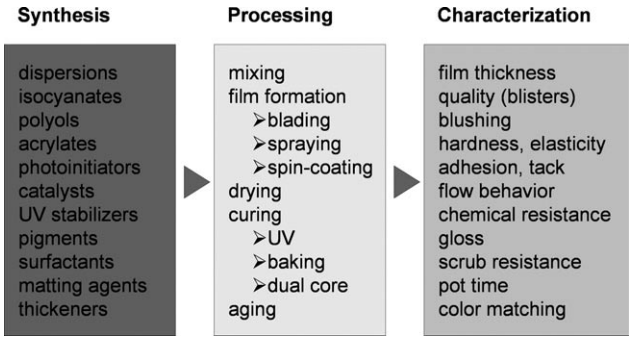

Figure 41. Multiparameter space for the formulation of coatings (from Ref. [379]).

ticity. The best materials with sufficient hardness but still acceptable elasticity can now be easily spotted.

Combinatorial methods to prepare and screen polymer formulations for biomaterials have been used successfully by the research group of Kohn. The development was driven by efficient parallel synthesis of suitable polymers, rapid screening assays for various cellular responses in the presence of the polymers, and semiempirical modeling using an artificial neural network to predict protein adsorption and cell growth.[380]

It is estimated that 46000 pieces of plastic float on every square mile of our oceans. The development of biodegradable plastic materials is thus of increasing environmental importance. Lochhead et al. have developed HT approaches to accelerate the search for such new materials. Within a three-month study, 2,4-dihydroxyphenol was identified as the only suitable coupling reagent out of 110 polyphenols for the preparation of biodegradable packing materials.[381]

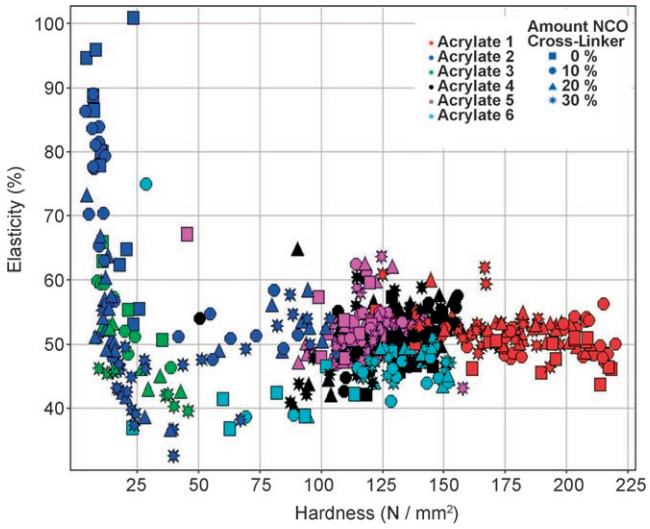

Figure 43. Effect of different types of acrylate binder and varying amounts of isocyanate cross-linker on the elasticity and hardness of UV coatings (from Ref. [379]).

6. Promises, Problems, and Successes

6.1. Promises

When introduced approximatly 12 years ago, the application of combinatorial chemistry in materials research promised:

- acceleration of basic research;
- fast discovery of knowledge;
- reduced development times;
- reduced time for products to the market;

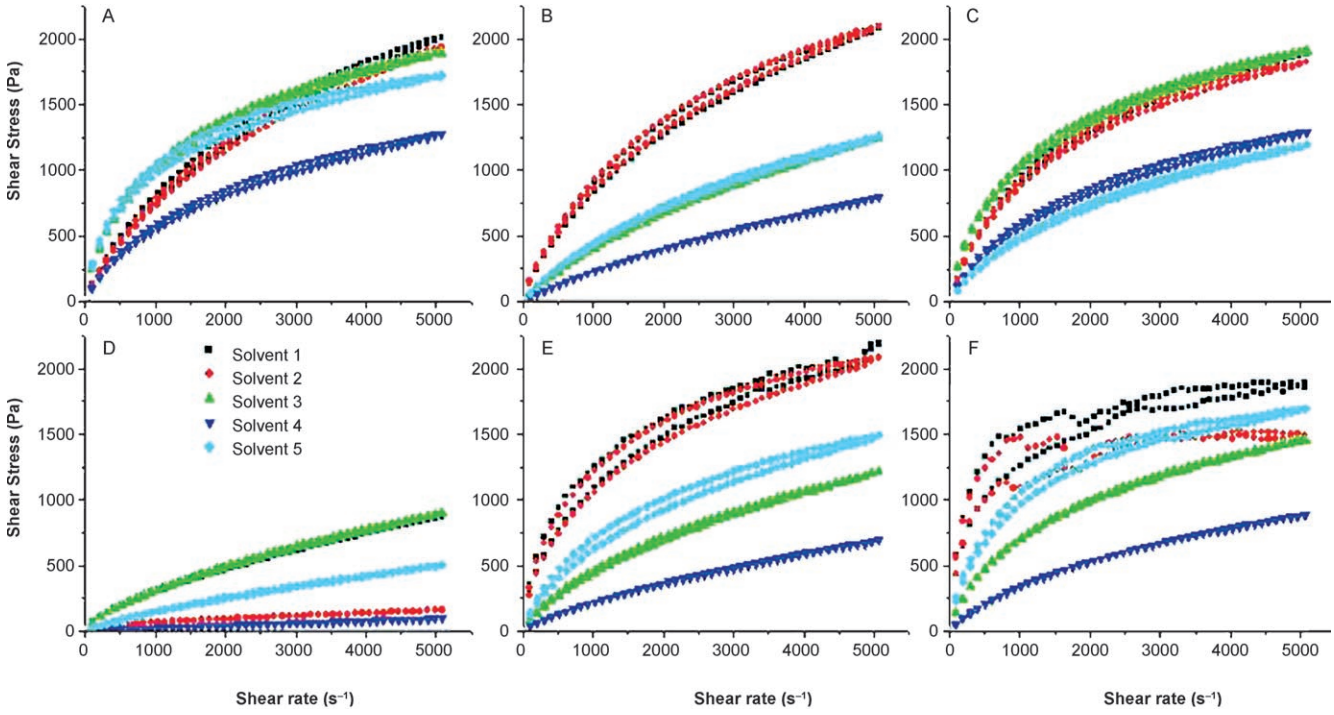

Figure 42. Development of paint coatings: optimization of the rheological behavior as a function of the thickener (A–F) and solvent (from Ref. [379]).

- rapid sampling of large parameter spaces;
- rapid collection of comparable data;
- discovery of new materials.

As documented in many examples in this Review, all of these promises have been fulfilled. HTE has developed into an extremely successful new technology and the last three promises above are also applicable to basic research. Unfortunately, most of the scientific community has still not realised how valuable the automated sampling of large parameter spaces really is. The most important advantages include reproducible preparation of materials and comparability of measured data. Such collections of comparable data allow the study of correlations and trends in ways never possible by conventional one-at-a-time experimentation.

6.2. Problems

Despite the many successful examples mentioned above, HTE cannot be applied to all problems. High-throughput not only generates data rapidly, it also generates false positives and negatives, of which the experimentor must be aware. There is no documention of how many HT applications have had to be abandoned because of the lack of agreement with data from conventional experiments. Poor HTT performance in individual cases may result from principal problems, but more likely they may be the result of a poor choice of technology. Many of the above mentioned examples are rather elaborate and document large efforts dedicated to the development of a suitable HT technique. When applying HTTs, it is essential in the early tests to already verify the agreement of the HT data with those obtained from conventional tests.

A general acceptance of HT techniques has not been reached and it is still often conceived as a means to replace intelligent planning by a large number of experiments. Many scientists in academia and industry have not realized the dramatic progress made in HTT and their view is still affected by the following prejudices:

- not suitable for the development of complex materials;
- findings or hits may not apply, since HT conditions often do not correspond with realistic production or conventional laboratory conditions;
- only a simple parallelization of experiments without use of scientific knowledge;
- suitable only for industrial developments;
- not suitable for basic research.

Most of these arguments have long been disproven by state of the art techniques in the field. It is a personal decision to accept or ignore this. Another more psychological barrier is to allow HT philosophies into the planning and execution of experiments—which many view as a threat to the conventional approaches of daily laboratory work.

More serious is the general lack of access to HT workflows and technologies. Many laboratories are not equipped for HTE and also lack experience and manpower. The installation of permanent HTTs in a laboratory requires relative expensive HT equipment and the use of complex software tools, which are also either very expensive or have to be developed in-house. The use of HT equipment may result in a dramatic increase in consumables (such as solvents or precursors), while the software requires at least one permanent staff member for proper use, maintenance, and adjustments. In academia, the former may become unaffordable, while the latter is often prohibitive. Another problem is interdisciplinarity, especially in academia. It is difficult to find a graduate chemistry student who is at the same time a good experimentalist, able to interface, construct, and modify equipment, and is aware of artificial intelligence and software tools. Furthermore, the permanent change of co-workers, who leave for first employment, does not allow the proper maintenance of sophisticated HT workflows by graduate students. For industry, the implementation of HTTs is therefore associated with high investments of capital and manpower and, because of the risk involved, smaller companies in particular are hesitant. These factors are responsible for the well-recognized lack of HTE in academia and smaller companies. The lack of presence in academia also leads to a lack of HTT in education, which furthermore reduces the future acceptance of these technologies. Although this is generally true, these arguments should not prevent scientists from implementing HTT in the laboratory, even if it is at a moderate level and on a small budget. If done carefully, even small levels of HT, such as running ten instead of one experiment at a time, can have dramatic effects on efficiency, as well as with additional benefits of increased comparability and reproducibility.

Complex synthesis procedures developed for the conventional preparation of catalysts or materials are often not suitable for automation, parallelization, and HTE. Here, alternative methods suitable for HT have to be developed before HTE can be applied. This often prevents the use of HTE in specific applications.

There are also solutions to a broader access to HTTs. HTT centers or institutes could be created, where workflows and software would be available for companies and academia to hire. One such institute, FLAMAC, has just been founded in Gent, Belgium, where partners can test or use workflows for coatings and developments in other formulations. In academia, departmental workflows could be installed, which could be shared similarly as has been the general practice with expensive analysis equipment (such as NMR, MS, or electron microscopy). In the area of laboratory equipment, many companies offer affordable systems of parallel reactors or laboratory robots, which can contribute to significant acceleration in academic laboratories or small- and medium-sized companies.

As evident from the many examples cited above, many specialized solutions exist for individual problems in materials research. The lack of general workflows or technologies furthermore reduces the broad use. Too many specialized solutions (hardware and software) and the complete lack of standards raise the barrier further.

Another problem is the broad lack of informatics tools for general uses, such as data bases, sophisticated visualizations, data mining, DoE, and automation of the control of work-

flows. A lack of affordable generalized software solutions is evident and is clearly responsible for the still broad use of Excel sheets in many laboratories. At present, the use of the sophisticated methods described above is limited to companies and a few laboratories. This situation will certainly change with time, as general software tools—such as the visualization and data-mining package Spotfire—continue to implement many of the accepted modeling and data-mining tools for general use.

6.3. Successes and Discoveries

Many success stories and discoveries in the HT area have already been summarized above. Some of these groundbreaking discoveries are a blue phosphor, a red phosphor, ethane dehydrogenation catalysts, catalysts for the water gas shift reaction, various new zeolites, a polyimide nanofiltration membrane, Cr-based and Fe-based catalysts for ethylene polymerization, CO oxidation catalysts, dry reforming catalysts, electrochemical sensor materials, dielectric materials, an optically transparent ferromagnet, and an optically transparent transistor. These successes are not only limited to materials and catalysts for industrial base chemicals, but also the development of catalytic processes for pharmaceuticals and pharmaceutical intermediates (not considered in this Review) is often under severe time pressure and can be speeded up significantly up by HTE. For example, Lefort et al. described their protocols used to accelerate the development of a catalytic process for the fabrication of an important intermediate through enantioselective hydrogenation of a substituted cinnamic acid derivative, which resulted in a multi-ton process at DSM.[382]

HTT has not only led to the acceleration of conventional synthesis and characterization through parallelization and automation, it has also led to many new synthesis methods and synthesis strategies, such as spatially resolved thin film deposition, composition-tolerant sol–gel methods, and gradient libraries for materials and polymers. HTTs have also led to many new characterization methods, such as rapid screening of the molecular-weight distribution of polymers, rapid screening of enantiomeric excess, parallel screening of heats of reaction by emissivity-corrected IR thermography, parallel screening of wettability, an increasing variety of 2D scanning methods, and laser-based techniques. The development of QCAR, QSAR, and QSPR have only become possible with HTTs. One might ask the question, why such a sudden flood of new methods, and why these methods are not used in conventional research? The answer is simple: demand. In conventional research the established methods are sufficient and their reliability is well known. For example, there was no need for a rapid determination of the molecular-weight distribution of polymers, so why bother? Furthermore, why use a new method with a larger error for single measurements?

It has been shown above that HTT can now routinely be applied to fast automated preparation, characterization, and testing of materials of many kinds. Reduced development times, higher success rates, and better reproducibility have led many companies to install their own HT operations (BASF, BP, Bayer, Degussa, DOW, Dupont, Exxon Mobile, GE, Henkel, UOP, etc.). Several HT companies have also been founded (Symyx Technologies, hte-AG, Avantium, Ilika, Bosch Lab Systems, Accelergy, etc.). For example, Symyx started operation in 1996 with 2 employees and today they have over 350 employees. The hte AG was founded in 1999 with 5 employees and now has over 100 employees. It is these specialized companies which push hardware and software developments as well as their integration to the boundaries of HTT that allow them to achieve productivities and throughput that regular R&D or academic laboratories can never reach. It is therefore not surprising that these technology leaders increasingly sell complete HT development plants or HT laboratories in the multimillion US$ price range. The increasing demand for such highly sophisticated systems also highlights the increasing trust and need for HTT on a larger scale.

Particularly difficult to report on is the actual products on the market that were developed by HTTs. HTT is still a young technology that is used by companies to save time and costs. It takes several years to get a product to market (scale up, customer-specific developments, production technology, patents, permissions, environmental evaluations, long-time performance, etc.). Most companies are very hesitant to reveal success stories, especially when associated with materials optimization, complex formulations, or more efficient catalysts. However, some first examples of HTT products have been revealed[383] and are summarized in Table 1.

Table 1: Summary of successful product developments based on HTT.

Developer	Customer	Product
Symyx	Agfa	radiography detector DirectriX
	DOW	catalyst for versify elastomers
	JSR	polymer for electronics applications
hte-AG	BASF	heterogeneous catalysts for intermediates
Arkema		silyl additive for antifouling boat paints
DOW		catalyst for asymmetric hydrogenation
		polymerization catalyst for propylene (SHAC)
UOP		C5–C6 isomerization catalyst
GE		catalyst for polycarbonate

7. Conclusions

In this Review with selected examples it has been shown that HTT has been validated in many areas of materials research and has been applied successfully to a wide area of applications, although many additional contributions in the literature worth mentioning could not be covered. HTTs have already led to many discoveries and the first products developed by HTE are on the market. Many research groups associated with basic research have not yet realized that many types of basic research can benefit from the introduction of parallel experiments and it is highly recommended that research groups think about the application of HTE methods. It is hoped that this article will stimulate some readers to apply HTE on a moderate level in their daily work.

HT methods have demonstrated their power and they are already on their way to becoming standard technologies. In the long run, laboratories and companies without HTTs will lose out against laboratories or companies using HTTs. More and more materials will be discovered, developed, or optimized by the use of HTTs, which could lead to a dramatic shift in the competitiveness. HTTs are becoming an increasingly important factor of R&D in industries and academia. The integration and broad use of HTT may become a decisive factor in maintaining technological advantages in a global market.

In contrast to drug development, where HTT already reaches sampling rates of 2 million samples per day, its perfection in materials research will advance more slowly because of the wide variation of technologies and the many isolated solutions. The important future quests for materials research, such as renewable energies, climate change, and growing problems with global food supply, will increasingly depend on HTT.

We thank the members of our research group, G. Frenzer, D. K. Kim, P. Rajagopalan, M. Krämer, N. Olong, M. Mentges, D. Rende, M. Seyler, and T. Weiss for their help with compiling the literature section. All the financial supporters over the last ten years, including MPG, BMBF, BMWA, DBU, Hoechst, Bayer, Creavis, Umicore, and Heraeus are also gratefully acknowledged. W.F.M. thanks the members of the "DECHEMA-Arbeitskreis Hochdurchsatzforschung", especially T. Brinz and W. Schrof, and their "Positionspapier Hochdurchsatztechnologien in der Materialforschung".[383]

Received: September 8, 2006
Published online: July 19, 2007

[1] D. Maclean, J. J. Baldwin, V. T. Ivanov, Y. Kato, A. Shaw, P. Schneider, E. M. Gordon, *Pure Appl. Chem.* **1999**, *71*, 2349 – 2365.
[2] F. Schueth in *Winnacker-Küchler Chemische Technik*, 5th ed. (Eds.: R. Dittmeyer, W. Keim, G. Kreysa, A. Oberholz), Wiley-VCH, Weinheim, **2004**, pp. 549 – 585.
[3] R. Hoogenboom, M. A. R. Meier, U. S. Schubert, *Macromol. Rapid Commun.* **2003**, *24*, 15 – 32.
[4] J. J. Hanak, *Appl. Surf. Sci.* **2004**, *223*, 1 – 8.
[5] J. J. Hanak in *Combinatorial Materials Science* (Eds.: X.-D. Xiang, I. Takeuchi), Marcel-Dekker, New York, **2003**, pp. 7 – 34.
[6] J. J. Hanak, *J. Mater. Sci.* **1970**, *5*, 964 – 971.
[7] R. Thomas, J. A. Moulijn, V. H. J. De Beer, J. Medema, *J. Mol. Catal.* **1980**, *8*, 161 – 174.
[8] J. G. Creer, P. Jackson, G. Pandy, G. G. Percival, D. Seddon, *Appl. Catal.* **1986**, *22*, 85 – 95.
[9] X.-D. Xiang, X. Sun, G. Briceno, Y. Lou, K.-A. Wang, H. Chang, W. G. Wallace-Freedman, S.-W. Chen, P. G. Schultz, *Science* **1995**, *268*, 1738 – 1740.
[10] E. Danielson, J. H. Golden, E. W. McFarland, C. M. Reaves, W. H. Weinberg, X. D. Wu, *Nature* **1997**, *389*, 944 – 948.
[11] B. Jandeleit, D. J. Schaefer, T. S. Powers, H. W. Turner, W. H. Weinberg, *Angew. Chem.* **1999**, *111*, 2648 – 2689; *Angew. Chem. Int. Ed.* **1999**, *38*, 2494 – 2532.
[12] R. Ramos, M. Menendez, J. Santamaria, *Catal. Today* **2000**, *56*, 239 – 245.
[13] M. Nele, A. Vidal, D. L. Bhering, J. C. Pinto, V. M. M. Salim, *Appl. Catal. A* **1999**, *178*, 177 – 189.
[14] F. A. Castillo, J. Sweeney, P. Margl, W. Zirk, *QSAR Comb. Sci.* **2005**, *24*, 38 – 44.
[15] http://www.dow.com, **2006**.
[16] *Experimental Design for High Throughput Materials Development* (Ed.: J. N. Cawse), Wiley, Chichester, **2003**.
[17] D. R. Bingham, R. Sitter, *Technometrics* **1999**, *41*, 62 – 70.
[18] L. A. Trinca, S. G. Gilmour, *Comput. Statistics Data Anal.* **2000**, *33*, 25 – 43.
[19] S. Bisgaard, M. Sutherland, *Qual. Eng.* **2003**, *16*, 157 – 164.
[20] A. Corma, M. J. Diaz-Cabanas, M. Moliner, C. Martinez, *J. Catal.* **2006**, *241*, 312 – 318.
[21] J. H. Van Drie, M. Lajiness, *Drug Discovery Today* **1998**, *3*, 274 – 283.
[22] T. Pötter, H. Matter, *J. Med. Chem.* **1998**, *41*, 478 – 488.
[23] R. C. Lewis in *Molecular Diversity in Drug Design* (Eds.: P. M. Dean, R. A. Lewis), Kluwer, Dordrecht, **1999**, pp. 221 – 248.
[24] J. S. Mason in *Molecular Diversity in Drug Design* (Eds.: P. M. Dean, R. A. Lewis), Kluwer, Dordrecht, **1999**, pp. 67 – 91.
[25] D. K. Agrafiotis in *The Encyclopedia of Computational Chemistry*, *Vol. 1* (Eds.: P. von R. Schleyer, N. L. Allinger, T. Clark, J. Gasteiger, P. A. Kollman, H. F. Schaefer, P. R. Schreiner), Wiley, Chichester, **1998**, pp. 742 – 761.
[26] J. Bajorath, *J. Chem. Inf. Comput. Sci.* **2001**, *41*, 233 – 245.
[27] D. K. Agrafiotis, J. L. Myslik, F. R. Salemme, *Mol. Diversity* **1998**, *4*, 1 – 22.
[28] *Concepts and Applications of Molecular Similarity*, (Eds.: M. A. Johnson, G. M. Maggiora), Wiley, New York, **1990**.
[29] R. D. Brown, Y. C. Martin, *J. Chem. Inf. Comput. Sci.* **1996**, *36*, 572 – 584.
[30] K. R. Changwon Suh, *QSAR Comb. Sci.* **2005**, *24*, 114 – 119.
[31] S. Sieg, B. Stutz, T. Schmidt, F. Hamprecht, W. F. Maier, *J. Mol. Model. (Online) 12*, 611 – 619.
[32] C. H. Reynolds, *J. Comb. Chem.* **1999**, *1*, 297 – 306.
[33] C. Klanner, D. Farrusseng, L. Baumes, C. Mirodatos, F. Schueth, *QSAR Comb. Sci.* **2003**, *22*, 729 – 736.
[34] C. Klanner, D. Farrusseng, L. Baumes, M. Lengliz, C. Mirodatos, F. Schüth, *Angew. Chem.* **2004**, *116*, 5461 – 5463; *Angew. Chem. Int. Ed.* **2004**, *43*, 5347 – 5349.
[35] D. Farrusseng, C. Klanner, L. Baumes, M. Lengliz, C. Mirodatos, F. Schueth, *QSAR Comb. Sci.* **2005**, *24*, 78 – 93.
[36] A. Corma, J. M. Serra, P. Serna, M. Moliner, *J. Catal.* **2005**, *232*, 335 – 341.
[37] M. Holena in *High-Throughput Screening in Chemical Catalysis* (Eds.: A. Hagemeyer, P. Strasser, A. F. Volpe), Wiley-VCH, Weinheim, **2004**, pp. 153 – 174.
[38] A. Holzwarth, P. Denton, H. Zanthoff, C. Mirodatos, *Catal. Today* **2001**, *67*, 309 – 318.
[39] B. Li, P. Sun, Q. Jin, J. Wang, D. Ding, *J. Mol. Catal. A* **1999**, *148*, 189 – 195.
[40] A. S. McLeod, L. F. Gladden, *J. Chem. Inf. Comput. Sci.* **2000**, *40*, 981 – 987.
[41] A. Eftaxias, J. Font, A. Fortuny, J. Giralt, A. Fabregat, F. Stüber, *Appl. Catal. B* **2001**, *33*, 175 – 190.
[42] J. H. Holland in *Adaption in Natural and Artificial Systems*, The University of Michigan Press, (1st ed. **1975**), **1992**.
[43] K. A. De Jong, PhD Thesis, University of Michigan, **1975**.
[44] D. E. Goldberg in *Genetic Algorithms in Search, Optimization and Machine Learning*, Addison Wesley, **1989**.
[45] D. X. Liu, H. L. Jiang, K. X. Chen, R. Ji, *J. Chem. Inf. Comput. Sci.* **1998**, *38*, 233 – 242.
[46] V. J. Gillet, W. Khatib, P. Willett, P. J. Fleming, D. V. S. Green, *J. Chem. Inf. Comput. Sci.* **2002**, *42*, 375 – 385.
[47] R. D. Brown, D. E. Clark, *Expert Opin. Ther. Pat.* **1998**, *8*.

[48] D. Wolf in *Principles and Methods for Accelerated Catalyst Design and Testing* (Eds.: E. G. Derouane, V. Parmon, F. Lemos, F. R. Ribeiro), Kluwer, Dordrecht, **2002**, pp. 125–133.
[49] D. Wolf, O. V. Buyevskaya, M. Baerns, *Appl. Catal. A* **2000**, *200*, 63–77.
[50] U. Rodemerck, M. Baerns, M. Holena, D. Wolf, *Appl. Surf. Sci.* **2004**, *223*, 168–174.
[51] D. Wolf, M. Baerns in *Experimental Design for Combinatorial and High-Throughput Materials Development* (Ed.: J. N. Cawse), Wiley, Hoboken, **2003**, p. 147.
[52] G. Grubert, E. V. Kondratenko, S. Kolf, M. Baerns, P. C. Van Geem, R. F. Parton, *Catal. Today* **2003**, *81*, 337–345.
[53] F. Clerc, D. Farrusseng, M. Lengliz, C. Mirodatos, S. R. M. Pereira, R. Rakotomalala, *Rev. Sci. Instrum.* **2005**, *76*.
[54] S. R. M. Pereira, F. Clerc, D. Farrusseng, J. C. van der Waal, T. Maschmeyer, C. Mirodatos, *QSAR Comb. Sci.* **2005**, *24*, 45–57.
[55] A. Corma, J. M. Serra, A. Chica in *Principles and Methods for Accelerated Catalyst Design and Testing* (Eds.: E. G. Derouane, V. Parmon, F. Lemos, F. R. Ribeiro), Kluwer, Dordrecht, **2002**, pp. 153–172.
[56] A. Corma, J. M. Serra, A. Chica, *Catal. Today* **2003**, *81*, 495–506.
[57] G. H. Jóhannesson, T. Bligaard, A. V. Ruban, H. L. Skriver, K. W. Jacobsen, J. K. Nørskov, *Phys. Rev. Lett.* **2002**, *88*, 255506.
[58] J. Greeley, T. F. Jaramillo, J. Bonde, I. Chorkendorff, J. K. Nørskov, *Nat. Mater.* **2006**, *5*, 909–913.
[59] A. Sundaram, V. Venkatasubramanian, *J. Chem. Inf. Comput. Sci.* **1998**, *38*, 1177–1191.
[60] R. Giro, M. Cyrillo, D. S. Galvao, *Chem. Phys. Lett.* **2002**, *366*, 170–175.
[61] R. Giro, M. Cyrillo, D. S. Galvao in *Materials Research Society Symposium Proceedings, 700, Combinatorial and Artificial Intelligence Methods in Materials Science*, **2002**, pp. 283–288.
[62] R. Giro, M. Cyrillo, D. S. Galvao, *Mater. Res.* **2003**, *6*, 523–528.
[63] I. Rechenberg, *Evolutionsstrategie '94*, Frommann-Holzboog, Stuttgart, **1994**.
[64] J. Klockgether, H.-P. Schwefel, *Proceedings of the 11th Symposium on Engineering Aspects of Magnetohydrodynamics*, Pasadena, **1970**, pp. 141–148.
[65] G. Kirsten, W. F. Maier, *Appl. Surf. Sci.* **2004**, *223*, 87–101.
[66] M. Holena, M. Baerns in *Experimental Design for Combinatorial and High-Throughput Materials Development* (Ed.: J. N. Cawse), Wiley, New York, **2003**, pp. 163–202.
[67] S. Kito, T. Hattori, Y. Murakami, *Appl. Catal. A* **1994**, *114*, L173–L178.
[68] T. Hattori, S. Kito, *Catal. Today* **1995**, *23*, 347–355.
[69] M. Sasaki, H. Hamada, Y. Kintaichi, T. Ito, *Appl. Catal. A* **1995**, *132*, 261–270.
[70] Z.-Y. Hou, Q. Dai, X.-Q. Wu, G.-T. Chen, *Appl. Catal. A* **1997**, *161*, 183–190.
[71] B. K. Sharma, M. P. Sharma, S. K. Roy, S. Kumar, S. B. Tendulkar, S. S. Tambe, B. D. Kulkarni, *Fuel* **1998**, *77*, 1763–1768.
[72] M. Holea, M. Baerns, *Catal. Today* **2003**, *81*, 485–494.
[73] S. Haykin, *Neural Networks: A Comprehensive Foundation*, Prentice Hall, New York, **1994**.
[74] K. Mehrotra, C. K. Mohan, S. Ranka, *Elements of Artificial Neural Networks*, MIT Press, Cambridge, **1997**.
[75] J. Zupan, J. Gasteiger, *Neural Networks for Chemists*, Wiley-VCH, Weinheim, **1993**.
[76] J. Zupan, J. Gasteiger, *Neural Networks in Chemistry and Drug Design: An Introduction*, Wiley-VCH, Weinheim, **1999**.
[77] M. A. Henson, *Comput. Chem. Eng.* **1998**, *23*, 187–202.
[78] *Scientific Applications of Neural Nets* (Eds.: J. W. Clark, T. Lindenau, M. L. Ristig), Springer, Berlin, **1998**.
[79] L. Glielmo, M. Milano, S. Santini, *IEEE-ASME Trans. Mechatronics* **2000**, *5*, 132–141.
[80] T. R. Cundari, J. Deng, Y. Zhao, *Ind. Eng. Chem. Res.* **2001**, *40*, 5475–5480.
[81] K. Omata, T. Umegaki, Y. Watanabe, M. Yamada, *J. Jpn. Pet. Inst.* **2002**, *45*, 192–195.
[82] S. Nandi, P. Mukherjee, S. S. Tambe, R. Kumar, B. D. Kulkarni, *Ind. Eng. Chem. Res.* **2002**, *41*, 2159–2169.
[83] A. Corma, J. M. Serra, E. Argente, V. Botti, S. Valero, *Appl. Catal. A* **2003**, *254*, 133–145.
[84] J. M. Serra, A. Corma, A. Chica, E. Argente, V. Botti, *Catal. Today* **2003**, *81*, 393–403.
[85] A. Corma, J. M. Serra, E. Argente, V. Botti, S. Valero, *ChemPhysChem* **2002**, *3*, 939–945.
[86] F. Larachi, *Appl. Catal. B* **2001**, *30*, 141–150.
[87] K. Huang, X.-L. Zhan, F.-Q. Chen, D.-W. Lü, *Chem. Eng. Sci.* **2003**, *58*, 81–87.
[88] L. Baumes, D. Farrusseng, M. Lengliz, C. Mirodatos, *QSAR Comb. Sci.* **2004**, *23*, 767–778.
[89] N. K. Roy, W. D. Potter, D. P. Landau, *Appl. Intelligence* **2004**, *20*, 215–229.
[90] E. J. Molga, *Chem. Eng. Process.* **2003**, *42*, 675–695.
[91] F. Inal, G. Tayfur, T. R. Melton, S. M. Senkan, *Fuel* **2003**, *82*, 1477–1490.
[92] G. Zahedi, A. Jahanmiri, M. R. Rahimpor, *Int. J. Chem. React. Eng.* **2005**, *3*, A8.
[93] A. Tompos, J. L. Margitfalvi, E. Tfirst, L. Végvári, *Appl. Catal. A* **2006**, *303*, 72–80.
[94] A. Tompos, J. L. Margitfalvi, E. Tfirst, L. Vegvari, *Appl. Catal. A* **2003**, *254*, 161–168.
[95] A. Tompos, J. L. Margitfalvi, E. Tfirst, L. Vegvari, M. A. Jaloull, H. A. Khalfalla, M. M. Elgarni, *Appl. Catal. A* **2005**, *285*, 65–78.
[96] L. A. Baumes, J. M. Serra, P. Serna, A. Corma, *J. Comb. Chem.* **2006**, *8*, 583–596.
[97] W. Härdle, L. Simar, *Applied Multivariate Statistical Analysis*, Springer, Berlin, **2003**, p. 486.
[98] T. Hastie, R. Tibshirani, J. Friedman, *The Elements of Statistical Learning—Data Mining, Inference and Prediction*, Springer, New York, **2003**, p. 533.
[99] J. Han, M. Kamber, *Data Mining—Concepts and Techniques*, 2nd ed., Morgan Kaufmann, San Francisco **2006**, p. 608.
[100] J. M. Caruthers, J. A. Lauterbach, K. T. Thomson, V. Venkatasubramanian, C. M. Snively, A. Bhan, S. Katare, G. Oskarsdottir, *J. Catal.* **2003**, *216*, 98–109.
[101] P. Ghosh, A. Sundaram, V. Venkatasubramanian, J. M. Caruthers, *Comput. Chem. Eng.* **2000**, *24*, 685–691.
[102] A. Böcker, G. Schneider, A. Teckentrup, *QSAR Comb. Sci.* **2004**, *23*, 207.
[103] A. Ohrenberg, C. von Törne, A. Schuppert, B. Knab, *QSAR Comb. Sci.* **2005**, *24*, 29–37.
[104] N. Adams, U. S. Schubert, *J. Comb. Chem.* **2004**, *6*, 12–23.
[105] N. Adams, U. S. Schubert, *QSAR Comb. Sci.* **2005**, *24*, 58–65.
[106] T. Ott, A. Kern, A. Schuffenhauer, M. Popov, P. Acklin, E. Jacoby, R. Stoop, *J. Chem. Inf. Comput. Sci.* **2004**, *44*, 1358–1364.
[107] M. Saupe, R. Födisch, A. Sundermann, S. A. Schunk, K.-E. Finger, *QSAR Comb. Sci.* **2005**, *24*, 66–77.
[108] http://www.hte-company.com, **2006**.
[109] D. Farrusseng, L. Baumes, C. Mirodatos in *High-Throughput Analysis* (Eds.: R. A. Potyrailo, E. J. Amis), Kluwer, New York, **2003**, pp. 551–579.
[110] F. Clerc, R. Rakotomalala, D. Farrusseng, *Proceedings of the International Symposium on Applied Stochastic Models and Data Analysis* **2005**, pp. 535–542.
[111] C. Suh, A. Rajagopalan, X. Li, K. Rajan, *Data Sci. J.* **2002**, *1*, 19–26.
[112] K. Rajan, C. Suh, A. Rajagopalan, X. Li, *Materials Research Society Fall Meeting*, *700*, **2001**, p. 7.5.

[113] "Molten Salts—Fundamentals to Applications": K. Rajan, A. Rajagopalan, C. Suh, *NATO Sci. Ser.* **2002**, *52*.
[114] C. Suh, A. Rajagopalan, X. Li, K. Rajan, *Materials Research Society Symposium Proceedings*, *804*, **2003**, JJ 9.23.1–9.
[115] C. Suh, K. Rajan, *Appl. Surf. Sci.* **2004**, *223*, 148 – 158.
[116] S. Sakahara, K. Yajima, R. Belosludov, S. Takami, M. Kubo, A. Miyamoto, *Appl. Surf. Sci.* **2002**, *189*, 253 – 259.
[117] A. Endou, C. Jung, T. Kusagaya, M. Kubo, P. Selvam, A. Miyamoto, *Appl. Surf. Sci.* **2004**, *223*, 159 – 167.
[118] K. Suzuki, Y. Kuroiwa, S. Takami, M. Kubo, A. Miyamoto, *Appl. Surf. Sci.* **2002**, *189*, 313 – 318.
[119] M. Kubo, M. Ando, S. Sakahara, C. Jung, K. Seki, T. Kusagaya, A. Endou, S. Takami, A. Imamura, A. Miyamoto, *Appl. Surf. Sci.* **2004**, *223*, 188 – 195.
[120] A. Frantzen, D. Sanders, J. Scheidtmann, U. Simon, W. F. Maier, *QSAR Comb. Sci.* **2005**, *24*, 22 – 28.
[121] B. J. Chisholm, R. A. Potyrailo, J. Cawse, R. Shaffer, M. Brennan, C. A. Molaison, D. Whisenhunt, B. Flanagan, D. Olson, J. Akhave, D. Saunders, A. Mehrabi, M. Licon, *Prog. Org. Coat.* **2002**, *45*, 313 – 321.
[122] R. A. Potyrailo, B. J. Chisholm, D. R. Olson, M. J. Brennan, C. A. Molaison, *Anal. Chem.* **2002**, *74*, 5105 – 5111.
[123] R. A. Potyrailo, D. R. Olson, G. Medford, M. J. Brennan, *Anal. Chem.* **2002**, *74*, 5676 – 5680.
[124] P. Cong, A. Dehestani, R. Doolen, D. M. Giaquinta, S. Guan, V. Markov, D. Poojary, K. Self, H. Turner, W. H. Weinberg, *Proc. Natl. Acad. Sci. USA* **1999**, *96*, 11077 – 11080.
[125] J. S. Paul, J. Urschey, P. A. Jacobs, W. F. Maier, F. Verpoort, *J. Catal.* **2003**, *220*, 136 – 145.
[126] J. S. Paul, P. A. Jacobs, P. A. Weiss, W. F. Maier, *Appl. Catal. A* **2004**, *265*, 185 – 193.
[127] R. B. van Dover, L. F. Schneemeyer, *Macromol. Rapid Commun.* **2004**, *25*, 150 – 157.
[128] W. H. Weinberg, H. W. Turner in *High-Throughput Screening in Chemical Catal.* (Eds.: A. Hagemeyer, P. Strasser, A. F. Volpe, Jr.), Wiley-VCH, Weinheim, **2004**, pp. 1 – 17.
[129] S. C. Sieg, C. Suh, T. Schmidt, M. Stukovski, K. Rajan, W. F. Maier, *QSAR Combi. Sci.* **2007**, *26*, 528 – 535.
[130] S. Sieg, B. Stutz, T. Schmidt, F. Hamprecht, W. F. Maier, *J. Mol. Model.* **2006**, *12*, 611 – 619.
[131] L. Harmon, *J. Mater. Sci.* **2003**, *38*, 4479 – 4485.
[132] J. C. Zhao, *Annu. Rev. Mater. Res.* **2005**, *35*, 51 – 73, 4.
[133] R. M. Walser, R. W. Bene, *Appl. Phys. Lett.* **1976**, *28*, 624 – 625.
[134] J. C. Zhao, X. Zheng, D. G. Cahill, *Mater. Today* **2005**, *8*, 28 – 37.
[135] J. C. Zhao, *Prog. Mater. Sci.* **2006**, *51*, 557 – 631.
[136] S. Huxtable, D. G. Cahill, V. Fauconnier, J. O. White, J. C. Zhao, *Nat. Mater.* **2004**, *3*, 298 – 301.
[137] H. M. Christen, I. Ohkubo, C. M. Rouleau, G. E. Jellison, Jr., A. A. Puretzky, D. B. Geohegan, D. H. Lowndes, *Meas. Sci. Technol.* **2005**, *16*, 21 – 31.
[138] H. M. Christen, S. D. Silliman, K. S. Harshavardhan, *Appl. Surf. Sci.* **2002**, *189*, 216 – 221.
[139] H. M. Christen, S. D. Silliman, K. S. Harshavardhan, *Rev. Sci. Instrum.* **2001**, *72*, 2673 – 2678.
[140] M. Lippmaa, T. Koida, H. Minami, Z. W. Jin, M. Kawasaki, H. Koinuma, *Appl. Surf. Sci.* **2002**, *189*, 205 – 209.
[141] S. Guerin, B. E. Hayden, *J. Comb. Chem.* **2006**, *8*, 66 – 73.
[142] X. D. Xiang, *Appl. Surf. Sci.* **2004**, *223*, 54 – 61.
[143] X. D. Xiang, *Annu. Rev. Mater. Sci.* **1999**, *29*, 149 – 171.
[144] X.-D. Xiang, *Appl. Surf. Sci.* **2002**, *189*, 188 – 195.
[145] R. B. Schwarz, W. L. Johnson, *Phys. Rev. Lett.* **1983**, *51*, 415 – 418.
[146] Y. K. Yoo, F. Tsui, *MRS Bull.* **2002**, *27*, 316 – 323.
[147] F. Tsui, P. A. Ryan, *Appl. Surf. Sci.* **2002**, *189*, 333 – 338.
[148] E. D. Specht, A. Rar, G. M. Pharr, E. P. George, P. Zschack, H. Hong, J. Ilavsky, *J. Mater. Res.* **2003**, *18*, 2522 – 2527.
[149] P. Ahmet, T. Nagata, D. Kukuruznyak, S. Yagyu, Y. Wakayama, M. Yoshitake, T. Chikyow, *Appl. Surf. Sci.* **2006**, *252*, 2472 – 2476.
[150] A. Ludwig, N. Zotov, A. Savan, S. Groudeva-Zotova, *Appl. Surf. Sci.* **2006**, *252*, 2518 – 2523.
[151] A. Ludwig, *Appl. Surf. Sci.* **2004**, *223*, 78 – 83.
[152] T. Friesen, J. Haupt, W. Gissler, A. Barna, P. B. Barna, *Surf. Coat. Technol.* **1991**, *48*, 169 – 174.
[153] P. F. Miceli, H. Zabel, J. E. Cunningham, *Phys. Rev. Lett.* **1985**, *54*, 917 – 919.
[154] J. Cui, Y. S. Chu, O. O. Famodu, Y. Furuya, J. Hattrick-Simpers, R. D. James, A. Ludwig, S. Thienhaus, M. Wuttig, Z. Zhang, I. Takeuchi, *Nat. Mater.* **2006**, *5*, 286 – 290.
[155] E. F. Kneller, R. Hawig, *IEEE Trans. Magn.* **1991**, *27*, 3588 – 3600.
[156] H. D. Chopra, M. R. Sullivan, A. Ludwig, E. Quandt, *Phys. Rev. B* **2005**, *72*, 054415.
[157] X. D. Xiang, X. Sun, G. Briceno, Y. Lou, K. A. Wang, H. Chang, W. G. Wallace-Freedman, S. W. Chen, P. G. Schultz, *Science* **1995**, *268*, 1738 – 1740.
[158] H. Koinuma, H. N. Aiyer, Y. Matsumoto, *Sci. Technol. Adv. Mater.* **2000**, *1*, 1 – 10.
[159] Z. W. Jin, M. Murakami, T. Fukumura, Y. Matsumoto, A. Ohtomo, M. Kawasaki, H. Koinuma, *J. Cryst. Growth* **2000**, *214/215*, 55 – 58.
[160] H. Minami, K. Itaka, H. Kawaji, Q. J. Wang, H. Koinuma, M. Lippmaa, *Appl. Surf. Sci.* **2002**, *197–198*, 442 – 447.
[161] T. Ohnishi, D. Komiyama, T. Koida, S. Ohashi, C. Stauter, H. Koinuma, A. Ohtomo, M. Lippmaa, N. Nakagawa, M. Kawasaki, T. Kikuchi, K. Omote, *Appl. Phys. Lett.* **2001**, *79*, 536 – 538.
[162] T. Ohsawa, K. Nakajima, Y. Matsumoto, H. Koinuma, *Appl. Surf. Sci.* **2006**, *252*, 2603 – 2607.
[163] S. Noda, Y. Kajikawa, H. Komiyama, *Appl. Surf. Sci.* **2004**, *225*, 372 – 379.
[164] J. F. Whitacre, W. C. West, B. V. Ratnakumar, *J. Electrochem. Soc.* **2003**, *150*, A1676 – A1683.
[165] Q. Wang, J. Perkins, H. M. Branz, J. Alleman, C. Duncan, D. Ginley, *Appl. Surf. Sci.* **2002**, *189*, 271 – 276.
[166] Q. Wang, L. R. Tessler, H. Moutinho, B. To, J. Perkins, D. Han, D. Ginley, H. M. Branz, *Mater. Res. Soc. Symp. Proc.* **2003**, *762*, 413 – 424.
[167] A. Ludwig, J. Cao, J. Brugger, I. Takeuchi, *Meas. Sci. Technol.* **2005**, *16*, 111 – 118.
[168] C. J. Taylor, S. Semancik, *Chem. Mater.* **2002**, *14*, 1671 – 1677.
[169] T. F. Jaramillo, S. H. Baeck, A. Kleiman-Shwarsctein, E. W. McFarland, *Macromol. Rapid Commun.* **2004**, *25*, 297 – 301.
[170] S. H. Baeck, E. W. McFarland, *Korean J. Chem. Eng.* **2002**, *19*, 593 – 596.
[171] S. H. Baeck, T. F. Jaramillo, A. Kleiman-Shwarsctein, E. W. McFarland, *Meas. Sci. Technol.* **2005**, *16*, 54 – 59.
[172] S. H. Baeck, T. F. Jaramillo, C. Braendli, E. W. McFarland, *J. Comb. Chem.* **2002**, *4*, 563 – 568.
[173] S. D. Beattie, J. R. Dahn, *J. Electrochem. Soc.* **2005**, *152*, C542 – C548.
[174] S. Jayaraman, A. C. Hillier, *J. Comb. Chem.* **2004**, *6*, 27 – 31.
[175] H. Karl, I. Grosshans, B. Stritzker, *Meas. Sci. Technol.* **2005**, *16*, 32 – 40.
[176] I. Grosshans, H. Karl, B. Stritzker, *AIP Conf. Proc.* **2003**, *680*, 690 – 693.
[177] I. Grosshans, H. Karl, B. Stritzker, *Mater. Sci. Eng. B* **2003**, *101*, 212 – 215.
[178] P. Huber, H. Karl, B. Stritzker, *Appl. Surf. Sci.* **2006**, *252*, 2497 – 2502.
[179] S. Groudeva-Zotova, H. Karl, A. Savan, J. Feydt, B. Wehner, T. Walther, N. Zotov, B. Stritzker, A. Ludwig, *Thin Solid Films* **2006**, *495*, 169 – 174.

[180] M. L. Bricker, J. W. A. Sachtler, R. D. Gillespie, C. P. McGonegal, H. Vega, D. S. Bem, J. S. Holmgren, *Appl. Surf. Sci.* **2004**, *223*, 109 – 117.
[181] L. Chen, E. G. Derouane, J. C. Vedrine, *Appl. Catal. A* **2004**, *270*, 157 – 163.
[182] I. Hahndorf, O. Buyevskaya, M. Langpape, G. Grubert, S. Kolf, E. Guillon, M. Baerns, *Chem. Eng. J.* **2002**, *89*, 119 – 125.
[183] S. Ozturk, S. Senkan, *Appl. Catal. B* **2002**, *38*, 243 – 248.
[184] U. Rodemerck, D. Wolf, O. V. Buyevskaya, P. Claus, S. Senkan, M. Baerns, *Chem. Eng. J.* **2001**, *82*, 3 – 11.
[185] C. Hoffmann, A. Wolf, F. Schüth, *Angew. Chem.* **1999**, *111*, 2971 – 2975; *Angew. Chem. Int. Ed.* **1999**, *38*, 2800 – 2803.
[186] D. E. Akporiaye, I. M. Dahl, A. Karlsson, R. Wendelbo, *Angew. Chem.* **1998**, *110*, 629 – 631; *Angew. Chem. Int. Ed.* **1998**, *37*, 609 – 611.
[187] D. E. Akporiaye, I. M. Dahl, A. Karlsson, M. Plassen, R. Wendelbo, D. S. Bem, R. W. Broach, G. J. Lewis, M. Miller, J. Moscoso, *Microporous Mesoporous Mater.* **2001**, *48*, 367 – 373.
[188] K. Choi, D. Gardner, N. Hilbrandt, T. Bein, *Angew. Chem.* **1999**, *111*, 3070 – 3073; *Angew. Chem. Int. Ed.* **1999**, *38*, 2891 – 2894.
[189] J. Klein, C. W. Lehmann, H. W. Schmidt, W. F. Maier, *Angew. Chem.* **1998**, *110*, 3557 – 3561; *Angew. Chem. Int. Ed.* **1998**, *37*, 3369 – 3372.
[190] J. M. Newsam, T. Bein, J. Klein, W. F. Maier, W. Stichert, *Microporous Mesoporous Mater.* **2001**, *48*, 355 – 365.
[191] Y. Song, J. Li, J. Yu, K. Wang, R. Xu, *Top. Catal.* **2005**, *35*, 3 – 8.
[192] C. Mellot Draznieks, J. M. Newsam, A. M. Gorman, C. M. Freeman, G. Férey, *Angew. Chem.* **2000**, *112*, 2358 – 2363; *Angew. Chem. Int. Ed.* **2000**, *39*, 2270 – 2275.
[193] L. M. Knight, G. J. Lewis, *Stud. Surf. Sci. Catal.* **2004**, *154A*, 171 – 179.
[194] P. Atienzar, A. Corma, H. Garcia, J. M. Serra, *Chem. Eur. J.* **2004**, *10*, 6043 – 6047.
[195] R. Wendelbo, D. E. Akporiaye, A. Karlsson, M. Plassen, A. Olafsen, *J. Eur. Ceram. Soc.* **2006**, *26*, 849 – 859.
[196] Special Issue of: *Macromol. Rapid Commun.* **2005**, *26*(4), 205 – 332.
[197] D. B. Wallace, M. E. Grove, *High-Throughput Anal.* **2003**, 469 – 490.
[198] A. Kamyshny, M. Ben-Moshe, S. Aviezer, S. Magdassi, *Macromol. Rapid Commun.* **2005**, *26*, 281 – 288.
[199] J. Wang, M. M. Mohebi, J. R. G. Evans, *Macromol. Rapid Commun.* **2005**, *26*, 304 – 309.
[200] J. Wang, J. R. G. Evans, *J. Comb. Chem.* **2005**, *7*, 665 – 672.
[201] Z. T. Cygan, J. T. Cabral, K. L. Beers, E. J. Amis, *Langmuir* **2005**, *21*, 3629 – 3634.
[202] T. N. Kim, K. Campbell, A. Groisman, D. Kleinfeld, C. B. Schaffer, *Appl. Phys. Lett.* **2005**, *86*, 201106.
[203] S. Bergh, S. Guan, A. Hagemeyer, C. Lugmair, H. Turner, A. F. Volpe, W. H. Weinberg, G. Mott, *Appl. Catal. A* **2003**, *254*, 67 – 76.
[204] S. Bergh, P. Cong, B. Ehnebuske, S. Guan, A. Hagemeyer, H. Lin, Y. Liu, C. G. Lugmair, H. W. Turner, A. F. Volpe, Jr., W. H. Weinberg, L. Woo, J. Zysk, *Top. Catal.* **2003**, *23*, 65 – 79.
[205] A. Guram, A. Hagemeyer, C. G. Lugmair, H. W. Turner, A. F. Volpe, Jr., W. H. Weinberg, K. Yaccato, *Adv. Synth. Catal.* **2004**, *346*, 215 – 230.
[206] R. A. Houghten, *Proc. Natl. Acad. Sci. USA* **1985**, *82*, 5131 – 5135.
[207] H. M. Geysen, R. H. Meloen, S. M. Barteling, *Proc. Natl. Acad. Sci. USA* **1984**, *81*, 3998 – 4002.
[208] A. Furka, F. Sebestyen, M. Asgedom, G. Dibo, *Int. J. Pept. Protein Res.* **1991**, *37*, 487 – 493.
[209] J. Klein, T. Zech, J. M. Newsam, S. A. Schunk, *Appl. Catal. A* **2003**, *254*, 121 – 131.
[210] J. C. Hulteen, D. A. Treichel, M. T. Smith, M. L. Duval, T. R. Jensen, R. P. Van Duyne, *J. Phys. Chem. B* **1999**, *103*, 3854 – 3863.
[211] C. L. Haynes, R. P. Van Duyne, *J. Phys. Chem. B* **2001**, *105*, 5599 – 5611.
[212] J. Hulliger, M. A. Awan, *Chem. Eur. J.* **2004**, *10*, 4694 – 4702.
[213] J. Hulliger, M. A. Awan, *J. Comb. Chem.* **2005**, *7*, 73 – 77.
[214] G. R. Newkome, B. J. Childs, M. J. Rourk, G. R. Baker, C. N. Moorefield, *Biotechnol. Bioeng.* **1999**, *61*, 243 – 253.
[215] R. A. Potyrailo, *TrAC Trends Anal. Chem.* **2003**, *22*, 374 – 384.
[216] R. A. Potyrailo, *Proc. SPIE-Int. Soc. Opt. Eng.* **2002**, *4578*, 366 – 377.
[217] S. M. Senkan, *Nature* **1998**, *394*, 350 – 353.
[218] A. Holzwarth, H. W. Schmidt, W. F. Maier, *Angew. Chem.* **1998**, *110*, 2788 – 2792; *Angew. Chem. Int. Ed.* **1998**, *37*, 2644 – 2647.
[219] H. Su, E. S. Yeung, *J. Am. Chem. Soc.* **2000**, *122*, 7422 – 7423.
[220] A. Holzwarth, W. F. Maier, *Platinum Met. Rev.* **2000**, *44*, 16 – 21.
[221] G. Kirsten, W. F. Maier in *High Throughput Screening in Chemical Catalysis* (Eds.: A. G. Hagemeyer, P. Strasser, A. F. Volpe), Wiley-VCH, Weinheim, **2004**, pp. 175 – 187.
[222] P. Cong, R. D. Doolen, Q. Fan, D. M. Giaquinta, S. Guan, E. W. McFarland, D. M. Poojary, K. Self, H. W. Turner, W. H. Weinberg, *Angew. Chem.* **1999**, *111*, 507 – 512; *Angew. Chem. Int. Ed.* **1999**, *38*, 483 – 488.
[223] S. Senkan, K. Krantz, S. Ozturk, V. Zengin, I. Onal, *Angew. Chem.* **1999**, *111*, 2965 – 2971; *Angew. Chem. Int. Ed.* **1999**, *38*, 2794 – 2799.
[224] M. Orschel, J. Klein, H. W. Schmidt, W. F. Maier, *Angew. Chem.* **1999**, *111*, 2961 – 2965; *Angew. Chem. Int. Ed.* **1999**, *38*, 2791 – 2794.
[225] P. Claus, D. Honicke, T. Zech, *Catal. Today* **2001**, *67*, 319 – 339.
[226] C. Hoffmann, H. W. Schmidt, F. Schuth, *J. Catal.* **2001**, *198*, 348 – 354.
[227] P. A. Weiss, J. W. Saalfrank, J. Scheidtmann, H. W. Schmidt, W. F. Maier in *High Throughput Analysis* (Eds.: R. A. Potyrailo, E. J. Amis), Kluwer/Plenum, New York, **2003**, pp. 125 – 153.
[228] P. A. W. Weiss, C. Thome, W. F. Maier, *J. Comb. Chem.* **2004**, *6*, 520 – 529.
[229] H. Wang, Z. Liu, J. Shen, *J. Comb. Chem.* **2003**, *5*, 802 – 808.
[230] M. T. Reetz, *Angew. Chem.* **2001**, *113*, 292 – 320; *Angew. Chem. Int. Ed.* **2001**, *40*, 284 – 310.
[231] M. T. Reetz, K. M. Kuhling, A. Deege, H. Hinrichs, D. Belder, *Angew. Chem.* **2000**, *112*, 4049 – 4052; *Angew. Chem. Int. Ed.* **2000**, *39*, 3891 – 3893.
[232] D. L. Wetzel, S. M. LeVine, *Science* **1999**, *285*, 1224 – 1225.
[233] T. X. Sun, *Biotechnol. Bioeng.* **1998**, *61*, 193 – 201.
[234] A. Karim, A. Sehgal, J. C. Meredith, A. J. Crosby, E. J. Amis in *High-Throughput Analysis* (Eds.: R. A. Potyrailo, E. J. Amis), Kluwer, New York, **2003**, pp. 33 – 56.
[235] H. Su, E. S. Yeung in *High-Throughput Analysis* (Hrsg.: R. A. Potyrailo, E. J. Amis), Kluwer/Plenum, New York, **2003**, pp. 57 – 76.
[236] T. X. Sun, G. E. Jabbour, *MRS Bull.* **2002**, *27*, 309 – 315.
[237] C. M. Snively, G. Oskarsdottir, J. Lauterbach, *Catal. Today* **2001**, *67*, 357 – 368.
[238] C. M. Snively, J. Lauterbach, *NATO ASI Ser. Ser. C* **2000**, *560*, 437 – 439.
[239] C. M. Snively, S. Katzenberger, G. Oskarsdottir, J. Lauterbach, *Opt. Lett.* **1999**, *24*, 1841 – 1843.
[240] A. Leugers, D. R. Neithamer, L. S. Sun, J. E. Hetzner, S. Hilty, S. Hong, M. Krause, K. Beyerlein, *J. Comb. Chem.* **2003**, *5*, 238 – 244.
[241] C. M. Snively, G. Oskarsdottir, J. Lauterbach, *Angew. Chem.* **2001**, *113*, 3117 – 3120; *Angew. Chem. Int. Ed.* **2001**, *40*, 3028 – 3030.

[242] K. L. A. Chan, S. G. Kazarian, *J. Comb. Chem.* **2005**, *7*, 185 – 189.
[243] R. J. Hendershot, R. Vijay, B. J. Feist, C. M. Snively, J. Lauterbach, *Meas. Sci. Technol.* **2005**, *16*, 302 – 308.
[244] R. J. Hendershot, W. B. Rogers, C. M. Snively, B. A. Ogunnaike, J. Lauterbach, *Catal. Today* **2004**, *98*, 375 – 385.
[245] T. Johann, A. Brenner, M. Schwickardi, O. Busch, F. Marlow, S. Schunk, F. Schuth, *Catal. Today* **2003**, *81*, 449 – 455.
[246] A. Nakayama, E. Suzuki, T. Ohmori, *Appl. Surf. Sci.* **2002**, *189*, 260 – 264.
[247] D. G. Hafeman, J. W. Parce, H. M. McConnell, *Science* **1988**, *240*, 1182 – 1185.
[248] Y. Zhang, X. Gong, H. Zhang, R. C. Larock, E. S. Yeung, *J. Comb. Chem.* **2000**, *2*, 450 – 452.
[249] H. Y. Cho, D. S. Hong, D. W. Jeong, Y. D. Gong, S. I. Woo, *Macromol. Rapid Commun.* **2004**, *25*, 302 – 306.
[250] X. J. Fan, M. Murakami, R. Takahasi, T. Koida, Y. Matsumoto, T. Hasegawa, T. Fukumura, M. Kawasaki, P. Ahmet, T. Chikyow, H. Koinuma, *Mater. Res. Soc. Symp. Proc.* **2002**, *700*, 55 – 60.
[251] T. Hasegawa, T. Kageyama, T. Fukumura, N. Okazaki, M. Kawasaki, H. Koinuma, Y. K. Yoo, F. Duewer, X.-D. Xiang, *Appl. Surf. Sci.* **2002**, *189*, 210 – 215.
[252] Y. Matsumoto, H. Koinuma, T. Hasegawa, I. Takeuchi, F. Tsui, Y. K. Yoo, *MRS Bull.* **2003**, *28*, 734 – 739.
[253] T. J. Silva, A. B. Kos, *J. Appl. Phys.* **1997**, *81*, 5015 – 5017.
[254] P. Ahmet, Y. Z. Yoo, K. Hasegawa, H. Koinuma, T. Chikyow, *Appl. Phys. A* **2004**, *79*, 837 – 839.
[255] A. Oral, S. J. Bending, M. Henini, *Appl. Phys. Lett.* **1996**, *69*, 1324 – 1326.
[256] A. Pross, A. I. Crisan, S. J. Bending, V. Mosser, M. Konczykowski, *J. Appl. Phys.* **2005**, *97*, 096105.
[257] W. C. Oliver, G. M. Pharr, *J. Mater. Res.* **1992**, *7*, 1564 – 1583.
[258] O. L. Warren, T. J. Wyrobek, *Meas. Sci. Technol.* **2005**, *16*, 100 – 110.
[259] N. Okazaki, H. Odagawa, Y. Cho, T. Nagamura, D. Komiyama, T. Koida, H. Minami, P. Ahmet, T. Fukumura, Y. Matsumoto, M. Kawasaki, T. Chikyow, H. Koinuma, T. Hasegawa, *Appl. Surf. Sci.* **2002**, *189*, 222 – 226.
[260] C. Gao, X. D. Xiang, *Rev. Sci. Instrum.* **1998**, *69*, 3846 – 3851.
[261] H. Odagawa, Y. Cho, H. Funakubo, K. Nagashima, *Jpn. J. Appl. Phys. Part 1* **2000**, *39*, 3808 – 3810.
[262] M. V. Mirkin, B. R. Horrocks, *Anal. Chim. Acta* **2000**, *406*, 119 – 146; G. Wittstock, M. Burchardt, S. E. Pust, Y. Shen, C. Zhao, *Angew. Chem.* **2007**, *119*, 1604 – 1640; *Angew. Chem. Int. Ed.* **2007**, *46*, 1584 – 1617.
[263] M. Black, J. Cooper, P. McGinn, *Meas. Sci. Technol.* **2005**, *16*, 174 – 182.
[264] M. Black, J. Cooper, P. McGinn, *Chem. Eng. Sci.* **2004**, *59*, 4839 – 4845.
[265] S. Jayaraman, A. C. Hillier, *J. Phys. Chem. B* **2003**, *107*, 5221 – 5230.
[266] T. Chikyow, P. Ahmet, K. Nakajima, T. Koida, M. Takakura, M. Yoshimoto, H. Koinuma, *Appl. Surf. Sci.* **2002**, *189*, 284 – 291.
[267] S. Vogt, Y. S. Chu, A. Tkachuk, P. Ilinski, D. A. Walko, F. Tsui, *Appl. Surf. Sci.* **2004**, *223*, 214 – 219.
[268] R. Cremer, S. Richter, *Surf. Interface Anal.* **2002**, *34*, 686 – 689.
[269] J. K. Park, K. J. Choi, K. N. Kim, C. H. Kim, *Appl. Phys. Lett.* **2005**, *87*, 031108.
[270] K. S. Sohn, D. H. Park, S. H. Cho, J. S. Kwak, J. S. Kim, *Chem. Mater.* **2006**, *18*, 1768 – 1772.
[271] K. S. Sohn, D. H. Park, S. H. Cho, B. I. Kim, S. I. Woo, *J. Comb. Chem.* **2006**, *8*, 44 – 49.
[272] H. Sano, T. Matsumoto, Y. Matsumoto, H. Koinuma, *Appl. Surf. Sci.* **2006**, *252*, 2493 – 2496.
[273] M. Thelakkat, C. Schmitz, C. Neuber, H. W. Schmidt, *Macromol. Rapid Commun.* **2004**, *25*, 204 – 223.
[274] X. N. Liu, H. B. Cui, Y. Tang, S. X. Huang, W. H. Liu, C. Gao, *Appl. Surf. Sci.* **2004**, *223*, 144 – 147.
[275] V. Z. Mordkovich, H. Hayashi, M. Haemori, T. Fukumura, M. Kawasaki, *Adv. Funct. Mater.* **2003**, *13*, 519 – 524.
[276] M. P. Taylor, C. W. Teplin, M. F. A. M. van Hest, J. L. Alleman, M. S. Dabney, L. M. Gedvilas, B. M. Keyes, B. To, P. A. Parilla, J. D. Perkins, J. D. Ginley, *Macromol. Rapid Commun.* **2004**, *25*, 344 – 347.
[277] S. Inoue, S. I. Todoroki, T. Konishi, T. Araki, T. Tsuchiya, *Appl. Surf. Sci.* **2004**, *223*, 233 – 237.
[278] S. Todoroki, S. Inoue, T. Matsumoto, *Appl. Surf. Sci.* **2002**, *189*, 241 – 244.
[279] J. T. Rantala, T. Kololuoma, L. Kivimaki, *Proc. SPIE-Int. Soc. Opt. Eng.* **2000**, *3941*, 11 – 18.
[280] S. J. Henderson, J. A. Armstrong, A. L. Hector, M. T. Weller, *J. Mater. Chem.* **2005**, *15*, 1528 – 1536.
[281] D. Rende, K. Schwarz, U. Rabe, W. F. Maier, W. Arnold, *Prog. Solid State Chem.* **2007**, *35*, 361 – 366.
[282] X. D. Xiang, *Biotechnol. Bioeng.* **1998**, *61*, 227 – 241.
[283] K. Fujimoto, K. Takada, T. Sasaki, M. Watanabe, *Appl. Surf. Sci.* **2004**, *223*, 49 – 53.
[284] K. Takada, K. Fujimoto, T. Sasaki, M. Watanabe, *Appl. Surf. Sci.* **2004**, *223*, 210 – 213.
[285] J. R. Dahn, R. E. Mar, A. Abouzeid, *J. Electrochem. Soc.* **2006**, *153*, A361 – A365.
[286] R. A. de Groot, F. M. Mueller, P. G. Engen, K. H. J. Buschow, *Phys. Rev. Lett.* **1983**, *50*, 2024.
[287] F. Tsui, L. He, L. Ma, *Mater. Res. Soc. Symp. Proc.* **2002**, *700*, 39 – 44.
[288] T. Ioroi, N. Fujiwara, Z. Siroma, K. Yasuda, Y. Miyazaki, *Electrochem. Commun.* **2002**, *4*, 442 – 446.
[289] T. Kobayashi, A. Ueda, Y. Yamada, H. Shioyama, *Appl. Surf. Sci.* **2004**, *223*, 102 – 108.
[290] S. Jayaraman, S. H. Baeck, T. F. Jaramillo, A. Kleiman-Shwarsctein, E. W. McFarland, *Rev. Sci. Instrum.* **2005**, *76*, 062227.
[291] E. Reddington, A. Sapienza, B. Gurau, R. Viswanathan, S. Saragapani, E. S. Smotkin, T. E. Mallouk, *Science* **1998**, *280*.
[292] B. C. Chan, R. Liu, K. Jambunathan, H. Zhang, G. Chen, T. E. Mallouk, E. S. Smotkin, *J. Electrochem. Soc.* **2005**, *152*, A594 – A600.
[293] S. Guerin, B. E. Hayden, C. E. Lee, C. Mormiche, J. R. Owen, A. E. Russell, B. Theobald, D. Thompsett, *J. Comb. Chem.* **2004**, *6*, 149 – 158.
[294] E. S. Smotkin, J. Jiang, A. Nayar, R. Liu, *Appl. Surf. Sci.* **2006**, *252*, 2573 – 2579.
[295] S. Guerin, B. E. Hayden, D. Pletcher, M. E. Rendall, J. P. Suchsland, *J. Comb. Chem.* **2006**, *8*, 679 – 686.
[296] R. Cremer, D. Neuschutz, *Int. J. Inorg. Mater.* **2001**, *3*, 1181 – 1184.
[297] R. Cremer, S. Dondorf, M. Hauck, D. Horbach, M. Kaiser, S. Kyrsta, O. Kyrylov, E. Munstermann, M. Philipps, K. Reichert, G. Strauch, *Z. Metallkd.* **2001**, *92*, 1120 – 1127.
[298] R. Cremer, D. Neuschutz, *Surf. Coat. Technol.* **2001**, *146–147*, 229 – 236.
[299] A. Borgschulte, R. Gremaud, S. de Man, R. J. Westerwaal, J. H. Rector, B. Dam, R. Griessen, *Appl. Surf. Sci.* **2006**, *253*, 1417 – 1423.
[300] P. Vandezande, L. E. M. Gevers, J. S. Paul, I. F. J. Vankelecom, P. A. Jacobs, *J. Membr. Sci.* **2005**, *250*, 305 – 310.
[301] I. F. J. Vankelecom, K. De Smet, L. E. M. Gevers, P. A. Jacobs, *Nanofiltration—Principles and Applications* (Eds.: A. I. Schäfer, A. G. Fane, T. D. Waite), Elsevier, Amsterdam, **2004**, Chap. 2
[302] M. Bulut, L. E. M. Gevers, J. S. Paul, I. F. J. Vankelecom, P. A. Jacobs, *J. Comb. Chem.* **2006**, *8*, 168 – 173.

[303] T. R. Boussie, C. Coutard, H. Turner, V. Murphy, T. S. Powers, *Angew. Chem.* **1998**, *110*, 3472 – 3475; *Angew. Chem. Int. Ed.* **1998**, *37*, 3272 – 3275.
[304] T. R. Boussie, V. Murphy, K. A. Hall, C. Coutard, C. Dales, M. Petro, E. Carlson, H. W. Turner, T. S. Powers, *Tetrahedron* **1999**, *55*, 11699 – 11710.
[305] T. R. Boussie, G. M. Diamond, C. Goh, K. A. Hall, A. M. Lapointe, M. Leclerc, C. Lund, V. Murphy, J. A. W. Shoemaker, U. Tracht, H. Turner, J. Zhang, T. Uno, R. K. Rosen, J. C. Stevens, *J. Am. Chem. Soc.* **2003**, *125*, 4306 – 4317.
[306] M. Stork, A. Herrmann, T. Nemnich, M. Klapper, K. Müllen, *Angew. Chem.* **2000**, *112*, 4544 – 4547; *Angew. Chem. Int. Ed.* **2000**, *39*, 4367 – 4369.
[307] D. J. Jones, V. C. Gibson, S. M. Green, P. J. Maddox, *Chem. Commun.* **2002**, 1038 – 1039.
[308] D. J. Jones, V. C. Gibson, S. M. Green, P. J. Maddox, A. J. P. White, D. J. Williams, *J. Am. Chem. Soc.* **2005**, *127*, 11037 – 11046.
[309] N. Adams, H. J. Arts, P. D. Bolton, D. Cowell, S. R. Dubberley, N. Friederichs, C. M. Grant, M. Kranenburg, A. J. Sealey, B. Wang, P. J. Wilson, A. R. Cowley, P. Mountford, M. Schroeder, *Chem. Commun.* **2004**, 434 – 435.
[310] P. Kolb, D. Demuth, J. M. Newsam, M. A. Smith, A. Sundermann, S. A. Schunk, S. Bettonville, J. Breulet, P. Francois, *Macromol. Rapid Commun.* **2004**, *25*, 280 – 285.
[311] T. R. Boussie, G. M. Diamond, C. Goh, K. A. Hall, A. M. LaPointe, M. K. Leclerc, V. Murphy, J. A. W. Shoemaker, H. Turner, R. K. Rosen, J. C. Stevens, F. Alfano, V. Busico, R. Cipullo, G. Talarico, *Angew. Chem.* **2006**, *118*, 3356 – 3361; *Angew. Chem. Int. Ed.* **2006**, *45*, 3278 – 3283.
[312] Z. J. A. Komon, G. M. Diamond, M. K. Leclerc, V. Murphy, M. Okazaki, G. C. Bazan, *J. Am. Chem. Soc.* **2002**, *124*, 15280 – 15285.
[313] M. Bäte, C. Neuber, R. Gisea, H.-W. Schmidt, *Macromol. Rapid Commun.* **2004**, *25*, 371 – 376.
[314] H. Pasch, P. Kilz, *Macromol. Rapid Commun.* **2003**, *24*, 104 – 108.
[315] J. C. Grunlan, D. L. Holguin, H.-K. Chuang, I. Perez, A. Chavira, R. A. J. Quilatan, A. R. Mehrabi, *Macromol. Rapid Commun.* **2004**, *25*, 286 – 291.
[316] J. C. Grunlan, A. R. Mehrabi, A. T. Chavira, A. B. Nugent, D. L. Saunders, *J. Comb. Chem.* **2003**, *5*, 362 – 368.
[317] R. A. Potyrailo, J. E. Pickett, *Angew. Chem.* **2002**, *114*, 4404 – 4407; *Angew. Chem. Int. Ed.* **2002**, *41*, 4230 – 4233.
[318] J. C. Meredith, A. Karim, E. J. Amis, *MRS Bull.* **2002**, *27*, 330 – 335.
[319] J. C. Meredith, A. P. Smith, A. Karim, E. J. Amis, *Macromolecules* **2000**, *33*, 9747 – 9756.
[320] C. G. Simon, Jr., N. Eidelman, Y. Deng, N. R. Washburn, *Macromol. Rapid Commun.* **2004**, *25*, 2003 – 2007.
[321] T. Terajima, H. Koinuma, *Macromol. Rapid Commun.* **2004**, *25*, 312 – 314.
[322] J.-F. Thaburet, H. Mizomoto, M. Bradley, *Macromol. Rapid Commun.* **2004**, *25*, 366 – 370.
[323] A. P. Smith, A. Sehgal, J. F. Douglas, A. Karim, E. J. Amis, *Macromol. Rapid Commun.* **2003**, *24*, 131 – 135.
[324] C. A. Tweedie, D. G. Anderson, R. Langer, K. J. Van Vliet, *Adv. Mater.* **2005**, *17*, 2599 – 2604.
[325] R. A. Potyrailo, P. J. McCloskey, R. J. Wroczynski, W. G. Morris, *Anal. Chem.* **2006**, *78*, 3090 – 3096.
[326] N. Eidelman, D. Raghavan, A. M. Forster, E. J. Amis, A. Karim, *Macromol. Rapid Commun.* **2004**, *25*, 259 – 263.
[327] M. B. Kossuth, D. A. Hajduk, C. Freitag, J. Varni, *Macromol. Rapid Commun.* **2004**, *25*, 243 – 248.
[328] D. A. Fischer, K. Efimenko, R. R. Bhat, S. Sambasivan, J. Genzer, *Macromol. Rapid Commun.* **2004**, *25*, 141 – 149.
[329] C. Gabriel, D. Lilge, M. O. Kirsten, *Macromol. Rapid Commun.* **2003**, *24*, 109 – 112.
[330] R. A. Potyrailo, R. J. Wroczynski, J. E. Pickett, M. Rubinsztajn, *Macromol. Rapid Commun.* **2003**, *24*, 123 – 130.
[331] A. Tuchbreiter, J. Marquardt, B. Kappler, J. Honerkamp, M. O. Kristen, R. Mülhaupt, *Macromol. Rapid Commun.* **2003**, *24*, 47 – 62.
[332] M. G. Sullivan, H. Utomo, P. J. Fagan, M. D. Ward, *Anal. Chem.* **1999**, *71*, 4369 – 4375.
[333] U. Simon, D. Sanders, J. Jockel, C. Heppel, T. Brinz, *J. Comb. Chem.* **2002**, *4*, 511 – 515.
[334] J. Scheidtmann, A. Frantzen, G. Frenzer, W. F. Maier, *Measurement Sci. Technol.* **2005**, *16*, 119 – 127.
[335] A. Frantzen, J. Scheidtmann, G. Frenzer, W. F. Maier, J. Jockel, T. Brinz, D. Sanders, U. Simon, *Angew. Chem.* **2004**, *116*, 770 – 773; *Angew. Chem. Int. Ed.* **2004**, *43*, 752 – 754.
[336] U. Simon, D. Sanders, J. Jockel, T. Brinz, *J. Comb. Chem.* **2005**, *7*, 682 – 687.
[337] M. Siemons, U. Simon, *Sens. Actuators B* **2006**, *120*, 110 – 118.
[338] T. J. Koplin, M. Siemons, C. Ocen-Valentin, D. Sanders, U. Simon, *Sensors* **2006**, *6*, 298 – 307.
[339] Y. Yamada, T. Kobayashi in *High-Throughput Analysis* (Eds.: R. A. Potyrailo, E. J. Amis), Kluwer/Plenum, New York, **2003**, pp. 247 – 259.
[340] G. Frenzer, A. Frantzen, D. Sanders, U. Simon, W. F. Maier, *Sensors* **2006**, *6*, 1568 – 1586.
[341] R. A. Potyrailo, *Angew. Chem.* **2006**, *118*, 718 – 738; *Angew. Chem. Int. Ed.* **2006**, *45*, 702 – 723.
[342] V. M. Mirsky, V. Kulikov, Q. Hao, O. S. Wolfbeis, *Macromol. Rapid Commun.* **2004**, *25*, 253 – 258.
[343] A. Apostolidis, I. Klimant, D. Andrzejewski, O. S. Wolfbeis, *J. Comb. Chem.* **2004**, *6*, 325 – 331.
[344] A. Corma, J. M. Serra, *Catal. Today* **2005**, *107–108*, 3 – 11.
[345] J. M. Serra, A. Corma in *High-Throughput Screening in Chemical Catal.* (Eds.: A. G. Hagemeyer, P. Strasser, A. F. Volpe, Jr.), Wiley-VCH, Weinheim, **2004**, pp. 129 – 151.
[346] A. Corma, J. M. Serra, P. Serna, S. Valero, E. Argente, V. Botti, *J. Catal.* **2005**, *229*, 513 – 524.
[347] J. Holmgren, D. Bem, M. Bricker, R. Gillespie, G. Lewis, D. Akporiaye, I. Dahl, A. Karlsson, M. Plassen, R. Wendelbo, *Stud. Surf. Sci. Catal.* **2001**, *135*, 461 – 470.
[348] M. L. Bricker, J. W. A. Sachtler, R. D. Gillespie, C. P. McGonegal, H. Vega, D. S. Bem, J. S. Holmgren, *Appl. Surf. Sci.* **2004**, *223*, 109 – 117.
[349] C. L. Staiger, D. A. Loy, G. M. Jamison, D. A. Schneider, C. J. Cornelius, *J. Am. Chem. Soc.* **2003**, *125*, 9920 – 9921.
[350] H. Wang, Z. Liu, J. Shen, H. Liu, *Catal. Commun.* **2004**, *5*, 55 – 58.
[351] A. Corma, M. J. az-Cabanas, M. Moliner, C. Martinez, *J. Catal.* **2006**, *241*, 312 – 318.
[352] M. Moliner, J. M. Serra, A. Corma, E. Argente, S. Valero, V. Botti, *Microporous Mesoporous Mater.* **2005**, *78*, 73 – 81.
[353] J. M. Serra, A. Corma, D. Farrusseng, L. Baumes, C. Mirodatos, C. Flego, C. Perego, *Catal. Today* **2003**, *81*, 425 – 436.
[354] A. Cantin, A. Corma, M. J. Diaz-Cabanas, J. L. Jorda, M. Moliner, *J. Am. Chem. Soc.* **2006**, *128*, 4216 – 4217.
[355] A. Corma, M. J. Diaz-Cabanas, J. L. Jorda, C. Martinez, M. Moliner, *Nature* **2006**, *443*, 842 – 845.
[356] Y. Liu, P. Cong, R. D. Doolen, H. W. Turner, W. H. Weinberg, *Catal. Today* **2000**, *61*, 87 – 92.
[357] Y. Liu, P. Cong, R. D. Doolen, S. Guan, V. Markov, L. Woo, S. Zeyss, U. Dingerdissen, *Appl. Catal. A* **2003**, *254*, 59 – 66.
[358] J. Urschey, A. Kuehnle, W. F. Maier, *Appl. Catal. A* **2003**, *252*, 91 – 106.
[359] D. Hancu, R. E. Colborn, R. Kilmer, *Prepr. Pap. Am. Chem. Soc. Div. Fuel Chem.* **2005**, *50*, 135 – 137.

[360] C. J. Brooks, J. Pigos, A. Hagemeyer, K. Yaccato, R. Carhart, M. Herrmann, A. Lesik, P. Strasser, A. Wolpe, H. Turner, H. Weinberg, *Prepr. Pap. Am. Chem. Soc. Div. Fuel Chem.* **2005**, *50*, 140 – 142.
[361] S. Duan, S. Senkan, *Ind. Eng. Chem. Res.* **2005**, *44*, 6381 – 6386.
[362] G. Grubert, S. Kolf, M. Baerns, I. Vauthey, D. Farrusseng, A. C. van Veen, C. Mirodatos, E. R. Stobbe, P. D. Cobden, *Appl. Catal. A* **2006**, *306*, 17 – 21.
[363] D. K. Kim, W. F. Maier, *J. Catal.* **2006**, *238*, 142 – 152.
[364] D. K. Kim, K. Stoewe, F. Mueller, W. F. Maier, *J. Catal.* **2007**, *247*, 101 – 111.
[365] K. Omata, A. Masuda, T. Mochizuki, Y. Watanabe, Sutarto, Y. Kobayashi, M. Yamada, *J. Jpn. Pet. Inst.* **2006**, *49*, 214 – 217.
[366] S. Senkan, M. Kahn, S. Duan, A. Ly, C. Leidholm, *Catal. Today* **2006**, *117*, 291 – 296.
[367] R. Borade, O. Bruemmer, A. Guram, A. Hagemeyer, H. Turner, X. Wang, H. Weinberg, *Chem. Eng. Commun.* **2005**, *192*, 1621 – 1635.
[368] S. Schuyten, E. E. Wolf, *Catal. Lett.* **2006**, *106*, 7 – 14.
[369] J. W. Saalfrank, W. F. Maier, *Angew. Chem.* **2004**, *116*, 2062 – 2066; *Angew. Chem. Int. Ed.* **2004**, *43*, 2028 – 2031.
[370] J. W. Saalfrank, W. F. Maier, *C. R. Chim.* **2004**, *7*, 483 – 494.
[371] W. F. Maier, J. Saalfrank, *Chem. Eng. Sci.* **2004**, *59*, 4673 – 4678.
[372] K. Yaccato, R. Carhart, A. Hagemeyer, A. Lesik, P. Strasser, A. F. Volpe, H. Turner, H. Weinberg, R. K. Grasselli, C. Brooks, *Appl. Catal. A* **2005**, *296*, 30 – 48.
[373] K. Gao, L. Yuan, L. Wang, *J. Comb. Chem.* **2006**, *8*, 247 – 251.
[374] P. J. Schmitz, R. J. Kudla, A. R. Drews, A. E. Chen, C. K. Lowe-Ma, R. W. McCabe, W. F. Schneider, C. T. Goralski, *Appl. Catal. B* **2006**, *67*, 246 – 256.
[375] S. Noda, H. Sugime, T. Osawa, Y. Tsuji, S. Chiashi, Y. Murakami, S. Maruyama, *Carbon* **2006**, *44*, 1414 – 1419.
[376] H. An, C. Kilroy, P. J. McGinn, *Catal. Today* **2004**, *98*, 423 – 429.
[377] N. E. Olong, K. Stoewe, W. F. Maier, *Appl. Catal. B* **2007**, *74*, 19 – 24.
[378] T. Schmidt, G. Frenzer, W. F. Maier in *Combinatorial amd High-Throughput Discovery and Optimization of Catalysts and Materials* (Eds.: R. A. Potyrailo, W. F. Maier), CRC Taylor & Francis, Boca Raton, **2006**, pp. 173 – 192.
[379] R. Iden, W. Schrof, J. Hadeler, S. Lehmann, *Macromol. Rapid Commun.* **2003**, *24*, 63 – 72.
[380] J. R. Smith, A. Seyda, N. Weber, D. Knight, S. Abramson, J. Kohn, *Macromol. Rapid Commun.* **2004**, *25*, 127 – 140.
[381] R. Y. Lochhead, C. T. Haynes, S. R. Jones, V. Smith, *Appl. Surf. Sci.* **2006**, *252*, 2535 – 2548.
[382] L. Lefort, J. A. F. Boogers, A. H. M. de Vries, J. G. de Vries, *Top. Catal.* **2006**, *40*, 185 – 191.
[383] http://www.dechema.de/HTT, **2006**.

